Sustainable Transport of Polymetallic Nodules

by

G.F.M. van Laar

to obtain the degree of Master of Science in Sustainable Energy Technology
at the Delft University of Technology,
to be defended publicly on Friday August 27, 2021

Student number:	4387775
Project duration:	October 22, 2020 – August 27, 2021
Thesis committee:	Dr. ir. H. Polinder, TU Delft, Supervisor
	Dr. D. J. Scholten, TU Delft
	Dr. ir. R. Schmehl, TU Delft
	Dr. ir. J. Breukels, Allseas Engineering BV
	August 21, 2021

Wind Energy Group, Faculty of Aerospace Engineering, Delft University of Technology &
Faculty of Electrical Engineering, Mathematics and Computer Science, Delft University of Technology

TU Delft

Allseas

Abstract

This research examines the possible pathways and available technologies that will help the shipping sector to achieve the climate goals set by the IMO. Reaching these goals will require financial incentives and policies regarding sustainability. These policies need to describe regulations at both international and regional level given the maritime sector's 3% contribution to GHG emissions (Tatar & ÖZER, 2018).
Previous research examines only the performances of the new technologies. This research includes both aspects to assess the different options, from the sustainable point of view as the business point of view.
The goal of this research was to investigate the possibilities to apply renewable energy sources to a vessel that transports polymetallic nodules from the Clarion-Clipperton Zone to Mexico in order to reduce the carbon footprint. Besides this, also look into which of these possibilities has the lowest costs. For this purpose, multiple propulsion drive train systems were examined which were based on the Panamax Leda C. The behavior of these new propulsion systems was examined to answer the following research question: "Which currently existing energy source(s) can be used to transport the polymetallic nodules from the Clarion-Clipperton Fracture zone to the coast of Mexico, a 2200 km route, and whose operational use is technically feasible in five years, in the most sustainable way and with the lowest costs?". To answer this research question, the following steps have been undertaken. First current technologies and their state, were analysed using technology readiness levels (TRLs). The known data was established which included the cargo, the requirements for the fleet, the total days at sea, total amount of nodules collected in one year and the buffer of the mining vessel. With this information an optimal base case was determined in terms of energy consumption and costs. The base case is a Panamax bulk carrier called the Leda C with a deadweight of 81526 dwt.
Two different key performance indicators (KPIs) were set to analyse the different performance systems. These KPIs are the emission reduction per tonne collected nodules in %/tonne and the costs per tonne collected nodules in $/tonne.
To examine the different propulsion systems, their performances had to be checked for this specific route. In this route analysis there is looked at the probability of the wind, which was necessary to calculate the performances of the wind assisted ship propulsion (WASP) systems.
Drive trains of the different propulsion systems were schematically given and analyzed to understand which systems should be implemented for the different propulsion systems. After this, the components of each propulsion was checked, looking at their performance, sizes and costs. The costs of the total drive trains of the different propulsion systems were elaborated. Finally, three different scenarios were chosen to examine the KPIs of the different propulsions.
It is concluded that the most cost-effective technology for the RE on board systems is the Flettner rotor and for the alternative fuels this is biofuel (HVO). The propulsion systems discussed in this research will only be attractive when the CO_2 tax will increase. It is concluded that the higher the carbon tax, the more attractive the alternative fuels become in terms of cost effectiveness.
The advice for Allseas will be, if nothing changes, to not install a sustainable energy propulsion system. Because all systems will be more expensive than the base case. If regulations make it necessary to reduce emissions, it is advised to install the Flettner rotor in hybrid with the current engine.

Keywords:
Wind assisted ship propulsion (WASP), solar system, Hydrogen, Ammonia, Biofuel, Fuel cell, Alternative propulsion system on board, Bulk carrier, transport, sustainability, innovation.

List of abbreviations

AC	Alternating Current
BAU	Business as usual
CAPEX	Capital Expenditure
CCZ	Clarion-Clipperton fracture zone
CDS	Climate Data Store
CO_2	carbon dioxide (carbon)
DC	Direct Current
DP	Dynamic Positioning
EEDI	Energy Efficiency Design Index
EEXI	Energy Efficiency Existing Ship Index
EU ETS	EU Emissions Trading System
FC	Fuel Cell
GHG emissions	Greenhouse Gas emissions
H_2	Hydrogen
H_2O	Water
HFO	Heavy Fuel Oil
HVO C_nH_{2n+2}	Hydrotreated Vegetable Oil
IC	Inflation Correction
ICE	Internal Combustion Engine
IMO	International Maritime Organization
KPI	Key Performance Indicator
LNG	Liquified Natural Gas
LPG	Liquid Propane Gas
MARVS	Maximum Allowable Relief Valve Setting (of a cargo tank)
MGO	Marine Gas Oil
MIDC	Maritime Industry Decarbonisation Council
N_2	Nitrogen
NH_3	Ammonia
NMC battery	Nickel Manganes Cobalt Oxide battery
NO_x	Nitric Oxide
O_2	Oxigen

O&M	Operating & maintenance
OPEX	Operational Expenditure
PEMFC	Proton Exchange Membrane Fuel Cell
SCR	Selective Catalytic Reduction
SMCR	Specified Maximum Continuous Rating
SOFC	Solid Oxide Fuel Cell
SO_x	Sulphur Oxide
WASP	Wind Assisted Ship Propulsion
WHR	Waste Heat Recovery

List of symbols

Symbol	Description	Units
ε_0	vacuum permittivity	$\mathrm{F\,m^{-1}}$
AWA	Apparent wind angle	$^\circ$
AWS	Apparent wind speed	$\mathrm{m/s}$
A	Area	$\mathrm{m^2}$
C	dimensionless coefficient (e.g. for drag model)	1
C_D	Drag coefficient matrix	$-$
C_L	Lift coefficient matrix	$-$
$C_{depreciation}$	Depreciation costs	\$
$C_{maintenance}$	Maintenance costs	\$
$C_{operation}$	Operating costs	\$
C_{total}	Total costs	\$
$C_{totfuel}$	Total fuel costs	\$
E_t	Energy for the transport vessel to go back and forth between CCZ and Mexico	MWh
F_D	Drag force matrix	kN
F_L	Lift force matrix	kN
F_i, j	Force matrix	kN
$MARVS$	Maximum allowable relief valve setting	MPa
MCR	maximum continuous rating	kW

NCR	normal continuous rating	kW
PN_a	Annual collected polymetallic nodules	tonne
$P_W ASP$	Power generated by the WASP system	kW
$SMCR$	Specified Maximum Continuous Rating	kW
TWA	True wind angle	°
TWS	True wind speed	m/s
V_s	Ship speed	knts
ρ_f	Fuel density	$\mathrm{kg/m^3}$
e	Energy content	MJ/kg
t_h	Time to load the transport vessel, is the same as the time to harvest the polymetallic nodules	days
t_s	Total time the transport fleet is at sea (250 days)	days
t_t	Travel time for the transport vessel to go back and forth between CCZ and Mexico	days
u	Energy density	MJ/L
v_h	Harvesting speed	tonne/h
DWT_{tv}	Deadweight tonnage of transport vessel	tonne

Contents

1 | Introduction

Approximately 90% of the world trade is performed by global shipping and this transport over sea is highly dependent on fossil fuels. Fossil fuels used in the marine sector are mostly heavy fuel oil (HFO) and marine gas oil (MGO). These fossil fuels emit green house gasses (GHGs) which have a huge environmental impact. GHG emissions in the industry are expected to have increased by 50-250% by 2050 compared with the GHG emissions in 2012, if left to business as usual (Rehmatulla, Parker, Smith, & Stulgis, 2017) (Nelissen et al., 2016). Besides this, the world is running out of fossil fuels. The shipping industry is also responsible for approximately 13% SOx and 15% NOx emissions of the global emissions. These emissions have a significant impact on human health (Tatar & ÖZER, 2018).

To conclude, GHG emissions, harmful emissions (such as SOx and NOx) and fuel consumption need to be diminished.

In 2016 the Paris Agreement was signed. Article 2 of the Paris Agreement aims to limit the global temperature to a maximum of 2 °C and pursues efforts to limit the rise to 1.5 °C before 2030. To achieve this goal, Article 4 states that the global peak of GHGs needs to be reached as soon as possible, thereby recognizing that peaking will take longer for developing country parties. Parties aim to achieve a balance between anthropogenic emissions by source and removals by sinks of GHGs (Moosmann, Urrutia, Siemons, Cames, & Schneider, 2019). Anthropogenic emissions are the emissions of various forms of carbon from combustion of fossil fuels (Hanania, Stenhouse, & Donev, 2016) and the global shipping industry, at the moment, accounts for nearly 3% of anthropogenic emissions (Tatar & ÖZER, 2018).

So, one step towards reaching this goal is to adjust the transportation over sea. To meet the Paris agreement, the International Maritime Organisation (IMO) agreed in April 2018 with a concept GHG strategy for the shipping sector to reduce emissions by at least 50% by 2050 compared to 2008 (Abbasov, 2020). The IMO is the main body that is currently responsible for developing and maintaining the regulatory framework concerning seas and is a specialized agency of the United Nations established in 1948. Its main purpose is to develop a set of rules for shipping that concern safety, environmental pollution, cooperation, legal disputes and shipping efficiency.

The IMO established a guideline in 2011 that new ships worldwide must comply with and have therefore introduced the Energy Efficiency Design Index (EEDI). The EEDI serves as a tool during the design stage which requires all new ships to meet a minimum level of energy efficiency. Furthermore, it is an index that estimates the amount of CO_2 in grams per transport work in tonne-mile. The EEDI is intended to define the energy efficiency of newly built ships and it depends on the machine power, speed of the ship and cargo weight (IRCLASS, 2014). Later, the IMO introduced an EEDI for existing ships, called Energy Efficiency Existing ships Index (EEXI). The goal of this EEXI is to reduce the operational carbon intensity of current vessels.

An attractive operational drive to meet the regulations set by the IMO, is immediate fuel savings. Direct fuel savings limit the risk of high price demand in the global crude oil markets (van der Kolk, 2020). Besides, the operational costs for HFO and MGO will likely increase due to the introduction of the Sulphur Cap in 2020 and the deliberate shift to alternative fuels such as hydrogen, ammonia and biofuels (Lloyd's Register, 2015).

Higher oil prices and the upcoming emission regulations are drivers for sustainable technology transports over sea and multiple projects are ongoing or already in use.

Decreasing speed has also a positive impact on decreasing the amount of GHG or harmful emissions and the use of new ship designs, especially the more hydrodynamic, can also provide solutions, but these will not be further discussed.
In this project only options with power that is generated from renewable energy sources are discussed; either power that can directly be used on ships or indirectly by means of e-fuel.
Various projects and studies on sustainable transports over sea have already been carried out.

DNV.GL, a classification society and advisor for the maritime industry, is the only body that compares these options altogether. In this study almost no concrete numbers are mentioned and DNV.GL has generalized the options that use wind as an energy source (DNV.GL, 2019).

Studies that do not generalize the options using wind, such as the PhD research of Nico van der Kolk (van der Kolk, Nico, 2020), of Giovanni Bordogna (Bordogna, 2020) and research of Petro Fagioni and Roland Schmehl (Faggiani & Schmehl, 2018a) focus on just one or two types of wind systems applied on different routes. These studies include a performance analysis and a cost analysis.
A research conducted by TNO, a Dutch organisation to enable application of knowledge, covered different types of fuels regarding the entire transport sector. This research can be used as guideline, but is only applicable for alternative fuels.
One research listed all possible options that will help the shipping sector to achieve the IMO's deep de-carbonisation targets (Mallouppas & Yfantis, 2021). This research remains only descriptive.
So most of the previous investigations only explained the performances of the new technologies, but none of these studies lists all the options and no study compares them with each other on both performances and total costs.
This research includes both aspects to assess the different options, from the sustainable point of view as the business point of view.
Possibilities concerning renewable energy directly generated on board which are currently under development, will be discussed here.

Projects using wind as a sustainable energy source are ships with wind assisted ship propulsion (WASP). These projects have especially the last couple of years been under development. Multiple WASP systems exist and can be split into six different categories (Nelissen et al., 2016). Examples of these WASP categories will be elaborated on further in the report. Firstly, the soft sails, these are conventional sails and are the first WASP systems used (Lloyd's Register, 2015). Rigid sails or wing sails can be compared with an aircraft wing. In the 1980's, the potential of this technology was first demonstrated by two ships, Shin Aitoku and Usuki Pioneer, but the interest faded to the sudden drop in oil prices (Bordogna, Markey, Huijsmans, Keuning, & Fossati, 2014). Currently, this technique often is combined with solar panels. Another category are the towing kites, which are kites connected to the bow of a vessel (Stam, 2020). Active sails needs to be turned on, after which they can then generate energy themselves. Rotors or turbosails are active sails. The rotor is a cylindrical structure on the deck of the vessel that rotates and with the use of the Magnus effect, energy is generated. The Magnus effects is the difference in air pressure on opposite sides of a rotating object (Lloyd's Register, 2015). Turbosails are suction

wings, which are non-rotating wings with vents and an internal fan or other device (CRAIN, 2010). Wind Turbines can also be used as WASP. At the moment there exist concepts for foldable wind turbines for commercial ships.

Energy generated from waves is another sustainable solution to reduce the amount of emissions using renewable energy. This can be done with the difference in energy at the water's surface (Liquid Robotics, Inc., 2020), with a patented wave power system that uses oscillating water columns that are integrated in the hull of a vessel (The Maritime Executive, 2017b) or with flaps attached to the ship that move up and down which causes the ship moving forward (Inhabitat, 2008).

Another renewable energy source that can be used for ships to reduce emissions, is solar energy. At the moment, the largest solar boat is a catamaran of 31 meters long and is powered by photo-voltaic solar panels consisting of 38,000 next-generation cells by SunPower.

Besides these current techniques, a lot of systems utilize a combination of renewable energy sources for ship propulsion. Many studies and concepts show that applying WASP decreases the amount of fuel and therefore emissions (van der Kolk, 2020), as well as the use of wave or solar energy. All these systems and concepts will be discussed further in chapter 2.

1.1 Allseas

The economic feasibility of using more sustainable options is reconsidered by maritime companies because of the higher oil prices and the upcoming emission regulations, including Allseas Engineering BV. Allseas is one of the major companies in the world that deals with offshore pipelay and subsea construction. One of the projects Allseas is involved in at the moment, is a deep-sea mining project in the middle of the Pacific Ocean in the Clarion-Clipperton Fracture Zone. This deep-sea mining project is planned to be executed in about 5 years.

Four km below the surface of the sea, there are critical metals that are necessary for a more sustainable transport (CCZ). Critical metals such as nickel, cobalt, manganese and copper are already in short supply and are needed for the use of batteries. The seafloor alone in the Clarion-Clipperton Fracture Zone contains 4.5 million square kilometers of polymetallic nodules containing these metals. The CCZ is divided into 25 areas, 16 areas are mining claims of approximately 1,000,000 km^2 and 9 areas of 160,000 km^2 are for conservation. A part of the zone is in possession of Allseas, this is the Nori D area, which is on the east side of the CCZ.
For Allseas to be profitable, two million tons of nodules need to be brought up from the sea floor to the surface every year and is shown in figure 1.1. The process to create EV batteries using nodules emits 75% less CO_2 than when these critical metals are extracted on land (The Metals Company, 2021). Besides this, other benefits are the not disrupted indigenous communities and the safer work conditions.

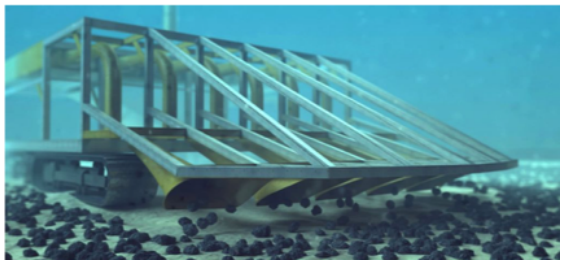

Figure 1.1: Allseas plans to scoop polymetallic nodules from the sea floor (Mining Magazine, 2019)

Once at the surface, these nodules have to be transported 1200 nm, which is more than 2000 km to the coast for processing. Deep sea mining requires a constant flow of transport to carry fuel and the nodules. This transport needs to be done as efficiently as possible bearing in mind the costs and the reduction of emissions. Figure 1.2 shows a graphic overview of this transport made by Vera Terlouw [1].

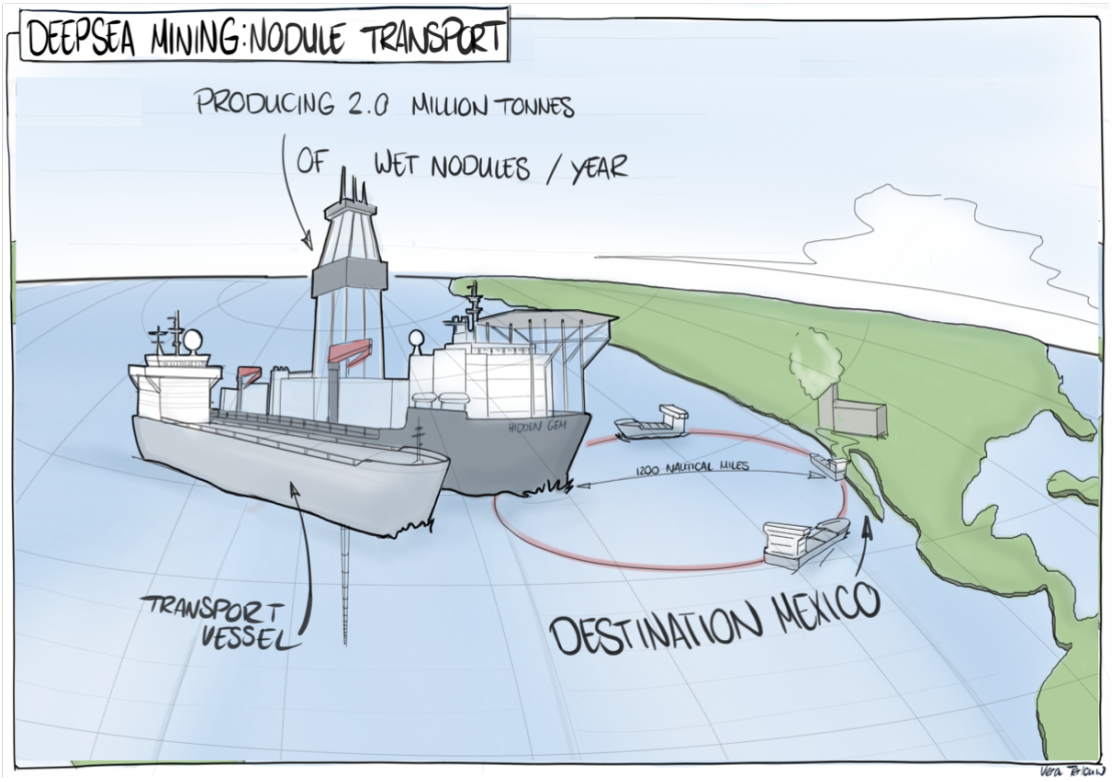

Figure 1.2: Graphic overview transport polymetallic nodules from CCZ to Mexico

[1] Vera Terlouw is a Naval Architect at Allseas

1.2 Research question

The goal of this project is to look at the various options that can be applied for this transport using sustainable energy sources. Besides this, the options must be feasible concerning the executability within a few years: the time it takes to execute the Deep-sea Mining project. The project is very dependent on the transport of the polymetallic nodules. Therefore, the research question is formulated as follows:

> *"Which transport options with using renewable energy source(s) can be applied to distribute the polymetallic nodules from the Clarion-Clipperton Fracture zone to the coast of Mexico, which is a 2200 km route in 5 years?"*

To answer this question, first options to transport the nodules from the CCZ to Mexico need to be examined. From this, technologies that can be applied to make the transport more sustainable, must be studied. Keeping in mind the boundary conditions for this transport, which needs to be examined first.
To compare these options on their feasibility, sustainability and affordability, a base case must be defined. Thirdly, the route, including external factors that need consideration when choosing the mode of transport or method, needs to be analysed. Subsequently, different modes of transport must be analysed regarding efficiency in terms of speed and financially. What methods are available to minimize kg/m_2 emissions and to reduce the amount of fuel? These methods need to be analysed and compared with the base case; what are the differences and similarities? Also, a cost-benefit analysis needs to be executed. With a cost-benefit analysis the strengths and weaknesses of the methods are estimated. This is needed to determine options which provide the best approach to achieving benefits while preserving savings, as well as providing a basis for comparing the methods with each other.

1.3 Approach and Thesis Structure

The project uses a System Engineering approach, which is a design approach used in the Bachelor's program at the Faculty of Aerospace Engineering, Delft University of Technology (TU Delft) (Melkert, Gibson, & Hulshoff, 2003). This project requires a design approach, because multiple design options need to be analysed. In the end the most feasible design(s) will be chosen. The choice will be based on prioritizing the factors costs, sustainability and speed.
The report has the following structure.
Chapter 2 elaborates on different current technologies mentioned in the introduction concerning feasibility, sustainability and financially, including their technology readiness levels. Chapter 3 gives a description of the transport. This includes a section about transport requirements: which factors are of importance, which values are assumed and which values can be neglected. This includes a base case as well. The base case is the starting point for transportation and has no sustainable assisted ship propulsion; in other words, point zero. Chapter 3 gives also an analysis of the route of transport, taking into account the current, wind and disturbances.
Chapter 5 gives an overview of the different drive trains for each option mentioned in the previous chapter. Then in chapter 6 the (new) energy sources needed for these drive trains are analysed on their performances concerning fuel and therefore emissions reduction for this route and transport. Also, other systems needed for these drive trains are selected and explained deeper in this chapter. After this, chapter 7 gives an analysis of the cost for the previous selected options. Chapter 8 gives an overview of different scenario's with the resulting key performance indicators (KPI's), including the resulting advice for Allseas. The report ends with the conclusions

and recommendations.

Introductory remark

As in the maritime sector preference is given to several specific units over SI units, these units are used in this thesis.
The following units are used and calculated in SI units:

Table 1.1: SI units and maritime units

Maritime unit	SI unit
10 knots	5.1444 m/s or 18,52 km/h
1 nm = 1 nautic mile	1852 m = 1.852 km
1 dwt = deadweight tonnage = maximum a ship can carry	1000kg

2 | Current state of technology

The vessel that transports the polymetallic nodules from the CCZ to the coast of Mexico should be compatible with the route, suitable to carry the polymetallic nodules and has to be stable during the transfer with the mining vessel. This chapter looks into what is already known about this transport. Different types of solutions that already exist to perform this shipment more sustainable, are analysed. Keep in mind that the Deep sea mining project is planned to be executed over 5 years, therefore a requirement of the outcome of the research question is that this shipment must be carried out within these years as well.

2.1 Transport options

This section describes the transport options, by discussing the fixed and assumed data needed for modelling a solution to transport the polymetallic nodules from the CCZ to the coast of Mexico. Some of this data is still not established yet, because the Deep-Sea mining project is still in concept phase. However, for this report, an assumed starting point for established data is used.

The established data is all the data of the route, the mining vessel and the cargo that is mostly certain. The route for the transportation of the polymetallic nodules has a distance of 1200 nm, which is 2200 km and is located between the CCZ and Mexico.
This transport needs to be done over sea. Vessels such as ships over sea, helicopters through the air, trains underground or a system with pipes may theoretically be used to transport the polymetallic nodules. Transport by air may be fast, but the collection of the nodules depends on the harvesting speed of the mining vessel. Besides this, the capacity of helicopters or airplanes is quite small, so the frequency of the cycle is very high. Also, helicopters are very expensive compared with ships and the range of a helicopter is not sufficient to make the 2200km trip.
Trains underground or a pipeline on the bottom of the ocean need to be placed at a depth of around 5km and the deepest pipeline installation has been placed at a depth of 2.5km. Next to this, the pipeline will wear out considerably if nodules are being pumped through,therefore maintenance and repair is badly needed. In addition, the pipe has to be placed in the CCZ, an area where several earth plates come together. Entire underwater mountains need to be traversed, not to mention the distance of 2200 km, which is even longer than the Nordstream 2 project. That project alone costed billions in installation.
From this it is deduced that ships are the most efficient, safe and cheapest way of transport the polymetallic nodules from the CCZ to the coast of Mexico.

2.2 Current emissions and fuel use in the shipping sector

As said before, the shipping section is a major contributor for global emissions. This is mostly because of the use of heavy fuel oil (HFO) and marine gas oil (MGO).

Since the 1960s HFO is the main fuel used in the maritime sector. At the moment approximately 77% of all fuel burned in marine engines is HFO (Maritime Industry Decarbonisation Council (MIDC), 2018). HFO has a high energy density, high carbon content and is relatively cheap. The relatively low costs of this fuel compared to cleaner fuel sources, is the main reason of its predominant use in the maritime sector. This fuel is a residue from the refining industry, it has a very high energy density, a high carbon content and is relatively low in price. HFO produces a lot of pollutants when used in an maritime engine, such as NOx, SOx and PM (Particulate Matter) and emits a lot of GHG (greenhouse gas) emissions (Maritime Industry Decarbonisation Council (MIDC), 2018) .
A change has to come to create a better environment, but also to keep in mind the capabilities of the shipping companies and the economic growth.
According to the International Transport Forum, a report of the OECD (Lucie Kirstein & Merk, 2018), 100% decarbonisation of the shipping section would be possible by 2035 when each of the following three options are implemented and combined. The first option to implement are technological measures, concerning improving energy efficiency and storage. The second option are operational measures include slow steaming, in other words, reduction of the speed of the vessel. The last option is renewable energy by using alternative fuels or wind or solar power (Lucie Kirstein & Merk, 2018). This master thesis focuses on the last option and alternative fuels, storage systems and projects with renewable energy generation on board will be discussed.

2.3 Technology readiness level

A method for classifying and understanding the current state of a technology is the system of technology readiness levels. TRLs indicate how far a technology is developed with specific phases. Here is TRL 1 the start of development of a technology and TRL 9 is when the technology is commercially available ("Grow", n.d.). Figure 2.1 gives an overview of the TRLs (TWI Ltd., 2021).
In this chapter section the current state of the technologies are explained and their TRLs are given.

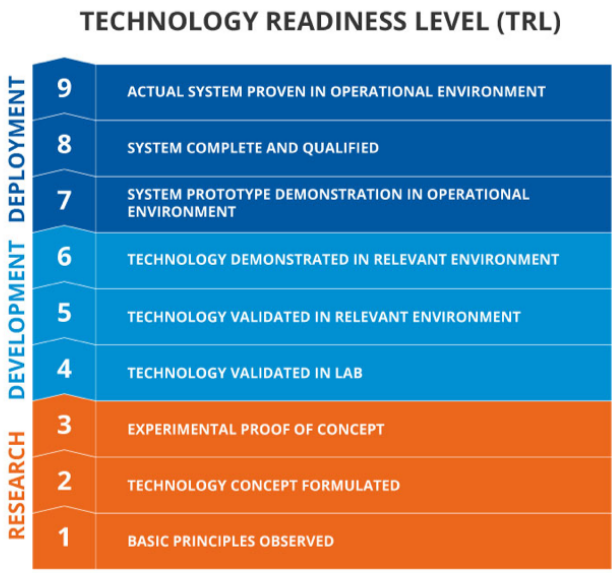

Figure 2.1: Technology readiness levels (TWI Ltd., 2021))

2.3.1 Alternative fuel

Replacing fossil fuel with 'clean' fuel, is a solution to decrease the amount of GHG or harmful emissions. Alternative fuels that are often mentioned in previous research are advanced biofuels, hydrogen, ammonia, LNG, LPG and methanol.

These alternative fuels can be divided into two categories: the first can reduce emissions up to 100% and the second can only decrease emissions for a certain amount. Note that almost for all alternative fuels, the engine and pipes need to be retrofitted.

The first category of alternative fuels that are often mentioned in previous research and can reduce emissions up to 100%, are advanced biofuels, hydrogen and ammonia.

There is a wide variety of production for biofuels, with a variety of feedstock and conversions. Advanced biofuels are second and third generation biofuels and produced using organic materials, from plants, bacteria or animals. It is estimated that biofuels are able to reduce carbon emissions by between 25% and 100% (Hsieh, 2017), which depends on the quality of the biofuel type and the way the bio feedstock is processed. As can be concluded from research done by DNV.GL ((DNV.GL, 2019)), the emissions of biodiesel depends on the production method. Marine biofuels are technically compatible with the existing marine engines, pipelines and bunker infrastructure. This is why biofuels are most suitable for retrofit. However, although advanced biofuels are already available in limited quantities, more knowledge on their performance and their physical properties might be required (Hsieh, 2017). Advanced biofuels therefore have the technology readiness level of around 4 and 5 as a lot of advanced biofuels are still under development and not deployed yet. Also, as biofuels are obtained from biomass or biomass residues, CO_2 is absorbed from plants and released in the atmosphere again. Because of these environmental implications, it is recommended to do more research into biofuels.

Producing (when from renewable energy sources) and using hydrogen will emit zero carbon

dioxide, zero sulphur oxide and zero nitrogen oxide, and can be used as fuel in different ways. The volumetric mass density of liquid hydrogen is 71 kg/m^3 and of hydrogen when stored as a compressed gas 23 to 38 kg/m^3, depending on the pressure, 700 to 300 bar. Comparing these densities with the density of HFO, the storage volume of liquid hydrogen is approximately five times the volume and as compressed gas it is 10 to 15 times the volume of HFO. When hydrogen is chemically bound, still some emissions occur (JSTRA & MLIT, 2020). Because of the reasons described above, liquid hydrogen has been chosen for this research.
The two most frequently used techniques to produce hydrogen is by steaming methane and by water electrolysis (Lucie Kirstein & Merk, 2018). With the last technique, renewable energy is used to split water into hydrogen and oxygen. When hydrogen is produced from water using renewable energy it emits almost no carbon emissions, while when it is obtained from methane (CH_4), it emits almost 90 times more (DNV.GL, 2019). Unfortunately, still a lot of research is necessary to make the production of sustainable hydrogen safe.
On board, a hydrogen fuel cell or an ICE (internal combustion engine) is used to convert chemical energy from hydrogen into electrical energy. Using a fuel cell emits again zero emissions. Using an ICE is more challenging. Uncontrollable pre-ignition events may occur due to the low ignition temperature of hydrogen and burning hydrogen mixed with air leads to high NOx emissions (Mallouppas & Yfantis, 2021). Besides this, DNV.GL (DNV.GL, 2019) states that hydrogen fuelled ICE for the maritime sector is less efficient than diesel engines.
Besides this, storage of hydrogen is subject to safety requirements. Liquid hydrogen needs to be stored at -256 °C and needs special pipes and storage tanks as hydrogen is an easily ignitable fuel wherefore more research must be done as well. Because of this, the TRL of commercially using hydrogen is set to 6 and the storage technology to 5. For retrofit this could be the toughest of alternative fuels to install.

Ammonia is another alternative fuel which can be used in the maritime sector. Comparing ammonia with hydrogen, an advantage of the liquid form of ammonia is that it allows more storage per cubic meter. However, for sustainable ammonia to become viable, it needs to be more competitive compared to conventional ammonia. At the moment, the production of conventional ammonia (and hydrogen) relies on 90% on fossil fuels (Healy & Graichen, 2019). Besides this, ammonia is very toxic. To change existing fuel tanks and pipes for ammonia fuel tanks and pipes, all needs to be double-walled to avoid severe consequences for example with leaks. Ammonia can be stored in the same tanks as LPG tanks (DNV.GL, 2019).
For ammonia, a combustion engine and a fuel cell can both be used to convert energy. When used in combustion engines, ammonia has serious disadvantages. The flammability range of ammonia is very narrow (15–28 vol%), ammonia has a high auto-ignition temperature (651 °C), a low laminar flame velocity (0.015 m/s) and still toxic emissions can occur. These factors complicate engine operations with ammonia. (Van Hoecke et al., 2021). To convert energy without emissions, for ammonia a fuel cell is necessary. The technology readiness level of sustainable ammonia is still between research and development phase and therefore set on 3-4.

It is essential for these alternative fuels that the production is performed by using renewable energy, otherwise there will be no full emission reduction compared with using MGO (Marine Gas Oil) or HFO (heavy fuel oil) (Lucie Kirstein & Merk, 2018).

The second category of alternative fuels can also reduce emission but not up to 100%. These alternative fuels include LNG, LPG and methanol. As these alternatives do not reduce emissions totally, these fuels are not examined further in this report. However, they are worth mentioning.

LNG stands for liquefied natural gas and is comparable with the composition of natural gas. The main element of LNG is methane (CH4), which has the lowest carbon content of fossil fuels. Therefore LNG emits the smallest amount of CO_2 emissions, 26% less then MGO and HFO,

when gas engines are used. The technology of using LNG for ships is already available. This is an advantage for retrofitting. LNG can also be used as hydrogen carrier for a fuel cell. However, for on-board use of LNG, either with a combustion engine or a fuel cell, there is still the issue of methane slip. Emissions from methane are detrimental to the overall environmental benefit of using LNG (Van Hoecke et al., 2021).
The alternative fuels from the first category, such as ammonia and hydrogen need a lot of storage space. A viable option could be by using LNG once a suitable and proper bunkering global infrastructure is available. However, from the point of view of the IMO to reduce carbon emissions, using LNG as an alternative fuel will not be sufficient (DNV.GL, 2019).

Another alternative fuel is LPG, liquefied petroleum gas, a mixture of propane and butane in liquid form and mostly used in the USA. This mixture enables particular characteristics of temperature and saturation pressure. LPG reduces kg/m^2 emissions by 17% using an internal combustion engine (DNV.GL, 2019). Like LNG, from the position to meet EEXI (explained in the introduction), LPG is not sufficient as a permanent solution.

The final alternative fuel discussed that could be used in the shipping sector as a possible strategy to lower kg/m_2 emissions, is methanol. Methanol is the most simple alcohol and has the lowest content of carbon and the highest content of hydrogen of all liquid fuels. Because of its simplicity, it can be made from different resources, such as natural gas and coal, but also from renewable energy sources like biomass or hydrogen. When methanol is produced from natural gas or coal, it can reduce CO_2 emissions by 10%. When methanol is yielded from renewable energy sources it reduces CO_2 emissions by 15% and higher when an ICE is used (DNV.GL, 2019). Methanol can be used as hydrogen carrier as well in combination with a fuel cell. When used as hydrogen carrier, methanol must be split. This reaction results in carbon emissions as well.

To conclude, the alternative fuels discussed could meet the expected content requirements for the shipping sector over the next decades. For the increasing consumption, a growth in production capacity for all alternative fuels is required, except for LNG. LNG is at the moment already in sufficient quantity to meet these requirements for the shipping sector for many years. However unfortunately, LNG will not be adequate in the long run. For zero emissions, alternative fuels need to be produced from renewable energy sources and without subsidies or taxation on CO_2 emissions, this could be a challenge.
In this report only alternative fuels of the first category are considered, as these have the potential to reduce emissions up to 100%. These alternative fuels are biofuel, hydrogen and ammonia. It is concluded that for biofuel the current engine can be used and both liquid hydrogen and ammonia need a fuel cell to emit zero emissions.

2.3.2 Storage systems

Energy storage systems like batteries, flywheels or super capacitors can supply power for zero-carbon electric propulsion. These storage systems remain relatively costly, although Bloomberg New Energy Finance estimated that by 2030 the pack prices of lithium batteries will be $73/kWh compared to $273/kWh in 2016. Although it is estimated that the electric vessel is the least profitable sustainable solution compared to alternative fuel options (Lloyd's Register, 2015), an all-electric vessel will expel almost no emissions when it comes from renewable energy generation. Still large improvements need to be made concerning battery capacity for longer voyages, but the current rapidly decreasing costs of battery technology and the competition, forces manufacturers to show the potential for broader use of batteries in the shipping sector. The range of the TRLs of storage systems is, due to this, wide, between 5 and 8, some are still under development, but a lot of storage systems are already complete and qualified. Sailing only on batteries

seems not feasible at the moment. The reason behind this is the low energy density of marine batteries. The energy density of the best performing commercial battery in 2018 was 2,434 kJ/l, compared to HFO with 39,970 kJ/l (Fulwood, 2021). The size and weight of such batteries currently prevents their application to deep-sea merchant vessels. Hybrid systems can therefore be a solution. Hybrid propulsion systems are the ones composed by different smaller engines, power storage units and a general power management system. This enables to counteract the effects of reduced power outtakes, to cope with energy peak demand and to focus more on lower emission while optimizing energy consumption at the same safety standards as before. Hybrid system implementation accounts for expenses that are 25% of the price of the main engine and can save up to 5% of generated power (TNO, 2013).

2.3.3 Energy generation on board

Renewable energy on board of a vessel can be generated with wind energy, wave energy or solar energy. In this section the currently existing concepts and projects of these types of renewable energy are discussed, again with their technology readiness levels. Only existing projects and concepts are mentioned as the system or technology needs to be installed the moment the execution of the deep sea mining project is started. From this section only the most feasible technologies will be chosen.

Wind assisted ship propulsion (WASP)

Projects for the shipping sector using wind as energy source are ships with wind assisted ship propulsion (WASP). The last years more research has been done to understand WASP better. It is estimated WASP has reduction of fuel of around 1-50%. But WASP depends on the operating speeds, hull, machinery, weather conditions, seasons and which route is taken, which makes WASP a propulsion with many uncertainties. WASP can be divided into six main categories: soft sails, wingsails, hull sails, towing kites, active sails and wind turbines (Nelissen et al., 2016).
These six categories can be divided into two types of WASP systems, the first type is direct propulsion and the second type provides indirect propulsion by connection to the drive train of the main engine. The direct propulsion system generates an aerodynamic thrust. The indirect propulsion system generates power. A disadvantage of an indirect WASP is its further loss of efficiency as it must be connected to the main engine.

Soft sail

The first category of the wind propulsion system is the propulsion by soft sail. This type of WASP is type 1. As said in the introduction, conventional sails are soft sails and was the first WASP used (Lloyd's Register, 2015). In 1978 research started to a project called Pinta-Rig by a German company Modern Merchant Sailing Vessel. The Pinta-Rig is only in research phase and further development is unclear (Nelissen et al., 2016). A technology that is ready for sale in 2020 is from Seagate Sail. Seagate Sail, an Italian company, has developed automatic delta sails. These delta sails are two collapsible booms automatically controlled with a complementary technology and shown in figure 2.2. This technology automatically regulates the vessel's engine as a function of the driving force from the wind (IWSA, 2016).

Figure 2.2: Delta wing sails of Seagate Sail (IWSA, 2016)

Figure 2.3: Ecoliner with Dyna-Rig (Dykstra-NA, 2013)

Other solutions with soft sail and still in test-phase are Fast-Rigs, which are automated square rigs stand free that provide wind assistance for vessels (Smart Green Shipping, 2020), the Neoline project and Dyna-Rig. The Neoline project is a project by Neoline, a French and Canadian company that plans to provide vessels with innovative duplex rigging and with an electric diesel auxiliary propulsion system (Neoline, 2020). Neoline has plans to operate pilot project vessels in the North Atlantic by 2020/2021. Dyna-Rig is a technology used for a design concept, the Ecoliner, created by Dykstra naval Architecs. Dyna-Rig is a concept rig of a square-rigged form (Dykstra-NA, 2013). The Ecoliner is a design concept of a multi-purpose cargo vessel shown in figure 2.3. The technology readiness level of the Dyna-Rig is in the last phase of the development stage and therefore set on 6.
Calculations of a study of (Rehmatulla et al., 2017) gives a reduction in emissions for soft sails between 10-50%, depending on the speed and the weather conditions.

Wingsail
Wing sail (or rigid sail) is similar to an aircraft wing and is often combined with solar panels (Lloyd's Register, 2015). Also Wingsails belong to WASP type 1 as this system directly generates a thrust force.
The Aquarius MRE System or EnergySail is a system that integrates both wind and solar power systems by using rigid sails, solar panels and energy storage models, shown on figure 2.4. Eco Marine Power is the Japanese company behind this advanced system and sea trails for this system started in 2016 (Eco Marine Power, 2016) and the goal of Eco Marine Power is to have everything ready by 2020 to build the Aquarius Eco Ship (Hellenic Shipping News, 2018).
Oceanfoil wing sail is another technology that uses wingsails to capture directional thrust from windpower. The oceanfoil wing sail consist of three aerofoils attached to a tail fin (The Maritime Executive, 2017a). The rigid opening sail (ROS) is a collapsible solar sail of the Australian company Ocius Technology Ltd. and can be used for bulkers, tankers and general cargo vessels (Nelissen et al., 2016). For the Auxiliary Sail Propulsion System (ASPS) the focus market are bulk carriers. The ASPS includes two masts both with three aerodynamic wings. These masts rotate automatically to exploit the power of the prevailing wind (Naaijen & Koster, 2014). The ASPS is shown in figure 2.5.
The wingsail is already commercially available and qualified (Nelissen et al., 2016), because of this, the TRL of wingsails is 8.

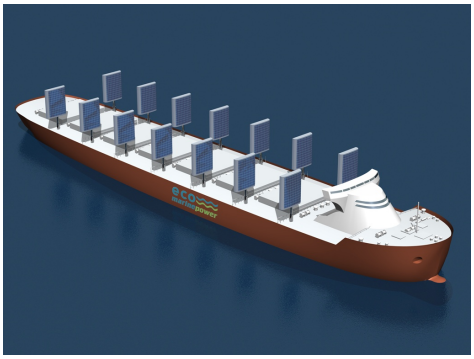

Figure 2.4: Aquarius Eco Ship by Eco Marine Power (Eco Marine Power, 2016)

Figure 2.5: ASPS for a cargoship of Windship Technology Ltd. (Naaijen & Koster, 2014)

Hull Sail

LadeAs is a Norwegian company that designed Vindskip, a hybrid merchant vessel driven by wind and LNG, shown in figure 2.6. The hull of the ship is above and below the water line which generates an aerodynamic lift (Shadbolt, 2015). This type of WASP cannot be retrofitted, but must be newly built because the entire hull shape is different.

Figure 2.6: The Vindskip carcarrier vessel disign of LadeAs (Shadbolt, 2015)

Towing Kite

Towing kites are kites connected to the bow of a vessel and can assist with the propulsion or generate thrust and electrical energy (Stam, 2020), therefore the belong to WASP type 1.
SkySails was the market and technology leader concerning automatic kite systems on ships (SKYSAILS GROUP, n.d.). This technology in practice turned out to be more unruly; kites turn out to be difficult in operations. However, kites have not entirely disappeared from the maritime sector. In 2019 the French company Airseas started with the Japanese company K-Line a seawing project concerning kites (Stam, 2020). Figure 2.7 shows the idea of the towing kite by Airseas.
A calculation of (Nelissen et al., 2016) shows a fuel savings between 1-32%, but the calculations of (Rehmatulla et al., 2017) show a reduction of fuel consumption of a constant 5%.
Kites are commercially available for ships, but also still under development to become applicable for larger ships. Because of this the TRL of kites is set on 5.

Figure 2.7: The Vindskip carcarrier vessel disign of LadeAs (Airseas, 2018)

Active sails

There are two different active sails, the Flettner rotor and the Turbosail.
The Flettner rotor uses the Magnus effect to rotate which generates a forward thrust (WASP type 1). The Magnus effects is the difference in air pressure on opposite sides of a rotating object (Lloyd's Register, 2015). The last couple of years a lot of research has been done in Flettner rotors. The Monorotor is a concept of a single rotor that is placed at the forepeak above the forecastle or at the aft of the Bridgeport Magnetics Group (Poulsen Hybrid, 2012). Magnuss Vertically-Variable Ocean Sail System (VOSS) is another concept using the Magnus effect, wherein a metal cylinder in an air stream a force roughly generates perpendicular to the air stream (Magnuss, 2020). C-Job Naval Architects have created a hybrid sailing concept for a cargo vessel, the so-called Flettner Freighter. This cargo ship is equipped with 4 Flettner rotors and a main engine that runs on LNG (C-job, 2015). ThiiiNKSail rotor is a concept of the Swiss company ThiiiNKSail and gives a works especially well for more narrow upwind tacks. This is due to the sail flaps that are fitted for the large scale rotors. For this concept the flettner rotors can be hydraulically folded onto a deck of the vessel (Thiiink, 2015).

Figure 2.8: The Norsepower Flettner Sail Solution (Norsepower, 2014)

Figure 2.9: Alycone - the Jacques Cousteau's Turbosail ship (Cousteau, 2011)

A technology that is already on the market is the Norsepower Rotor Sail Solution, which is a more modern version of the Flettner rotor and is fully automated. This solution is mainly designed for ships bigger than 5,000 deadweight tonnage (dwt), so tankers, bulk carriers and RoRo vessels (Norsepower, 2014). Figure 2.8 shows the Norsepower Flettner Sail Solution.
Thus, Flettner rotors are already commercially available and have proven it is a reliable tech-

nology in operational environment, therefore the TRL is set on 9. (Rehmatulla et al., 2017) calculated that this technology reduces fuel consumption between 10% at 20 knots and 30% at 10 knots. Another calculation provides a reduction of fuel consumption between 2 and 24% for a single Flettner rotor ((Nelissen et al., 2016)).

Another active sail technology, non-rotating and fan-driven, is the Turbosail (Cousteau, 2011) and shown in figure 2.9. This concepts is comparable with suction wings. Suction wings are non-rotating foils with vents and an internal fan or other device and is developed by CRAIN (CRAIN, 2010). An advantage of this technology is mainly the possibility to use bigger foils, which can produce a greater force forward (Econowind, 2019). This turbosail technology is still under development but almost in the deployment phase, the TRL is therefore 6.

Wind Turbine

Wind turbines can also be used as WASP and are assigned to WASP type 2, indirect propulsion, as the WASP system is connected to the drive train of the main propulsion system. Because of this, the energy generation of the wind turbines is not dependent on the wind direction, only on the wind speed. However, as the wind turbines are connected to the main drive train, their total efficiency will reduce.
The company ProPit has developed a concept for foldable wind turbines for commercial ships. These turbines produce not only electricity, but also thrust force forward (Carlson & Nilsson, 2014). The concept of these foldable wind turbines is shown in figure 2.10. Another company that has made a concept concerning the use of wind turbines on ships, is Inerjy. The concept is called EcoVert, which is a vertical-axis wind turbine. Currently Inerjy is busy with a demonstration vessel, because up to now land-only EcoVert exist (Inerjy, 2015).
The technology of the wind turbine is qualified and available, however, it the technology has not yet proven to be applicable in operational environment, therefore the TRL is set on 8 and not 9.

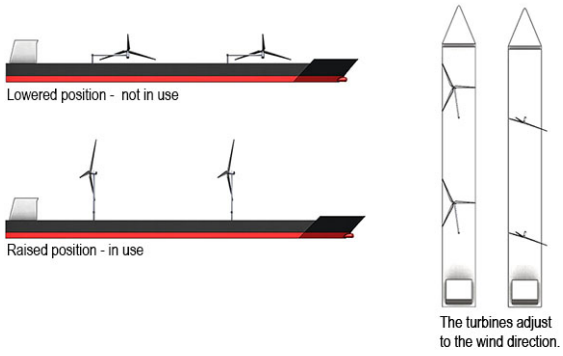

Figure 2.10: Foldable wind turbines onboard commercial ships to reduce fuel consumption of ProPit (Carlson & Nilsson, 2014)

Waves

Waves are holding power and can therefore be used as an innovative energy source on ships to reduce emissions.
Autonaut and the Wave Glider are Uncrewed Surface Vessels (USV). These are small ocean robots of circa 5 meters that use the waves for propulsion. Concerning the propulsion, this

technology exploits the difference in energy at the water's surface (Liquid Robotics, Inc., 2020). At the moment it is only used for research into autonomous systems and oceanographic studies (Autonaut, 2020) (Ridden, 2018).
The Canadian company ZShips is preparing a patented wave power system that uses oscillating water colums that are integrated in the hull of a vessel. The concept is to convert wave energy into stored energy in the form of compressed air which can be used as potential energy or on demand to generate energy (The Maritime Executive, 2017b).
The Suntory Mermaid is a 9.5 meter catamaran that neither has an engine nor sails, but moves only by the energy of waves (Donker, van Herwaarden, Stuurman, & van Zutphen, 2010). The flaps attached to the ship move up and down which causes the ship moving forward. These flaps are connected to a spring that keeps them in the right position. The direction of the waves is inconsequential, but the speed of the ship is limited to 5 knots and is not yet applicable for larger vessels (Inhabitat, 2008).

Solar

The world's largest solar boat at the moment is 31 meter long and is powered by photovoltaic solar panels consisting of next-generation cells by SunPower. The Tûranor Planet Solar, which is the name of this catamaran has made a world tour in 2011 (Pilato, 2012).

A concept of an emission-free ship that is powered by solar energy and hydrogen is made the Japanese company NYK Group and is called the NYK Super Eco Ship 2050. The pure car and truck carier (PCTC) is designed together with the companies MTI and Elomatic and is part of NYK's management plan. The ship does not only uses solar energy and hydrogen to reduce the emissions, the ship is also remodeled to decrease water friction, reducing weight of the hull and uses waves as well, for propulsion. All of these measures would result in a zero-emission vessel (Offshore Energy, 2018). The NYK Super Eco Ship 2050 is shown in figure 2.11.
Solar panels for ships are not yet commercially available and still under development. However the knowledge about this technology already exist. Because of this, the TRL for solar panels on ships is set on 6. Solar sails is a technology still in concept phase and on the beginning of development and therefor set on TRL 4.

Figure 2.11: NYK Super Eco Ship 2050 (Offshore Energy, 2018)

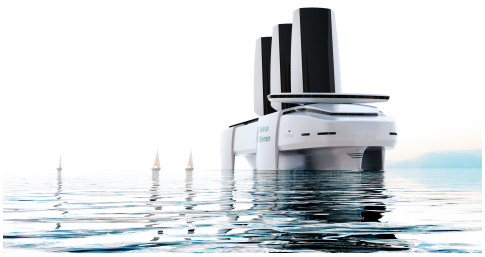

Figure 2.12: The Orcelle (Cummins, 2012)

A system that utilizes a combination of renewable energy sources, is the design of the ship Orcelle, from the Scandinavian company Wallinson Wilhelmson (Donker et al., 2010). The ship uses waves like the Suntory Mermaid, described above. Because this movement is similar to that of the movement of a dolphin, the ship is named Orcelle. The Orcelle is a cargo ship with

a length of 250 meters and a top speed of 27 knots. The planned dates for building this ship are around 2025 (Cummins, 2012). Figure 2.12 shows the concept of the Orcelle.

2.4 Conclusion

It can be concluded that the only feasible way to transport the polymetallic nodules over sea, is by ship.
Also a lot of systems utilize a combination of renewable energy sources for ship propulsion. Many studies and concepts show that applying these systems will decrease the amount of fuel and therefore emissions (van der Kolk, 2020), WASP as well as the use of wave or solar energy. Almost all these systems are still in concept phase and the range of reduction is very wide. Therefore research needs to be done to get more certainty around these different sustainable alternatives. As a lot of these systems are still at a very early stage of development, these will not be discussed further in this report. This is because, as said before, the execution of this project depends on Allseas's deep-sea mining project which is planned to start in about 5 years.

A multi criteria analysis was used in an early stage of the research, to compare the different technologies and search for similarities, differences and opportunities to choose which technologies are examined further, can be found in appendix A (propulsion performance is calculated by dividing the lift over the drag coefficients of the WASP systems, addressed further in chapter 6).
There are two types of WASP systems. Type 1 uses the wind force and direction with a direct thrust, this applies to all mentioned WASP systems minus the wind turbine. Type 2 is when the wind is used indirectly when it is connected to the drive train of the main engine; this applies for the wind turbine.
In this report it is assumed that the alternative fuels are from renewable energy sources to have zero carbon emissions.
A summary of the TRLs of the most promising and feasible options for this project are given in figure 2.13.

Alternative fuel or technologies	TRL
Alternative fuels	
Biofuels	4/5
Ammonia	3/4
Hydrogen	6 (storage systems: 5)
Alternative technologies	
Batteries/electrical	5/8
Alternative energy generation	
Wind	
Soft sails	
Kites	5
Dyna rig	6
Wing sails	
Wing sail	8
Active sail	
Turbo sails	6
Flettner rotor	9
Other	
Wind turbine	8
Solar	
Solar panels	6
Solar in sails	4

Figure 2.13: Summary TRLs of current technologies

For this project thesis, the route and the cargo are known. With this information the selected different technologies can be compared to conclude which of them or a combination, fits best with the transport requirements set in chapter 3.
The goal of this project is to look at the various options by using renewable energy sources that can be applied for this transport over sea in five years and to analyse which option would be the fastest, cheapest and most sustainable. The various options will be compared with a base case to examine their performances concerning emission reduction and costs. From this chapter can be concluded that adapting a new vessel to a new energy source, the total new propulsion system could function more efficient. However, it is expected that every new type of energy source, will fit best when combined with a newly built vessel, in terms of efficiency. Besides this, using an existing ship is more sustainable as its materials are re-used which is expected to be less expensive than newly built. Therefore, retrofitting is chosen to implement the new energy sources on the base case. It needs to be noted that the new systems must fit with the base case to be feasible. For example, the space on the deck, the size of the engine room and capacity of the fuel tanks are important for this.

As this project is commissioned by Allseas, to formulate an advice, not only the performances of the examined systems are important, also the the costs of each propulsion system. Thus, this research does examine the systems from two sides, from a sustainable point of view and from a business point of view. This is as well the gap found in the literature examined. None of the previous research examined has listed all the renewable energy source options for ships and examined them from both sides with each other and the base case.
In this report, from this comparison, an advice for Allseas can be formed. Therefore, the new research question is as follows:

> *"Which currently existing energy source(s) can be used to transport the polymetallic nodules from the Clarion-Clipperton Fracture zone to the coast of Mexico, a 2200 km route, and whose operational use is technically feasible in five years, in the most sustainable way and with the lowest costs"*

3 | Transport description

This chapter gives a description of the transport itself. In other words, this chapter gives the fixed and determined data needed for modelling a solution to transport the polymetallic nodules from the CCZ to the coast of Mexico. This delineation includes requirements for this shipment, a base case and a route analysis. Transport Requirements examine what is already known and certain about this transport. Some of these data have not been fully established yet, because the Deep-Sea mining project is still in concept phase. However, for this report, it is assumed that these data are fixed. This chapter also gives a base line, section 3.2, to which the new model(s) can be compared with and the route is analyzed in section 3.3. Lastly, a tool to compare the new installed propulsion systems with the base case, the key performance indicators (KPI) is explained in 3.4.

3.1 Transport Data and Requirements

In this section the transport data and requirements will be discussed. These requirements are necessary to have a more complete picture of the operation and to find out what the best fit will be, to transport the polymetallic nodules. First a functional flow diagram is shown to give an overview of the shipment of the polymetallic nodules. Secondly, the established data is presented. Last, all the requirements for this transport are explained with a requirements discovery tree. The requirements discovery tree is used to make sure nothing is overlooked.

3.1.1 Established data

The established data is all the data of the route, the mining vessel and the cargo that is certain. The route for the transportation of the polymetallic nodules has a distance of 1200 nm, which is 2200 km and is located between the Clarion Clipperton Zone (CCZ) and Mexico.

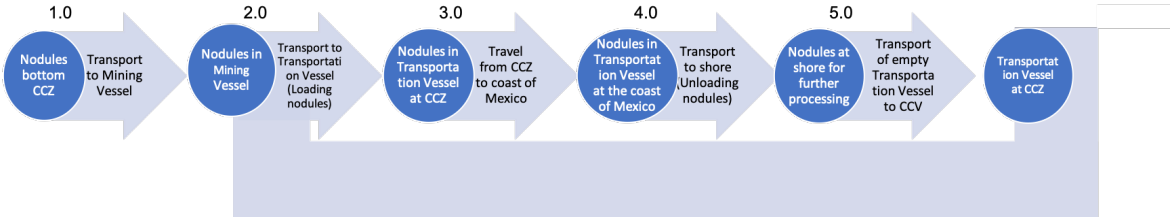

Figure 3.1: Flow Diagram of the Deep-Sea mining operation including the transport to shore

Figure 3.1 shows the Flow Diagram of transport of the Deep-Sea mining operation. First,

the polymetallic nodules are vertically transported from the bottom of the pacific to the mining vessel, secondly the nodules are placed from the mining vessel to a transport vessel, then the nodules are transported from the Clarion Clipperton Zone (CCZ) to the coast of Mexico where the transportation vessels are unloaded and lastly the empty transportation vessels return to the mining vessel to do the entire cycle again.

A summary of the established data is shown in table 3.1[1]. With the first part, 333tonne of nodules are vertically transported per hour. The mining vessel, named the Hidden Gem, has a buffer of 20,000 to 25,000 tonne, which takes about 60 hours to fill. The transfer of the nodules from the Hidden Gem to the transport vessel can be done in different ways. To transport the nodules, they can be in dry state or in wet state (slurry). For this investigation, the assumption is made that the nodules will be transported in dry state as more nodules can be shipped. For this project the transfer is not taken into account. However, possibilities of the transfer of the nodules from the Hidden Gem to the transport vessel are examined and can be found in Appendix C.
In table 3.1 the total days at sea are 250 days. Because delays can occur, this number is not 365 days.

Table 3.1: Summary established data

Route	From CCZ to coast of Mexico
Route distance	1200 [nm] (2200 [km])
Annual collection of nodules	2 [million tonnes]
Collection nodules from CCZ by Hidden Gem (v_h)	333 [tonne/h]
Buffer Hidden Gem	20,000-25,000 [tonne]
Total days at sea	250 [days]
Maximum significant wave height at CCZ	3.5 [m] period of 20[s]
Average significant wave height at CCZ	2 [m] period of 14[s]
Current at CCZ	1 [kts]
Wind at CCZ	up to 30 [kts] (15.5 [m/s])

3.1.2 Transport requirements

In this subsection the transport requirements are given. These have been selected using a requirement discovery tree[2], given in appendix B.

The transport requirements needed for a sustainable transport of polymetallic nodules from the CCZ to the coast of Mexico are divided into six sub categories, the characteristics of the fleet, the route requirements, the environmental requirements, the economic requirements, the freight distribution and the social requirements.

Characteristics of the fleet

To define the characteristics of the fleet, the type of transport needs to be determined. From chapter 2 it is concluded that the most efficient way to transport the polymetallic nodules is by ship. According to (Cepowski & Kacprzak, 2019) several types of ships could be used to

[1] This data is conceptual and released by Allseas.

[2] This is a tool to organize and display the requirements in a hierarchical tree structure. In this report it is used to give an overview and to not forget aspects for this transport.

transport the polymetallic nodules: an adapted tanker that transports the nodules in a wet state in cargo tanks, an adapted bulk carrier that transports the nodules also in a wet state but in a hold equipped with a bilge-drainage system or a standard bulk carrier that transports the nodules in dry state. As said before, the nodules in dry state is assumed.

Besides this, the fuel type and the amount of emission of the fleet need to be established. The fleet should also be equipped to carry the polymetallic nodules. Polymetallic nodules have a density of 2 to 3 tonne/m^3 and cargoes with a density of more than 1.78 tonne/m^3 are defined as heavy cargo. Therefore, polymetallic nodules in any state of run-of-mine (ROM) need to be treated by regulations as heavy cargo (Abramowski & Cepowski, 2013). ROM nodules are the nodules directly from the mine, so in this case, from the bottom of the CCZ. The transport vessel must also be compatible with the Hidden Gem, mainly depending on the type of transfer of the nodules.

Another sub requirement of the characteristics of the fleet is the constant flow to transport the polymetallic nodules. A constant flow of carriers is needed, because the mining vessel collects 333 tonnes of nodules per hour and does not take a break when harvesting starts. This is between two to three million tonnes of ore per year and the Hidden Gem has a buffer of maximum 25,000dwt. It should be determined how many transport vessels are necessary for a constant flow and what size these vessel have. In other words, what is the frequency of transport cycle, the travel time and the number of transfers.

So, the requirements of characteristic of the fleet are as follows: the fleet must consist of heavy cargo vessels (this is established in IMO regulations), it must always have a ship alongside the Hidden Gem for a continues flow of nodules transportation and it must be able to sail 2200km. The characteristics of the fleet, without adjustments for a sustainable assisted technology will be determined in 3.2, the base case.

Route

The route that needs to be travelled is from the east part of the Clarion Clipperton Zone to the coast of Mexico. An analysis of the route needs to be performed to understand what the fleet has to endure. For this analysis weather data of this route needs to be collected, such as the wind, waves, current and storms. An overview of this analyse will be given in 3.3. Requirements set for this route is that the average magnitudes of the current, waves and wind must not exceed the safety requirements set by the IMO for heavy cargo vessels.

Environmental

The amount of noise, GHG emissions and harmful emissions, such as SOx and NOx are subject to the environmental requirements. The amount of noise must comply with the regulations drawn up by the IMO. The emissions from transport are needed to compare different sustainable technologies, which assist the transport vessel, with the base case and with each other. An assumption for this report is that the upstream emissions will be neglected. Besides this, the different sustainable technologies applied need to be compliant with environmental regulations of the IMO, for this report this is assumed. Also, the availability, production and economy of alternative fuels is assumed.
For the comparison between the base case and the base case with sustainable assisted technologies, a requirement is that there should be some reduction of emissions.

Economic

The economic requirements consist of the energy consumption and the cost of the transport. The energy consumption means the type of energy used for this transport. Two cases are considered, a base case and a sustainable case. With the energy intensity is meant how much energy an energy source can deliver.

The cost of the transport are surcharges of international waters, the costs for the fuel consumption, the harbour costs and the costs of the crew. Costs that are not mentioned in the discovery tree, but are also included, are the operating costs, the Stopford CAPEX (Stopford, 2009), the maintenance costs and the capital costs. CAPEX is capital expenditure, which are costs the company incurs to benefit in the future, such as engines, storage and processing costs. The costs of the base case are determined in section 3.2 and the different concepts are determined in chapter 6.

Freight distribution

The freight distribution consists of the supply and the demand of the polymetallic nodules. It is the system and process by which goods are collected, transported and distributed within the environment.

The supply depends on the control of the loading area in the CCZ, or in other words, how much polymetallic nodules are collected per hour. As said before, the speed of harvesting the nodules from the bottom of the CCZ is 333 tonne nodules per hour. The demand is the global demand for polymetallic nodules. This depends on the market and is hard to predict. The demand also depends on how much the processing site at the shore can handle. For this report the demand of the nodules is not taken into account.

Social

The last transport requirement is regarding safety; a social aspect with legal and ethical requirements. The base case, as well as the sustainable concept will both have to comply with the regulations drawn up by the IMO. When meeting these regulations, it is assumed that the social requirements will be met, therefore the social aspects are not further investigated in this thesis.

3.2 The Base Case

In this section the base case is given. This base case is needed as a comparison for vessels equipped with different renewable energy assisted ship propulsion, so this base case will be used as a reference model. The reference ship needs to meet the requirements necessary to transport the polymetallic nodules set in section 3.1. Section 3.2 describes first the fleet characteristics. The fleet characteristics includes data such as how many ships are needed for a constant flow of transport and the matching sizes of the vessel. The required amount of energy and the total costs per fleet is analysed to find an optimum for this specific transport. Section 3.2.2 gives the main particulars of the chosen reference ship and the amount of emissions corresponding to this reference ship.

3.2.1 Fleet characteristics

To define the characteristics of the entire fleet, it is necessary to know how many ships are needed and their size. It is assumed that the transport vessels of the same fleet should all have the same

size. This to simplify the calculation and to simplify prospective modification for sustainable assisting technologies. Another assumption made is that the transport vessels can be fully loaded to their maximum capacity.

Besides the number of ships and their sizes, the energy consumption and costs are analysed to conclude the optimum for this base case. Data that needs to be kept in mind is given in table 3.1.

Duration round trip, fleet size and frequency

In this subsection, the duration of a round trip, the fleet size and the number of full cycles made annually per ship size are given. This is necessary to establish the optimum fleet for this transport and to determine the total energy consumption and the costs of this fleet. Table 3.2 shows this information per ship size.
Ship sizes are given in deadweight tonnage (dwt). Deadweight is the weight a ship can carry. The sizes of the vessels are grouped in size categories. Ships with a deadweight between 10,000 and 35,000 are called Handysize, between 35,000 and 60,000 are called Handymax, between 60,000 and 85,000 are called Panamax and between 85,000 and 180,000 Capasize. It is assumed when the nodules are transferred in dry conditions, they are transported with a bulk carrier and when transferred in wet conditions, they are transported with a tanker.
The average speed of the vessels is given in knots. As shown in table 3.2, this is almost the same for each ship size. This is the reason why the travel return time is also almost the same per ship size. The time to load the transport vessel depends on the collection nodules from CCZ by the mining vessel, the Hidden Gem. Thus the harvesting speed is the limiting factor for the transfer.

Table 3.2: Duration of a round trip, the fleet size and the number of full cycles made annually per ship size

Dry bulk carrier					
Name	DWT	knts	Travel time return (with sea-margin of 15%) [days]	# full cycles annualy	# vessels needed
Handysize	10,000	13.5	8.5	200	8
	20,000	14.0	8.2	100	5
	30,000	14.5	7.9	67	4
Handymax	35,000	14.5	7.9	57	3
	40,000	14.5	7.9	50	3
	45,000	14.5	7.9	44	3
	50,000	14.5	7.9	40	3
	55,000	14.5	7.9	36	3
Panamax	60,000	14.5	7.9	33	3
	63,000	14.5	7.9	32	3
	70,000	14.5	7.9	29	3
	75,000	14.5	7.9	27	2
	82,000	14.5	7.9	24	2
Capezise	85,000	14.5	7.9	24	2
	105,000	14.5	7.9	19	2
	125,000	14.5	7.9	16	2
	150,000	14.5	7.9	13	2
	175,000	14.5	7.9	11	2

The loading time of the transport vessel in days or the harvesting time (t_h) is calculated using equation 3.1. The dwt of the transport vessel (DWT_{tv}) is divided by the harvesting speed and

divided by 24, the number of hours in day. v_h is the harvesting speed.

$$t_h = \frac{\frac{DWT_{tv}}{v_h}}{24} \tag{3.1}$$

Equation 3.2 shows the calculation of the number of vessels needed. In this equation the 250 days at sea (t_s) are divided by the 2 mtonne annual collected polymetallic nodules (PN_a). This is multiplied by the travel return time, divided by the deadweight of the transport vessel and rounded up. 'Ceil' in this formula means rounded up. The travel return time (t_t) is given in table 3.2, which is the duration of one round trip in days.

$$\#vessels = ceil\left(\frac{t_t \cdot \frac{t_s}{PN_a}}{DWT_{tv}}\right) \tag{3.2}$$

How many cycles annually must be made, is calculated with equation 3.3. Here the 2 mtonne of nodules is divided by the deadweight of the transport vessel.

$$\#cycles = \frac{PN_a}{DWT_{tv}} \tag{3.3}$$

Energy consumption

The total energy consumption per fleet is given in this subsection. The higher the energy consumption, the higher the fuel consumption and the more emissions. For the fleet it is most optimal in terms of sustainability to have low energy and fuel consumption. HFO is the fuel assumed to determine the base case, as this is the most common and mostly used fuel in the maritime sector. The annual energy consumption per 1000 collected nodules is shown in table 3.3.

Table 3.3: Annual energy consumption per ship size

Dry bulk carrier					
Name	DWT	SMCR [kW]	Energy consumption per return [MWh]	Total annual energy consumption [MWh]	Energy consumption per annual collected nodules [MWh/ 1000 t nodules]
Handysize	10,000	2550	521	104267	52
	20,000	3940	777	77674	39
	30,000	5090	969	64590	32
Handymax	35,000	5760	1096	62651	31
	40,000	6150	1171	58531	29
	45,000	6400	1218	54143	27
	50,000	7225	1375	55006	28
	55,000	8049	1532	55712	28
Panamax	60,000	8450	1608	53614	27
	63,000	8670	1650	52390	26
	70,000	9080	1728	49381	25
	75,000	9280	1766	47104	24
	82,000	9500	1808	44104	22
Capezise	85,000	9700	1846	43443	22
	105,000	11180	2128	40534	20
	125,000	13050	2484	39744	20
	150,000	14450	2750	36673	18
	175,000	16250	3093	35350	18

SMCR is the Specified Maximum Continuous Rating. This is the maximum power output the engine of a vessel can produce, while running continuously at safe limits and conditions. The total energy consumption is the energy consumption needed for the return multiplied by the total amount of cycles made in one year. The SMCR is calculated with the assumption that for this transport the vessel is sailing in a straight line from the CCZ to Mexico and back. However, keep in mind that the vessel is not always sailing at maximum power.
The annual energy consumption for the return (E_t) is calculated using equation 3.4.

$$E_t = \frac{SMCR \cdot t_t \cdot \#cycles \cdot 24}{1000} \tag{3.4}$$

Figure 3.2 shows the energy consumption per 1000 collected nodules per ship size. As the energy consumption depends mostly on the total number of cycles made annually, the energy consumption decreases for larger ship sizes. From a deadweight of 80,000 and higher the energy consumption differs not that much anymore.

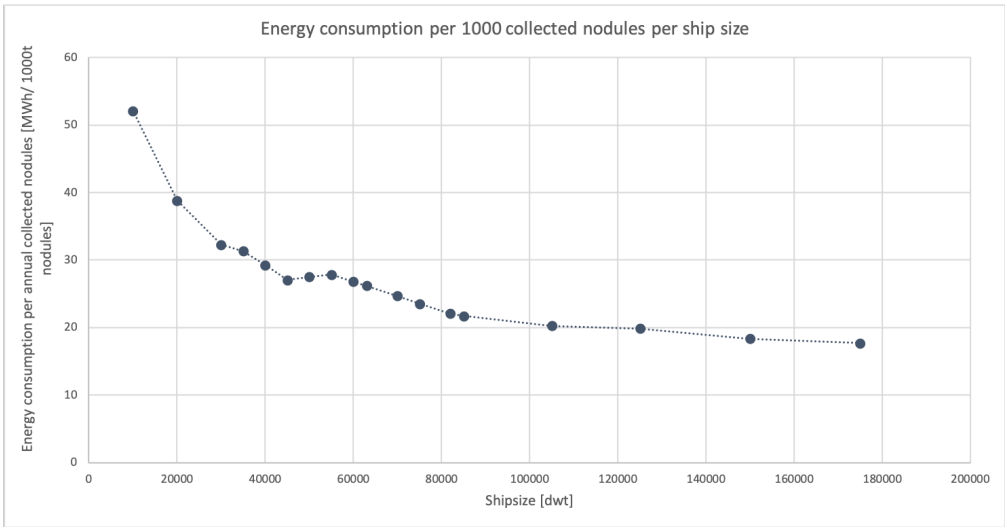

Figure 3.2: Annual energy consumption per ship size

Costs

From the customer point of view, the base case is optimal when the costs are lowest. In this section the total costs per fleet size is calculated and presented. The data, percentages and formulas are from (Stopford, 2009).

The total costs for each fleet consist of the total costs of one ship multiplied by the amount of vessels needed plus the annual costs for fuel consumption. Table 3.5 gives the data used for calculating these costs. The inflation correction is 1.24. Öko-Institut e.V., a German Institute for applied ecology has stated that for a Panamax bulk carrier the fuel costs (HFO) are estimated at $450/tonne (Healy & Graichen, 2019), also the fuel bunker price at the moment is around 450$ per tonne consumption fuel (Ship & Bunker, 2021).

Table 3.4: Operation costs

Included	
Manning costs	42%
Stores and lubricants	14%
Repairs and maintenance	16%
Insurance	12%
General costs	16%
Excluded	
Cargo handling cost	
Port cost	

Table 3.5: Used data costs

Inflation correction (IC)	1.24
Fuel price (HFO)	450 [$/t]

The total costs of one ship include the operating costs, which are shown in table 3.4, the periodic maintenance per year. This is 2% of the stopford CAPEX. The stopford CAPEX are funds used by Allseas to acquire, upgrade, and maintain physical assets. Besides this, the total costs of one ship also includes depreciation per year, which is 6% of the inflation correction and the yearly capital costs. The yearly capital costs is the interest or dividend and debt repayment, this is 20% of stopford CAPEX. The costs per fleet is given in table 3.6.

$$
\begin{aligned}
C_{total}[m\$] = \\
&(C_{operation} \\
&+ C_{maintenance}(2\%CAPEX) \\
&+ C_{depreciation}(6\%IC) \\
&+ C_{capital}(20\%CAPEX)) \cdot \#fleet \\
&+ C_{totfuel}
\end{aligned}
$$

Table 3.6: Total annual costs (Stopford, 2009)

Dry bulk carrier											
Name	DWT	Stopford CAPEX [m$]	With inflation correction [m$]	Operating cost* p.a. [m$]	Costs fuel consumption per year for entire fleet [m$/year]	Periodic maintenance per year [m$]	Depreciation per year [m$]	Yearly capital cost [m$]	# vessels needed	Total annual costs [m$]	Costs per ton nodules [$/tonne nodules]
Handysize	10,000	24	30	1.2	12.5	0.5	1.8	4.8	8	78.2	39.1
	20,000	26	32	1.2	6.4	0.5	1.9	5.2	5	50.6	25.3
	30,000	27	33	1.2	4.4	0.5	2.0	5.4	4	41.2	20.6
Handymax	35,000	28	35	1.3	4.1	0.6	2.1	5.6	3	32.6	16.3
	40,000	29	36	1.3	3.8	0.6	2.2	5.8	3	33.4	16.7
	45,000	30	37	1.4	3.6	0.6	2.2	6.0	3	34.1	17.1
	50,000	31	38	1.4	3.7	0.6	2.3	6.2	3	35.3	17.6
	55,000	32	40	1.5	3.8	0.6	2.4	6.4	3	36.5	18.3
Panamax	60,000	33	41	1.6	3.6	0.7	2.5	6.6	3	37.6	18.8
	63,000	34	42	1.7	3.6	0.7	2.5	6.8	3	38.5	19.3
	70,000	36	45	1.8	3.4	0.7	2.7	7.2	3	40.6	20.3
	75,000	38	47	1.9	3.2	0.8	2.8	7.6	2	29.3	14.7
	82,000	40	50	1.9	3.0	0.8	3.0	8.0	2	30.4	15.2
Capezise	85,000	41	51	1.9	3.0	0.8	3.1	8.2	2	31.0	15.5
	105,000	47	58	2.0	2.8	0.9	3.5	9.4	2	34.4	17.2
	125,000	52	64	2.0	2.8	1.0	3.9	10.4	2	37.4	18.7
	150,000	59	73	2.0	2.6	1.2	4.4	11.8	2	41.3	20.7
	175,000	65	81	2.0	2.5	1.3	4.8	13.0	2	44.8	22.4

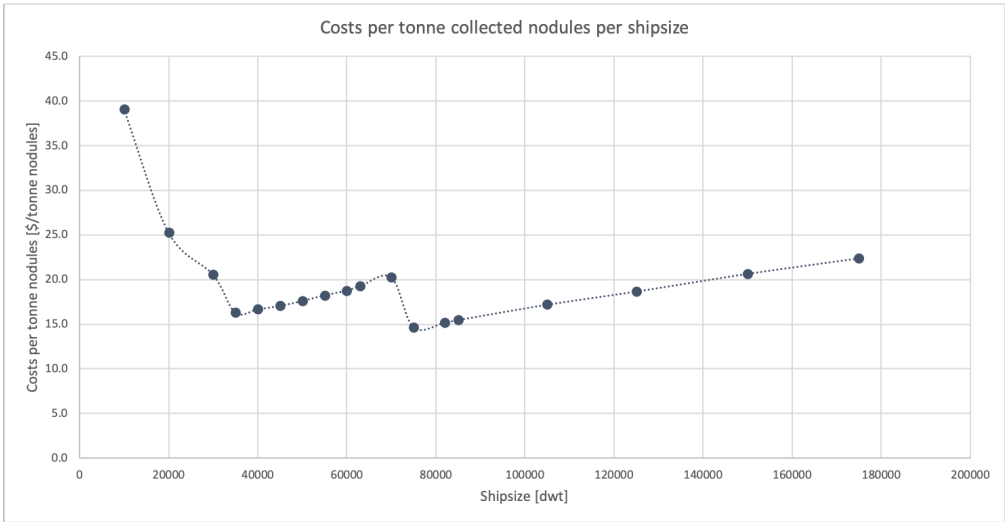

Figure 3.3: Annual costs per collected nodule per ship size

Figure 3.3 displays the costs per tonne collected nodules per ship size for each fleet. The staircase shape in this graph can be explained with steps in the number of vessels needed per fleet for each ship size. The optimum for the costs is for a ship size of 75000 dwt.

Conclusion

To conclude, the most efficient base case for this transport is a dry bulk carrier with a dead weight of 75000 dwt. As a buffer of 10% is profitable, a reference ship is chosen with a dead weight of approximately 82000 dwt to have this over-capacity. This ship size has the lowest costs and, as said before, of this ship size, the energy consumption doesn't decrease that much anymore. The fleet size will then be two ships.

3.2.2 Specifications Reference Ship

A reference ship that is close to the outcomes of the previous calculations is given in this subsection and is used as a base line to compared with for calculations further in this report. The reference ship is a Panamax bulk carrier, named Leda C and shown in figure 3.4. This ship is build in 2011 with 81,526 dwt and IMO 9583768. The specifications of this ship are provided in table 3.7. Panamax bulk carriers are suitable to transport coal, ore, phosphorites, salt and grain cargo and therefore this resulted in the conclusion that the ship is also suitable to transport dry polymetallic nodules.

Figure 3.4: Panamax Leda C (marinetraffic.com, 2011)

There are a few reasons why the Panamax Leda C was chosen as reference ship. According to Smulders (2017) this Panamax bulk carrier can serve as floating breakwater. Using this older Panamax ship also has an economic advantage as the limitation on the width of Panamax ships has to be changed by the completion of the Panama Canal expansion in 2016 (Smulders, 2017). Companies such as Dykstra Naval Architects (Dykstra-NA, 2013) and Blue WASP (van der Kolk, 2020) use Panamax ships for WASP and therefore these ships are suitable for this case study. A study (Vos, 2019) says that this ship has a great stability which enables the option to apply a large sail area, plus to enhance stability for loading at sea.

Table 3.7: Specifications Panamax bulk carrier, Leda C (marinetraffic.com, 2011) (Target Marina S.A., 2011)

Vessel name	**Leda C**
Length	229 [m]
Beam	32.24 [m]
Height	15.99 [m]
Average draft	11.2 [m]
Freeboard	4.59 [m]
Dead weight tonnage	81526 [tonne]
Gross tonnage	44600 [tonne]
Maximum speed	18.6 [knots]
Average speed	9.5 [knots]
Installed power	9470 [kW]
RPM	91
Propeller diameter	6.4 [m]
Rudder span	10 [m]
Rudder height	7 [m]

The energy consumption and costs of the reference fleet (2 vessels) is determined with the data of the Panamax Leda C and shown in table 3.8. 14.5 knots is held as the speed at which the calculations are made. The SMCR used in the previous calculation to determine the reference vessel, is not the average power of the Panamax Leda C. The Leda C consumes 26.8ton/day HFO

when sailing 14.5knts (Target Marina S.A., 2011).
When in the near future the renewable energy propulsion systems work better with a lower speed, the speed of the reference ship can be adjusted to this new speed and a new energy consumption and annual costs will be displayed. When the speed decreases below a certain level, a third vessel is needed to guarantee continuity of the transport of the nodules. Another solution could then be a larger reference ship; so for this reduction of ship speed, the maximum number of reference vessels must stay two, otherwise the total costs will be much higher. The impact of speed on energy and fuel consumption will become more clear as it will be explained in chapter 4.

Table 3.8: Energy consumption and costs of the reference fleet

Reference fleet	
Speed	14.5 [knots]
Annual fuel consumption fleet	6700 [tonne]
Annual energy consumption fleet	75,000 [MWh]
Annual costs fleet	30 [m$]
Day rate fleet	82200 [$/day]

Keep in mind that the chosen vessel is used for all energy generation systems. A different sized vessel could benefit one of these systems. The deliberate choice for only one vessel size was made to have a clearer comparison and not too many variables.

Fuel and emissions of the base case

The last part discussed in this section, to define the base case, are the emissions emitted by the reference ship. The emissions depend on the fuel consumption and the fuel type. The total annual fuel consumption for two bulk carriers with a deadweight of 81,526dwt is determined to be around 6700 tonne with a ship speed of 14.5 knts and the fuel type of the reference ship is HFO.
Table 3.9 shows the emission factors for an operation at sea for bulk carriers with dry cargo. With the given information, the bottom data of table 3.9 gives the total annual emissions that occur for the required two Panamax bulk carriers.

Table 3.9: Emission factors for "at sea" operation for bulk carrier with dry cargo (Entec, 2002)

	NO_x	SO_2	CO_2	HC
Bulk Carrier with Dry Cargo [kg/tonne fuel]	92	54	3179	3
Total annual emissions [tonne]	1150	675	39,338	38

The costs of the base case are calculated in section 3.2.1. For two bulk carriers of 82,000dwt these are rounded 30 million$ per year.

3.3 Route Analysis

This section explains the methods and data bases used to describe certain aspects of the environmental conditions between the Nori D area of the Clarion Clipperton Zone and Mexico, shown in figure 3.5. The Nori D area is on the east side of the Clarion Clipperton Zone. The parameters that were visualized are the significant wave height, current speed, wind speed and wind direction.

Figure 3.5: Route between CCZ and Mexico

3.3.1 Current

The database used to download the current speed is HYCOM. HYCOM is a coordinate ocean model that offers real time ocean prediction system outputs such as salinity, water surface elevation, water temperature and the Northern and Western component of the current speed.

The data was manually classified into months, for each month the minimum, maximum and average value is calculated for the 23 years of available data. Figure 3.6 shows a plot of the current in a year in knots of a point in the CCZ with coordinates: latitude 19 and longitude -126.

From figure 3.6 it can be concluded that the magnitude of the current speed is approximately 0.1 knots, which is about 0.05 m/s. The current speed is higher during springtime and is lower during autumn. Current can affect ships during their journey, a ship sailing against the current needs more fuel and sailing with the current will reduce fuel consumption to maintain the sailing speed. As the ship sails both ways the ship will both benefit from the current as see it as a disadvantage. To experience the current as little as possible, it would be advisable to sail during autumn. However, as the hurricane season is from June to November with peaks in September and October (Sea World, 2020), it would be more advisable to sail in December to May and accept the advantages and disadvantages of the current.

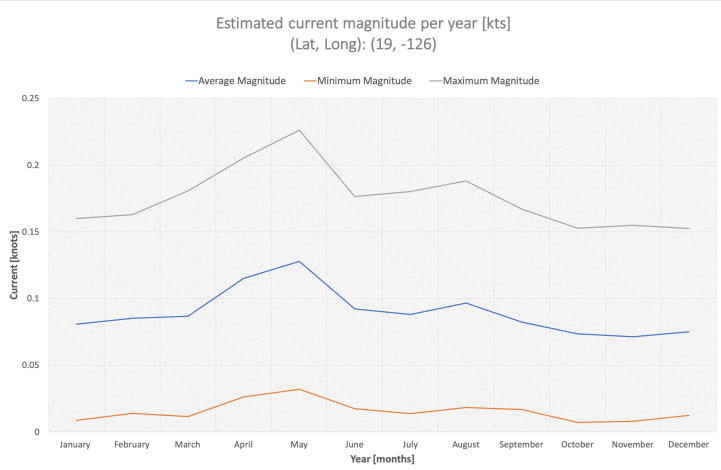

Figure 3.6: Estimated current magnitude in a year

3.3.2 Waves

The data for the significant wave height was downloaded from the Climate Data Store (CDS), a website that offers information about Earth's climate. The parameters downloaded consist of the significant wave height of the first, second and third swell partition for 1993 to 2015 and can be seen in the figure bellow again of a point in the CCZ with latitude 19 and longitude -126 as coordinates.

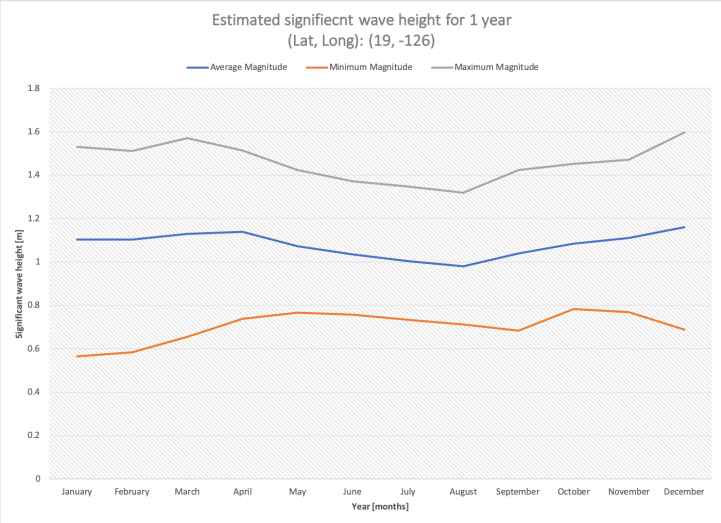

Figure 3.7: Significant wave height in a year

As can be seen in the figure, the significant wave height does not change that much during the year. An explanation of this could be that the average is taken along the years and high peaks are filtered out. This data is mostly important when is looked into assisted ship propulsion by waves. Later in this report this will be discussed further.

3.3.3 Wind

For the wind data, Era interim (1989-2019) and the Blueroute application of Marin are used. With this application the shortest route can be estimated. The route is from the east of the CCZ to Mexico, so around: Latitude, Longitude (19, -126) to Latitude, Longitude (20.6, -105) as co-ordinates. Two wind statistics were calculated, one for the voyage from the extraction point to Mexico and one for the return voyage, with the wind angle relative to the ship's longitudinal axis, i.e. the direction where the ship is sailing to. To calculate this, the wind probability matrix relative to the north for this route is used, given in appendix D. Percentage of occurrence of True Wind Angles and True Wind Speed for both voyages are shown in figure 3.8 and figure 3.9. In these figures the different colors are different magnitudes of wind speed at a height of 10m.

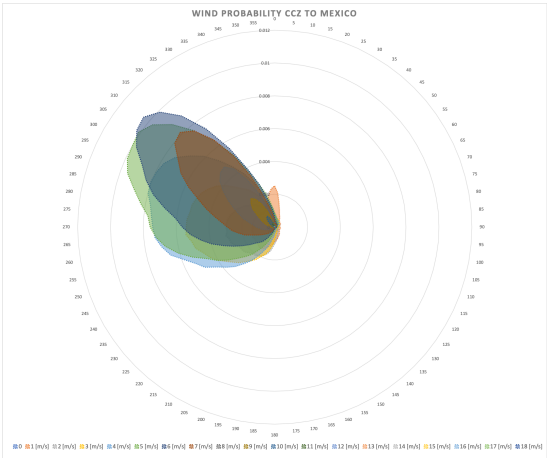

Figure 3.8: Percentage of occurrence of True Wind Angles and True Wind Speed relative CCZ to Mexico

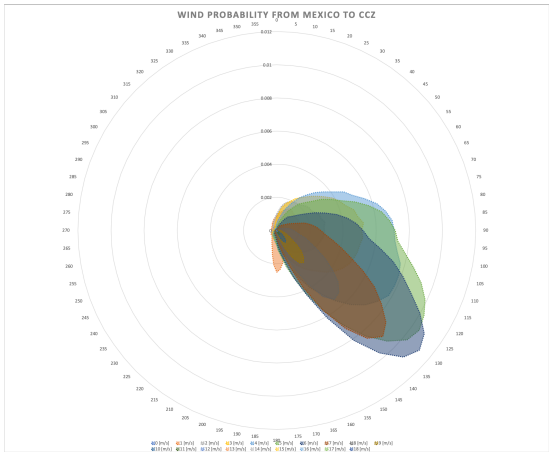

Figure 3.9: Percentage of occurrence of True Wind Angles and True Wind Speed relative CCZ to Mexico

As can be seen in the figures above, for the voyage from the CCZ to Mexico, the wind will come mostly from North-West, seen from the ship and for the voyage from Mexico to the CCZ this is the other way around, the wind will come mostly from South-East, seen from the ship. This wind data is necessary to estimate the which WASP system fits best for this route and is used in the next chapter.

3.4 Key performance indicators

Key performance indicators (KPIs) are used to evaluate the success of a result. It is a tool that measures a type of performance. As there will be multiple systems potentially useful, KPIs will be used to compare these systems with each other.

The goal of this report is to find out which of the propulsion systems, discussed in the next chapters, can transport the polymetallic nodules in the most sustainable way that is economically and technically feasible. In section 3.1 it is assumed that the systems used for propulsion are feasible. To compare the sustainability of the different systems with the base case, the emission reduction is expressed in percentage per tonne collected nodule, relative to the base case. This percentage is the total emission reduction of the new installed systems, compared with the total

annual emission of the reference ship, the Panamax Leda C, stated in section 3.2.
The KPI to examine the economic feasibility is total costs of each propulsion system expressed in costs per tonne collected nodules. The total costs are the costs are the total expenses over 30 years of this specific propulsion system. The total costs are divided by the total collected nodules in those 30 years.
The two KPIs are as follows :

- Emission reduction per tonne collected nodules [%/tonne]
- Costs per tonne collected nodules [$/tonne]

These KPIs will be used in chapter 8 to examine the different propulsion systems and to analyse and compare them with each other and the base case.

In this chapter, a baseline has been explained. Requirements for this transport, a reference vessel, the conditions for the route and the two assessment keys have been formed. The information from this chapter is used for all further calculations in this research. In addition, the base case is used as comparison material for the sustainable solutions. In the next chapter, the sources of these sustainable propulsion systems will be discussed.

4 | New propulsion source

In this chapter, the information given in chapters 2 and 3 come together. The route and transport are known, the systems to make the transport more sustainable are sorted out and in this chapter the sources of these (new) propulsion systems are examined.
For alternative fuel as a new energy source, new tanks and piping systems need to be installed. The data such as size and weight of the new tanks are given, so that a comparison with the current tank can be made.

For assisting propulsion using WASP systems or solar systems, their physical placement on board must be decided and their size can be determined. The performances of the WASP systems on board of the Leda C for this specific transport are analysed, using the wind data from section 3.3.

4.1 Propulsion source: base case

As already mentioned in chapter 3.2, the fuel for propulsion the reference vessel is heavy fuel oil (HFO). The fuel is stored in tanks. The sizes of these tanks depend on the energy consumption and on the efficiency of the drive train of the base case. In this section the sizes of the current installed fuel tanks are given and information about HFO is provided to have a clear point of comparison. The drive train of the base case and its total efficiency will be discussed in chapter 5.

HFO is stored in a type A tanks, close to the engine room. Type A tanks adapt to the hull and shape of the ship. To ensure fuel feed to the main engine, the temperature of these tanks is maintained at an even temperature between +75°C and +90°C. 4000 m^3 is the total fuel tank capacity for the Panamax Leda C (Target Marina S.A., 2011). Table 4.1 shows the specifications of the tanks of the Panamax Leda C.

Table 4.1: Specifications HFO tank reference ship (Target Marina S.A., 2011)

Tank type	Type A
Temperature	75-90 [°C]
MARVS	0 [Mpa]
Total capacity tanks	4000 [m^3]

4.2 Propulsion source: alternative fuels

Alternative fuels as new energy suppliers provide chemical energy which can be converted into ultimately mechanical energy that drives the propellers. A new tank and new piping system is necessary for some of these alternative fuels when comparing it with the tank and piping system of the base case. In this section the storage equipment is analysed for each of the alternative fuels.

Biofuel

The most promising biofuels for ships at the moment are renewable diesel fuels (biodiesel) and liquid biogas (LBG). Most popular biodiesels are hydro-treated vegetable oil (HVO), biomass-to-liquids (BTL) and fatty acid methyl esters (FAME) (DNV.GL, 2019). According to DNV.GL, HVO and SVO (straight vegetable oil) are best for replacing heavy fuel oil. And according to another study on biofuel options for shipping, HVO is currently the most compatible and ready for fuel production (Platform Duurzame Biobrandstoffen, 2018). Because of these reasons, HVO is chosen to continue with in this research as the advanced biofuel.
Comparing HVO with HFO, these fuels are quite similar. Therefore the tanks and the piping system can stay mostly the same (DNV.GL, 2019) (Neste Oil, 2018). The density and energy density of HVO and HFO differ somewhat, HVO has a density of 780 kg/m^3 and an energy density of 34.4 MJ/L and HFO has a density of 1010 kg/m^3 and an energy density of 35 MJ/L. This and the new sizes of the tanks with HVO are given in table 4.3. Keep in mind that the current tank capacity at 100% is 4000 m^3.

Hydrogen

Hydrogen (H2) is a non-toxic gas. For shipping, it can be stored as a cryogenic liquid, as compressed gas or chemically bound. When hydrogen is stored in liquid form, it has to be placed in a tank with installed temperatures of below 20 Kelvin (–253 °C) at 1 bar or at higher temperatures, 33 Kelvin (–240 °C), at the "critical pressure" of hydrogen, 13 bar (DNV.GL, 2019). As mentioned earlier in chapter 2, this form of hydrogen is chosen for this research.
Liquid hydrogen has a lot of characteristics that need to be taken into account when looking at new storage equipment, e.g. its boiling point is extremely low (–253 °C), its ignition energy is low, its combustion range is wide, its visibility of flames is low and hydrogen causes 'embrittlement' of metal. Because the temperature of liquefied hydrogen is extremely low, a high-performance heat insulation system is required (DNV.GL, 2019). For this system to be safe, large ancillary equipment, such as safety valves, need to be developed and installed (JSTRA & MLIT, 2020).
Because liquid hydrogen has a low energy density, a larger volume is required for the same amount of energy, with as a consequence that larger-capacity fuel tanks are needed. It is preferred to have a small fuel tank capacity as it does not affect the available cargo space too much.

A huge advantage of using hydrogen as a fuel, is that hydrogen lacks high amounts of impurities (depending on the source but assumed here are as being pure enough) that it can be used directly with no need for de-hydrogenation, refinement, or other processes. Thus, besides the tank and a high-performance heat insulation system, no other equipment is needed. It is assumed that all the specifications of the hydrogen storage tanks are compliant with the IGF Code of the IMO. The IGF Code is the International Code of Safety for Ships using Gases or Low-flashpoint Fuels (DNV.GL, 2016).

Another assumption made regarding the tanks to be installed in the Panamax Leda C would be that these are Type C cylindrical tanks made of stainless steel, see figure 4.1. The size of type

C tanks ranges from 1,000 m^3 to 20,000 m^3 (DNV.GL, 2016). So, the number of tanks and its size can be adjusted to the available place on board of the Panamax Leda C.
When the maximum allowable relief valve setting of a cargo tank (MARVS) of the Type C tank is set at 0.2 Mpa, the IGF code states that the pressure shall maintain below the set pressure for a period of 15 days (DNV.GL, 2019). The specifications of the hydrogen tank is given in table 4.2.

Table 4.2: Specifications hydrogen tank (DNV.GL, 2019)

Tank type	Type C
Temperature	-253 [°C]
MARVS	0.2 [Mpa]

The fuel tank capacity required for each ship was considered based on the distance and the fuel consumption rate, both given in section 3.2. The capacity of the base case is 4000 m^3. The properties of the hydrogen and its fuel tank size compared with HFO is given in table 4.3. As shown in this table, the hydrogen tank capacity is more than four times the capacity of the HFO tank. This could be a problem as the cargo space need to be increased to make place for the hydrogen tanks. To calculate the necessary capacity of the tank, the efficiency of the total drive train of the propulsion system using hydrogen is needed, this is given in section 6.6.

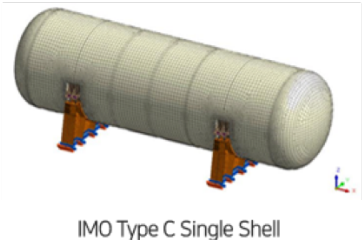

Figure 4.1: IMO type C tanks with single shell (left) and with double shell (right) (DSEC, 2016)

Ammonia

Comparing ammonia with other alternative fuels, it can be said that ammonia is a fire-retardant fuel. However, ammonia is very toxic, can damage the respiratory tract and the lungs in a short time and has an extremely strong, irritating smell (MAN Diesel A/S, 2020). Because of these fuel properties, the piping and the type C tank must be double layered, as a buffer for a leak. The single shell C tank is shown in figure 4.1, so for ammonia the same type tank is needed but with two layers.

Another property of ammonia is that it is corrosive to copper and plastics with a nickel concentration higher than 6%. Teflon can be used as sealing material and needs to be placed on all the piping (JSTRA & MLIT, 2020).

The lower energy content of ammonia is 18.6 MJ/kg, which is around 46% of that of HFO (40.5 MJ/kg). Ammonia requires a tank capacity about 2.7 times greater than that of the existing HFO tank, given in table 4.3. Besides this, the ammonia fuel tank must be a self-contained tank with heat-insulating construction. Therefore, the capacity must be two to three times greater than the existing HFO tanks, which may influence the cargo hold area. A cylindrical horizontal IMO Type C tank was chosen for this concept design.

The storage requirements of ammonia are quite similar to the fuel tank requirements of LPG-fueled ships, so LPG storage tanks can be used for ammonia-powered ships (JSTRA & MLIT, 2020).
The use of ammonia as the main fuel can lead to a reduction in the total cargo capacity when all the ammonia tanks are placed below deck. However, it is believed that there is sufficient space on the deck of the Panamax Leda C and as a result, like the hydrogen tanks, the ammonia tanks could be placed on deck. Because ammonia changes into a gas under atmospheric pressure, it can spread widely in a short time in the event of a leak. In such a case, there are likely to be health risks for people on and near the ships. For safety, therefore, additional measures are required to prevent leakage on deck and other measures, including venting the outside of the double pipe.

Table 4.3: Summary storage tanks for alternative fuels (MAN Diesel A/S, 2020) (JSTRA & MLIT, 2020) (DNV.GL, 2019)

Energy storage type	Fuel density	Energy content	Energy density	Fuel tank size relative to HFO
	[kg/m3]	[MJ/kg]	[MJ/L]	
HFO	1010	40.5	35	1
Biofuel (HVO)	780	44.1	34.4	1.1
Hydrogen (H2) (liquid, -253℃)	71	120	8.5	4.2
Ammonia (NH3) (liquid, -33℃)	682	18.6	12.7	2.7

4.3 Propulsion source: wind

Propulsion by means of wind can be done with different technologies. The most feasible and promising technologies at present were outlined in chapter 2. These wind assisting ship propulsion (WASP) systems are the kite, Dyna Rig, Wing sail, Turbo sail, Flettner rotor and Wind turbine. These systems can be divided in two types of WASP systems. The first type is when the wind force is used directly and the WASP system is not connected to the main drive train but the propulsion is supported by an aerodynamic thrust formed by the wind. The second type is when the WASP system generates power from wind and is connected to the drive train of the main engine.
In this section both type of WASP systems will be discussed. To understand how the power generation of these WASP systems is calculated, first hand calculations are made. For a more accurate calculation of the energy generation of the WASP systems, different models are used.
The size of the deck is 7383m^2; this is 1.1 the size of a football field. Assuming sufficient deck space and the WASP systems would not interfere with cargo hold openings and cargo handling, the dimensions, numbers and placement of the WASP systems have been determined. Research into the sizes, numbers and placement of the WASP systems for this ship size has already been worked out. For the kites this is done by Fagioni and Schmehl (Faggiani & Schmehl, 2018a), for the WASP systems, Dyna Rig, Wing sail, Flettner Rotor and Turbo sail by van der Kolk (van der Kolk, Bordogna, Mason, Desprairies, & Vrijdag, 2019) and for the wind turbines by Bøckmann (Eirik Bøckmann, 2011). The sizes and numbers of the WASP systems are given in table 4.4.
The aerodynamic thrust does not only depend on the area of the wind propulsion system, but also on its aerodynamic characteristics (lift and drag coefficients), which are dependent on the shape of the device and on whether it is an active device (Flettner rotor) or a passive device

(wingsail)[1]. The lift and drag coefficients of each of these WASP systems are known and given in table 4.4. For the wind turbine the power coefficient (C_P) 16/27 is taken, also known as the Betz limit (Eirik Bøckmann, 2011).

Table 4.4: Sizes, numbers, lift and drag coefficients WASP systems (Faggiani & Schmehl, 2018a), (van der Kolk et al., 2019), (Eirik Bøckmann, 2011)

	Kites	**Dyna rig**	**Wing sail**	**Turbosail**	**Flettner rotor**	**Wind turbine**
Number(#) [-]	1	5	8	12	6	1
Area [m^2]	640[2]	-	-	-	-	-
Height[m]	-	34	36	20	30	20
Width/diameter [m]	-	14.6	9	3	5	38
C_L [-]	1.25	2	3	7.5	10	-
C_D [-]	0.3	1	1	2.2	3.3	-
C_P [-]	-	-	-	-	-	$\frac{16}{27}$

The structure of this section is as follows, first the manual calculations are made, then performance prediction models are explained that are used for more accurate calculations and finally a summary table is given of the power reduction compared to the base case in percentage.

4.3.1 Hand calculations

To understand how the WASP systems function, first hand calculations were executed.
The performances of the WASP system depend mostly on the aerodynamic forces on the WASP system. The aerodynamic forces are the wind forces working on the vessel and the WASP system. The relative wind force working on the WASP system consists of the force of the wind (true wind speed (TWS) with true wind angle (TWA)) and the force of the wind originated by the speed of the vessel (V_s).

These calculations can be divided in WASP type 1 (thrust force) and WASP type 2 (power generation).

WASP type 1

WASP systems of type 1 depend on both wind direction and wind speed. For WASP type 1, the force of the wind and the force of the wind originated by the speed of the vessel result in a drag and a lift force, F_D and F_L, which will induce a thrust force. The drag force is parallel to the relative wind flow (the apparent wind speed (AWS) with apparent wind angle (AWA)) and the lift force is perpendicular to the apparent wind speed. This is shown in figure 4.2.

[1]Information from Giovanni Bordogna, expert on WASP systems and co-founder of the company BlueWASP

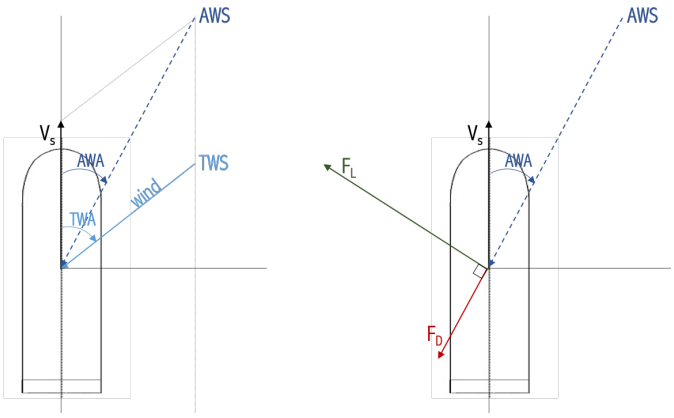

Figure 4.2: Aerodynamic forces acting on Panamax Leda C

The lift and drag forces can be calculated as follows:

$$F_L = \frac{1}{2}\rho_a C_L A(AWS)^2 \tag{4.1}$$

$$F_D = \frac{1}{2}\rho_a C_D A(AWS)^2 \tag{4.2}$$

In these formulas ρ_a is the density of the air, A is the area of the WASP system, AWS is the resulting wind speed and C_D and C_L are the drag and lift coefficients of each WASP system. The resulting thrust force can be calculated using equation 4.3. In this equation n is the number of WASP systems installed (Daluar Hussain Sumon, 2017)(Traut et al., 2014).
Keep in mind, the AWS for kites also includes the kite's velocity vector tracing the circle pattern; for these manual calculations this is not taken into account.

$$F_{WASP} = n(F_L sin(AWA) - F_D cos(AWA)) \tag{4.3}$$

For the hand calculations, the mean true wind speed and mean true wind angle were taken from the wind probability matrix for the CCZ to Mexico and the return route. These wind probability matrix was shown in polar plots section 3.3 and are explained as well in appendix D. The average wind speed is about 9.5 knts (≈5 m/s) and from CCZ to Mexico the wind comes in from about 50°and from Mexico to CCZ from about 130°, with the wind angle relative the longitudinal axis of the ship.

The main engine of the vessel must deliver a certain power to propel the ship. This power depends on the total drag force of the vessel (D_s), the speed of the vessel (V_s) and the total propulsion efficiency (η_t). This total efficiency links the power at the main drive train with the mechanical power that propels the ship. It takes into account the friction of the bearings of the shaft, the propeller efficiency in the water and the hull shape (Pietro Faggiani, 2017). Without the WASP system, the power that the engine should deliver (P_m) would be:

$$P_m = \frac{0.5144 \cdot V_s}{\eta_T} \cdot D_s \tag{4.4}$$

In this formula 0.5144 is used to convert the ship speed (V_s) from knots to m/s.

The thrust force of the WASP system (F_T) can be subtracted directly from the drag force of the ship leading to a lower power to keep the same speed as:

$$P_{m,WASP} = \frac{0.5144 \cdot V_s}{\eta_T} \cdot (D_s - F_{WASP}) \tag{4.5}$$

One can also see the equivalent power that the WASP system is delivering as:

$$P_{WASP} = \frac{0.5144 \cdot V_s}{\eta_T} \cdot F_{WASP} \tag{4.6}$$

So, P_{WASP} is as well the power reduction at the engine. For these hand calculations it is assumed, the propulsion efficiency is constant and set to 0.7 if a value is not specified and verified (van der Kolk, Nico, 2020).

WASP type 2

Wind turbine belongs to WASP type 2, which only depends on the wind speed. The wind turbine can turn and does not generate thrust force, but generates power. For wind turbines, the power is calculated with equation 4.7(Daluar Hussain Sumon, 2017), here instead of a lift and drag coefficient, a power coefficient is taken into account, which is given in table 4.4.

$$P_{WT} = \frac{1}{2}\rho_a C_P A (AWS)^3 \tag{4.7}$$

For the hand calculations, the equivalent power delivered by the WASP system for three ship speeds 9 en 12 en 14 knts, is calculated.
The active sails need to be start up in order to rotate. According to Bordogna this is 115kW max, for these sizes. These tables are given in appendix E. Table 4.5, shows the percentages of these hand calculations for a ship speed of 12knts.

Table 4.5: Hand calculations of the fuel savings in percentages of total fuel consumption WASP type 1 system for a ship speed of 12 knts ($\approx 6.2 m/s$)

WASP systems	**Fuel reduction in %**
Kite	3 [%]
Dyna rig	10 [%]
Wing sail	18 [%]
Turbo sail	13 [%]
Flettner rotor	21 [%]
Wind turbine	4 [%]

If the ship's speed is not too high, the apparent wind will come in less straight from the front relative to the bow, it is generally easier to get more efficiency from the WASP system [3]. This can be seen from the outcomes in table 4.5.

[3]Information from Anton Kistjes, WASP expert and project manager at Marin

4.3.2 Performances WASP type 1

In reality, calculating the performances of the WASP systems is a bit harder as more variables need to be taken into account. For the more accurate calculations of the type 1 WASP systems, two different models are used. For the kites the kite model, (Faggiani & Schmehl, 2018a) and for the other WASP type 1 systems, (van der Kolk et al., 2019).

Kite model

For the kites a model is used programmed by Pietro Faggiani and Roland Schmehl (Faggiani & Schmehl, 2018a). This model takes the shortest route from A to B (or B to A). Depending on the angle between the sailing direction and the wind, the model takes the traction of a maneuvering kite (which has been already optimized before-hand).At the end it sums up all the contributions along the route and gives the amount of fuel that has been saved by using the traction of the kite. The traction of the kite is a more complex traction than with the other WASP systems because also the movements of the kite itself must be taken into account, these force vectors are shown ini figure 4.3 . In this model the tether length is fixed and the AWS includes the vectorial sum of the TWS, the velocities due to the ship motion and the velocities due to movements of the kite (Pietro Faggiani, 2017).

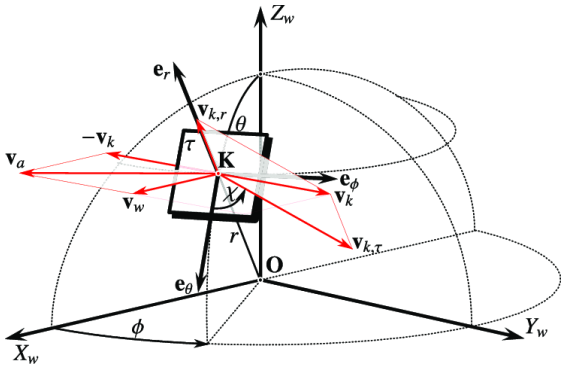

Figure 4.3: kite decomposition (Pietro Faggiani, 2017)

Delft WASP vessel model

The Delft WASP vessel model made by Giovanni Bordogna and Nico van der Kolk (van der Kolk et al., 2019) is used for the other WASP type 1 systems to predict how much power they generate. These WASP systems include, the dyna rig, wing sail, turbosail and flettner rotor. This model is a tool to predict these WASP performances, with the underlying principle, an equilibrium of forces working on the vessel with emphasis on interaction effects (van der Kolk, 2020), shown in figure 4.4

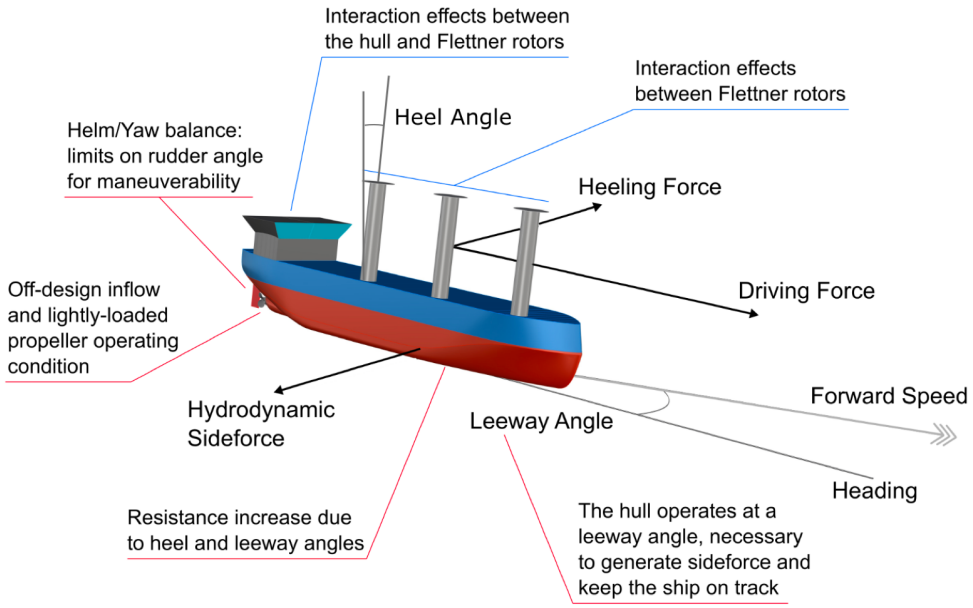

Figure 4.4: Key components of the Delft WASP vessel model, example with 3 Flettner rotors (van der Kolk et al., 2019)

The environmental forces, such as the wind, current and waves, are given and analysed in section 3.3. The aerodynamic forces include forces on the WASP system. The desired wind thrust force is generally accompanied by a transverse aerodynamic force, known as the heeling force, see figure 4.4. This undesired heeling force and associated moment need to be balanced by corresponding hydrodynamic reactions. These hydrodynamic forces are the forces on the hull and the propeller thrust (Boonstra, 2020). It is assumed that the rudder of the vessel adjusts perfectly to the heading angle of the vessel and can therefore be ignored. The Delft WASP vessel model finds the equilibrium between the aerodynamic and hydrodynamic forces and moments with the use of an optimisation routine (van der Kolk et al., 2019). The system is solved in four degrees of freedom: surge, sway, roll and yaw.
Data also neglected to simplify these calculations, are the scale effects (Bordogna, 2020).

$P_W ASP$ is the WASP contribution to the total propulsive requirement (Bordogna, 2020). The expression used for $P_W ASP$ in the Delft WASP vessel model, appears also in the EEDI formula set by the IMO (IMO, 2013) and is as follows:

$$f_{eff} \cdot P_{eff} = \frac{0.5144 \cdot V_s}{\eta_T} \sum_{i=1}^{m} F(V_s)_{i,j} \cdot W_{i,j} - \sum_{i=1}^{m} P_{activesail}(V_s)_{i,j} \cdot W_{i,j} \tag{4.8}$$

In this formula:

- $f_{eff} \cdot P_{eff}$ is the available effective power in kW delivered by the WASP system. The product of availability and power is a result of a matrix operation, this is why f_{eff} and P_{eff} are combined. The matrix operation addresses each wind condition with a probability and a specific wind propulsion system force.

- 0.5144 is used to convert the ship speed (V_s) from knots to m/s.
- η_T [4] is the total efficiency of the main propulsion system of the ship. This is set to 0.7 if a value is not specified and verified (van der Kolk, Nico, 2020).
- $F(V_s)_{i,j}$ is the force matrix of the WASP system
- $W_{i,j}$ wind probability matrix of this specific route. Both the polar diagram of this matrix of the route from the CCZ to Mexico and back are given in section 3.3.
- $P_{activesail}$ is a matrix with the same dimensions as $F(V_s)_{i,j}$ and $W_{i,j}$ and is the power demand in kW for active sails to turn them on. For non-active sails $P_{activesail}(V_s)_{i,j}$ is not included.

This formula is the same principle as equation 4.6. Three large differences; First, as more degrees of freedom, the thrust force $F_W ASP$ is in this formula a force matrix. Secondly, power is needed for the active sails to start to spin, this is integrated in the formula as the active sails to spin, $P_{activesail}$ as a function of the ship speed. Thirdly, to find out whether a certain type of wind propulsion is beneficial for the specific route, the formula is multiplied by the wind probability matrix. The polar plot of this wind probability matrix was given in section 3.3 and in appendix D.

The performance of the ship with wind propulsion is calculated in the form of a polar diagram. This diagram shows the engine's net fuel consumption for all wind directions (true wind angles)[5].

Knowing the fuel consumption of the reference vessel, the amount of fuel saved due to the WASP systems can be calculated by subtracting these two numbers from each other. The results of the performances for this model are presented in a polar plot, an example is given in figure 4.5 for 6 Flettner rotors for a ship speed of 9, 12 and 14 knots. The axes of the polar plot are from the vessels' point of view, with the bow of the vessel directly into the wind, so TWA is 0°. In the polar plot the fuel savings are shown which are the differences of fuel consumption between the vessel with the Flettner rotor case and the base case, which varies depending on the wind conditions.
The fuel savings in percentages are the average fuel savings of the whole route, from the CCZ to Mexico and back, which are compared with the same ship, sailing at the same speed but without wind assistance.

[4] An efficiency value for the main propulsion system (η_T) is prescribed by the IMO. This value is taken into account as within the EEDI, the WASP systems are seen as systems to reduce power, not to generate power, because they must be placed hybrid, combined with a main propulsion system

[5] Method explained by Alex Grasman, project manager at Marin

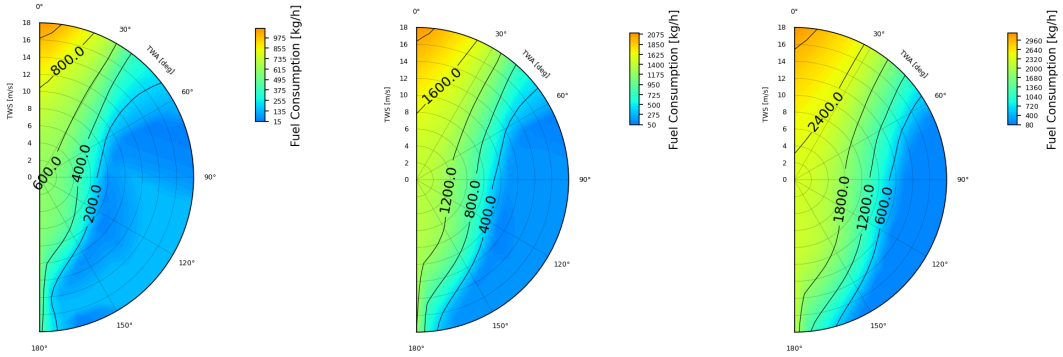

Figure 4.5: Polar plots of the fuel consumption Leda C with 6 Flettner rotors when, from left to right, the ship speed is 9, 12 and 14 knots using the Delft vessel WASP model (Bordogna, 2020)

For each of the WASP type 1 systems, the performances as a percentage of the fuel consumption as it would be without using the WASP system, are calculated for 9, 12 and 14 knts, given in appendix G.
Keep in mind that Flettner rotors and Turbo sails are sails that need to be started up by first putting energy into them. The rotors start to rotate (Flettner rotor), or air is extracted (Turbosail). This energy is added of their fuel consumption. For both sails a maximum of 115kW is worked with[6]. These sails are then able to generate considerable lift forces, while a common lift over drag ratio compared to conventional sails is guaranteed. The advantage of these sails is that they require little surface area to generate a lot of (propulsive) power. That is why this is pleasant for the field of view around the bulk carrier [7]. The results of the model are shown in figure 4.6 and also given in a table in appendix G.

4.3.3 Performances WASP type 2

For calculating the performances of WASP type 2, the wind turbine, a different model is used from (Eirik Bøckmann, 2011). Instead of using the EEDI formula, the aerodynamic thrust on the wind turbines is converted into power as the output of a wind turbine is power and not thrust. The net power of the wind turbine is the power generated by the wind turbine minus the power required to overcome the drag force of the ship at a certain ship speed (Eirik Bøckmann, 2011). Looking at stability issues, the increased heel angle due to the wind turbine in this model is negligible.
Comparing the wind turbine model with the hand calculations, for the wind turbine model the overall efficiency factor of the driving mechanism is added. This efficiency calculation is based on all components transmitting the power between the wind turbine and the propeller as well as the forward force of the propeller itself. According to (Talluri, Nalianda, Kyprianidis, Nikolaidis, & Pilidis, 2016), this efficiency (ηg) is 85%.

$$P_{WT} = \frac{1}{2}\eta g \rho_a C_P A (AWS)^3 \tag{4.9}$$

[6]Information received from Giovanni Bordogna, expert on WASP systems and co-founder of the company BlueWASP
[7]Information received from Alex Grasman, project manager at Marin

4.3.4 Results

Comparing the simplified calculations with the calculations done with the Delft WASP vessel model and with the kite model, the fuel reduction results differ. This is due to the fact that the model does not work with an average wind speed and direction, but takes into account the wind probability of all wind speeds and directions. Also, only x and y forces of the wind are included in the simplified calculation. In reality, there is a z-component as well. When the WASP system is used directly, this z-component can be neglected. However, when the WASP system is used to generate energy then this component should be taken into account. Especially when a kite is considered, when generating energy, the pulling force of the kite has influence on how much energy is generated.
Also, the resistance of the current, waves and hull need to be taken into account as well as these will affect the WASP systems. Because of this, the results shown in table 4.7 are used further in this report.

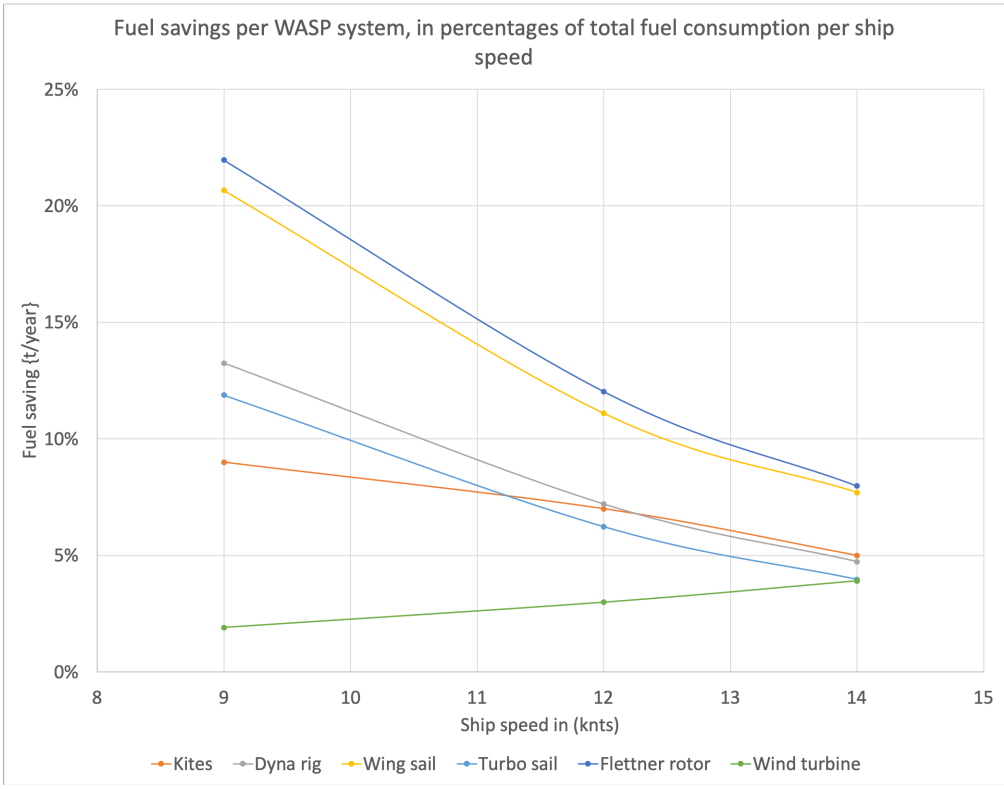

Figure 4.6: Performances WASP systems in terms of percentages fuel reduction

The ship speeds tested are 9, 12 and 14 knts, the results can be seen in figure 4.6, also given in a table in appendix G . The slower the vessel is sailing, the lower the fuel consumption and the higher the fuel savings will be. With a theoretical ship speed of 14knts, and with WASP systems and an installed power of 9470kW (see table 3.4 in section 3.2), it is not possible to reach that high speed. In this respect, a lower ship speed is more feasible and more optimal in terms of fuel reduction.

As already stated before, sailing is not possible with only the use of WASP systems. The

conclusion can be drawn from the research results that this is demonstrated and the propulsion systems with WASP need to be combined with the current engine to reach the speed of 12 knts.

Knowing the capacity of the vessel, which is 81526 dwt, the annual collection of nodules (2 million) and when sailing 250 days per year, the lowest ship speed can be calculated, to have a constant flow of transportation and a constant fleet size of two vessels. A graph of this fuel consumption vs ship speed can be found in appendix F(Healy & Graichen, 2019). In this appendix is looked at the costs as function of the ship speed of this reference speed. The resulting ship speed is 12 knts. Below this ship speed an extra vessel is necessary for the continuous flow of transport of the polymetallic nodules. The ship speed of 14.5 knts was assumed in chapter 3.2, however the ship speed of 12 knts is used further in this report. The data such as the fuel consumption and day rate fleet for this new ship speed, are shown in table 4.6 and are used in the rest of this research.

Table 4.6: Energy consumption and costs of the reference fleet

Reference fleet	
Speed	12 [knots]
Annual fuel consumption fleet	5000 [tonne]
Annual energy consumption fleet	56,000 [MWh]
Annual costs fleet	29.5 [m$]
Day rate fleet	80800 [$/day]

Looking at figure 4.6, the best outcomes are obtained using the Flettner rotor. It can be concluded that the aerodynamic thrust does not only depend on the area of the wind propulsion system, but also on its aerodynamic characteristics (lift and drag coefficients), which are dependent on the shape of the device. Besides this, the aerodynamic thrust depends on whether the WASP system is an active device (Flettner rotor and Turbosail) or a passive device (wingsail). The results are expressed in terms of % fuel savings compared with the same ship sailing at the same speed, but without wind assistance.

The fuel reduction of the wind turbines increases with a higher ship speed, this is because the wind turbine does not depend on the wind direction, only on the incoming wind speed. Of all the WASP systems, the lowest fuel reduction is reached by the wind turbine. For this wind velocity, a large turbine is necessary to create useful power and its size is limited on the vessel. Besides this, the wind turbine does not generate a direct thrust, but the power generated needs to be connected to the main engine, which will result in further loss of efficiency.
The kite has a certain optimum, its percentages of fuel reduction does not increase as much as that of the other WASP type 1 systems.
It can be concluded that the fuel savings with the WASP systems are not really high, the most probable reason for this is that it is not a very windy area. Table 4.7 shows the resulting fuel reduction in percentages when the ship speed is 12 knts, these percentages are used for the first KPI, which was explained in chapter 3.

Table 4.7: Fuel savings in percentages of total fuel consumption the WASP system for a ship speed of 12 knts ($\approx 6.2m/s$)

WASP systems	**Fuel reduction in %**
Kite	7 [%]
Dyna rig	7.2 [%]
Wing sail	11.1 [%]
Turbo sail	6.2 [%]
Flettner rotor	12 [%]
Wind turbine	3 [%]

4.4 Propulsion source: solar

The IMO (IMO MEPC.1/Circ. 815) describes a formula to calculate the auxiliary power reduction due to the PV power generation system with equation 4.10 (IMO, 2013) .

$$P_{AEeff} = I \cdot \mu \cdot A_{wd} \tag{4.10}$$

P_{AEeff} is the total net electric power (kW) generated by the PV power generation system. I is the the solar irradiance in W/m^2. This solar radiation intensity depends on the direct radiation perpendicular to the surface, defined by the weather data, the Albedo or reflection index and the different angles between the board and the solar rays (Julià, Tillig, & Ringsberg, 2020). For this calculation the average solar irradiance on main global shipping routes is taken, which is 200 W/m^2 (Mallouppas & Yfantis, 2021). This number of 200 W/m^2 is somewhat higher than when the surface of the entire globe, including land mass, is taken: 166 W/m^2 (Tamalm, 2004) .

μ is the total efficiency of the PV cells on board of the vessel. This total efficiency depends on the reference efficiency and temperature of the cell determined by the manufacturer, the temperature coefficient of the cell material, the temperature of the PV cell and an conversion efficiency, as the solar panels are connected to the main propulsion system (Julià et al., 2020). The total efficiency for solar panels on board of the vessel are between 16-18% (Mallouppas & Yfantis, 2021). Note that this model does not account for shadow losses.

A_{wd} is the whole deck area (7382m^2). It is assumed that the panels are placed on the entire deck area and do not interfere with the ship operations or other systems onboard. Solar can also be installed on wingsails, these have an area of 2592 m^2. With this formula the power generated with the PV cells installed on board or installed in the wingsails, is given in table 4.8. In this table the fuel savings are given as a percentage of the total fuel consumption. How much power is generated with the solar panels is given as a percentage of the installed power. This corresponds with the percentage of fuel reduction.
Only 3% of the total energy generated with HFO can be replaced with solar energy, so a reduction of 3% of the fuel consumption. A reason for this relatively low reduction is that half of the time the solar system cannot generate energy. Besides this, the ship required a lot of energy, Because of this a solar system of a large area is needed and the area is limited on the vessel.

Table 4.8: Fuel savings (percentages if total fuel consumption

Solar	**Fuel reduction in %**
Solar panels	3 [%]
Solar on wing sails	1 [%]

In addition to the source of a new system, to place a new propulsion system on a ship, a drive train must be installed. A drive train is the group of components of the ship that deliver power to the propellers. In the next chapter, these components are analysed.

5 | Drive train propulsion systems

Both alternative fuels and different renewable energy sources on board have already been analysed in chapter 5. To implement and install these new renewable energy systems, adjustments need to be made to the current propulsion system. In this chapter the drive trains of the different propulsion systems of the base case and sustainable alternatives will be analysed to understand how they work and what other systems are needed for them to operate. Besides this, the efficiency and the sizes of these components have to be taken into account to determine the fuel consumption and to analyse the placement and installation of the new propulsion system.

The drive trains of the propulsion systems are schematically given with blocks. These blocks are shown in figure 5.1. ES in the diamond-shaped blocks stands for 'energy source'. There are three types of energy sources: fuels, wind and solar. Fuels can be divided into biofuels, hydrogen and ammonia. The performances of these energy sources for this transport are already examined in chapter 4.

Within the blocks the energy conversions are given (ex. Ch $\rightarrow$ E) to give a more clear picture what happens in a certain system.

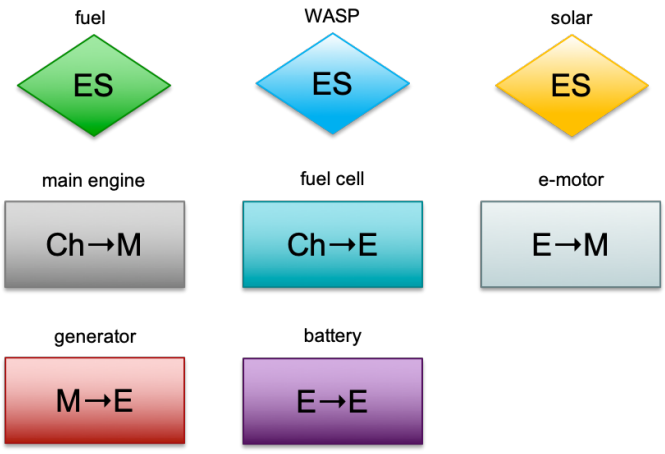

Figure 5.1: Overview of blocks used in the drive trains

Keep in mind that for clear comparison with the base case, all the new renewable energy systems are installed individually. There is investigated what equipment is needed for each system separately. This does not alter the fact that propulsion systems can be combined.

5.1 Drive train base case

The main propulsion system is shown schematically in figure 5.2. In this overview ES is the energy supply, for this engine this is heavy fuel oil (HFO), explained in chapter 4. The HFO goes to a fuel pump to the main engine. In the main engine chemical energy is converted to mechanical energy, this energy goes directly to the propellers; no gearbox is installed. Because of this, only the efficiency of the main engine will be taken into account, this is described in chapter 6. The conversion of the energy is indicated in the box with Ch $\rightarrow$ M, chemical to mechanical energy. ES in this figure stands for energy source.

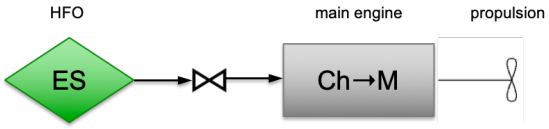

Figure 5.2: Schematic propulsion system of the base case

The main and only propulsion system of the base case is a two stroke engine, and is placed in an engine room of approximately 1000 m^3, shown in figure 5.3. This figure is given as an illustration how large the engine room is (small illustrations of men are shown in this figure) and to show that when the engine is taken out, much space is left. This can be convenient for the propulsion systems with alternative fuels that need more fuel storage. The engine shown in the figure is the MAN 6S60MC-C (MARK 8)(TIER II)[1] (Target Marina S.A., 2011). With a maximum continuous rating (MCR) of 10.170 kW at 93.0 rpm and a normal continuous rating (NCR) of 9.153 kW at 89.8 rpm (MAN Diesel A/S, 2010).

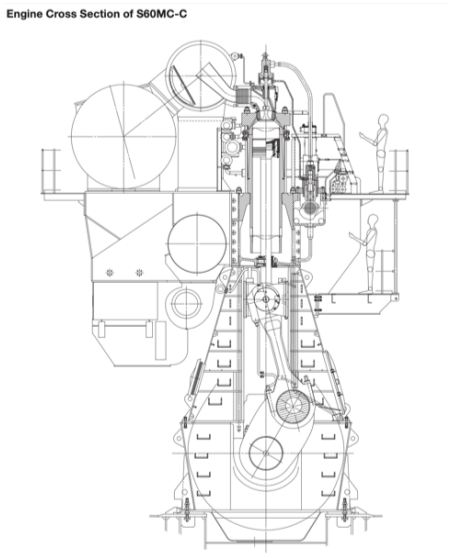

Figure 5.3: Engine cross section of s60mc-c (MAN Diesel A/S, 2010)

[1] In this engine name: 6 is the number of cylinders; S is the stroke/bore ratio, S=Super long stroke; 60 is the diameter of piston in cm; M is the engine programme; C is the concept, C=Camshaft controlled; C is the design, C=Compact engine; MARK 8 is mark number 8; TIER II is the emission regulation, IMO Tier level

The annual emissions that originate from the base case are previously discussed in section 3.2, which include NO_x, SO_2, CO_2 and HC.

5.2 Drive train biofuel

As stated in chapter 4, to retrofit advanced biofuel, such as hydrotreated vegetable oil (HVO) not a lot has to change for the current propulsion system (Maritime Industry Decarbonisation Council (MIDC), 2018). HVO can be stored in the same tanks as HFO and also the internal combustion engine (ICE) of the base case can be used (DNV.GL, 2019). The schematic overview of this propulsion system using HVO as energy source is given in figure 5.4.

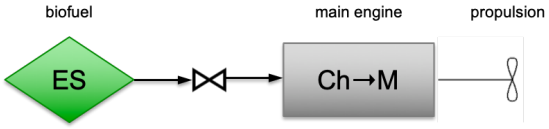

Figure 5.4: Schematic propulsion system using HVO

The structure of HVO is C_nH_{2n+2} and is free of of aromatics, oxygen and sulfur (Dimitriadis et al., 2018). The reaction that occurs within the ICE is as follows:

$$C_nH_{2n+2} \xrightarrow{N_2 + O_2} NO_2 + H_2O + CO_2$$

N_2 and O_2 are from the the atmosphere to the HVO within the ICE where combustion takes place. As can be seen from the chemical equation, still CO_2 is emitted. As said in chapter 2, it assumed that advanced biofuels are carbon neutral when produced with renewable energy. The produced carbon dioxide by biofuel is largely absorbed from the air by the plants as they grow (when other factors that limit plant growth are sufficiently available) (DeCicco, 2016), theoretically resulting in zero emissions. Another greenhouse gas emitted is NO_2. For this emissions selective catalytic reduction (SCR) catalysts are installed to reduce NO_x emissions. The SCR catalyst is elaborated in section 6.5.

5.3 Drive train hydrogen

In chapter 4 is looked at the storage facilities for liquid hydrogen on board of the vessel. In this section the components of the drive train necessary for hydrogen, is looked into.
In chapter 6, these different components of the propulsion system of hydrogen wll be individually elaborated.

Stated in chapter 2, the converting of the liquid hydrogen from chemical energy to mechanical energy for propulsion can be done in ICE and in a fuel cell (FC) combined with an electric motor. It was concluded that hydrogen fuelled ICE has multiple challenges and is less efficient.
On the other hand, using pure hydrogen in fuel cells does eliminate emissions other than water from ships completely. As there are no emissions and with a view to a sustainable future, the fuel cell as energy converter is chosen here. It is assumed that to change the energy converter from the contemporary ICE to a FC, the current combustion engine has to be replaced entirely.

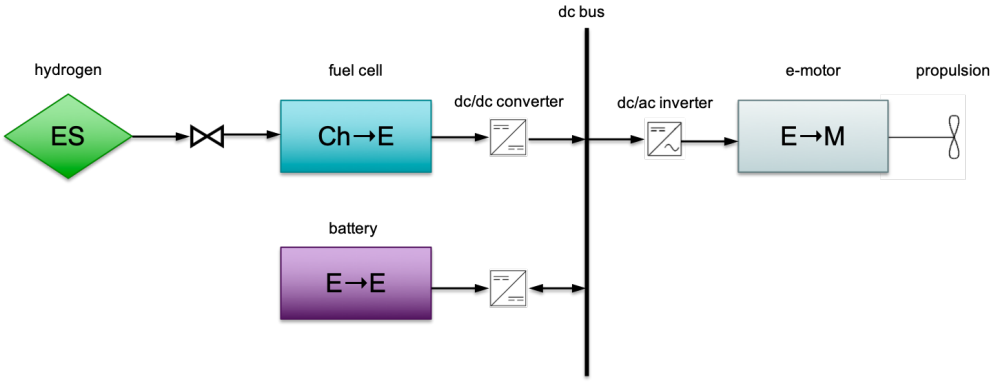

Figure 5.5: Schematic propulsion system using hydrogen

In figure 5.5 the schematic overview of the propulsion system using hydrogen is given. In the fuel cell chemical energy is converted into electrical energy. The chemical reaction that occurs within the fuel cell is as follows:

$$2H_2 \xrightarrow{O_2} 2H_2O$$

As can be seen, only water comes out. The fuel cell is connected with a dc/dc converter to a dc bus. A dc/dc converter is a device that changes a source of a direct current (DC) from one voltage level to another. This is necessary to have the same voltage level on the dc bus. A bus is a common connection to which any number of loads are connected in parallel, all being fed more-or-less the same voltage. A dc connection is chosen here instead of an alternating current (AC) connection, because most renewable energy sources are dc connected. From the dc bus the energy goes to a dc/ac inverter, which inverts the direct current to an alternating current. It is assumed that the electric motor is ac. Reasons for this choice are explained in chapter 6. The electric motor turns electrical energy into mechanical energy which starts the propellers.
Parallel to the fuel cell a battery is placed. The battery is not used here as main propulsion system but as a buffer. All these systems are elaborated in chapter 6.

5.4 Drive train ammonia

Like hydrogen, ammonia can be used as fuel in the combustion engine or fuel cell.

According to MAN in 2018 (Lindstrand, 2021), ammonia engines could be in operation in a short time as ammonia can be used as fuel in an engine equipped liquid propane gas (LPG) with only small adjustments. Unfortunately some emissions will still be formed with an ICE. Therefore, an ammonia fuel cell is chosen for this drive train.

Ammonia as fuel for a fuel cell system can be used as a hydrogen carrier or in pure form. When ammonia is used as hydrogen carrier, a cracker is necessary to split the hydrogen from ammonia. For this report it is assumed that ammonia will directly be used as this is more efficient, so no cracker is installed (Kim, Roh, Kim, & Chun, 2020). Figure 5.6 shows the schematic overview of the propulsion system using ammonia.

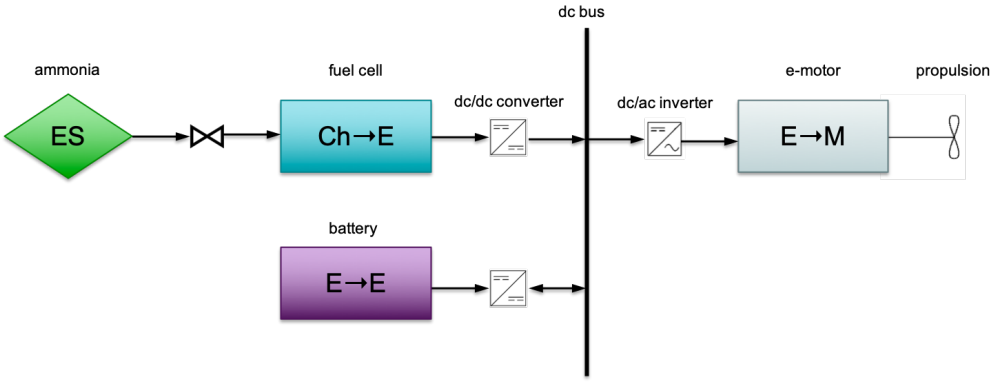

Figure 5.6: Schematic propulsion system using ammonia

Like hydrogen, a fuel cell is installed to convert chemical energy into electrical energy without emissions. The chemical reaction that takes place in the fuel cell is as follows:

$$4NH_3 \xrightarrow{3O_2} 2N_2 + 6H_2O$$

The battery and the fuel cell are connected to a dc bus which goes to an electric motor.
One system that also needs to be installed in order to run completely on ammonia, is a ventilation system. The main challenge of using ammonia as a fuel is the fact that ammonia is highly toxic. Regarding this known safety issue, ammonia has already been treated as the liquefied gas cargo, a refrigerant and as an SCR reductor in ships (Kim et al., 2020). So, the measures for these may enable the next step in enabling ammonia as a safe fuel. In chapter 6 the ventilation system will be discussed.

5.5 Drive train WASP

To sail the speed determined in chapter 3, it is expected that the ship cannot sail with a WASP system only, so the current engine is still needed. Therefore, the WASP system is combined with the main drive train. In chapter 6, the performance of the WASP system is examined and this postulation can be confirmed.
The energy generated with the WASP system can be used in different ways. The first possibility is when the WASP system is not connected to the drive train of the propulsion system, but directly propels the vessel. When a WASP system is used in this way, as said before, the performance of the system doesn't depend only on the wind velocity, but also on the direction of the wind. This is noted as WASP type 1. The layout of these drive trains is shown in figure 5.7.

Active sails like Turbosails or Flettner rotors, require some energy to start. When they run, these sails generate energy like the other type 1 WASP systems. Because of this, a generator is placed before these WASP systems. This is not shown in the drive train as it is assumed for these active sails that this is included within these systems.

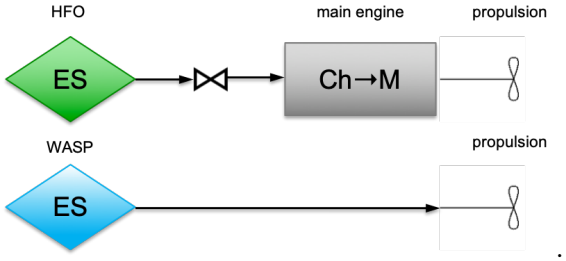

Figure 5.7: Schematic propulsion system using wind assist, WASP type 1 (direct)

Secondly, the WASP system can also be connected to the drive train of the main engine. When the energy generated with the WASP system is used in this way, the WASP system is only dependent on the velocity of the wind. This is previously noted as WASP type 2, which includes the wind turbine.

For this drive train it is assumed that all the systems are connected in parallel to a dc bus which is connected to an electric motor that is connected to the propellers. With this layout the current engine can be removed and potentially replaced with a fuel cell for propulsion with an alternative renewable fuel. An schematic overview of this layout is given in figure 5.8

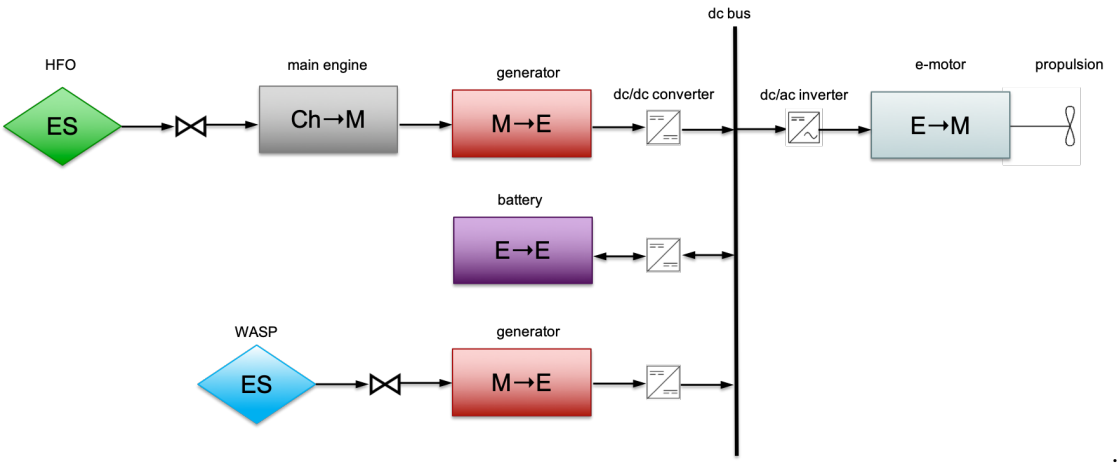

Figure 5.8: Schematic propulsion system using wind assist, WASP type 2 (indirect, wind turbine)

The WASP system is connected with a generator to the dc bus, this is because the energy generated from the WASP system is mechanical energy. This mechanical energy is converted to electrical energy using the generator. In general, renewable energy sources produce dc.
For the main engine to be connected to the dc bus, also a generator is needed.
The battery functions as a buffer or to turn on active sails.

5.6 Drive train solar

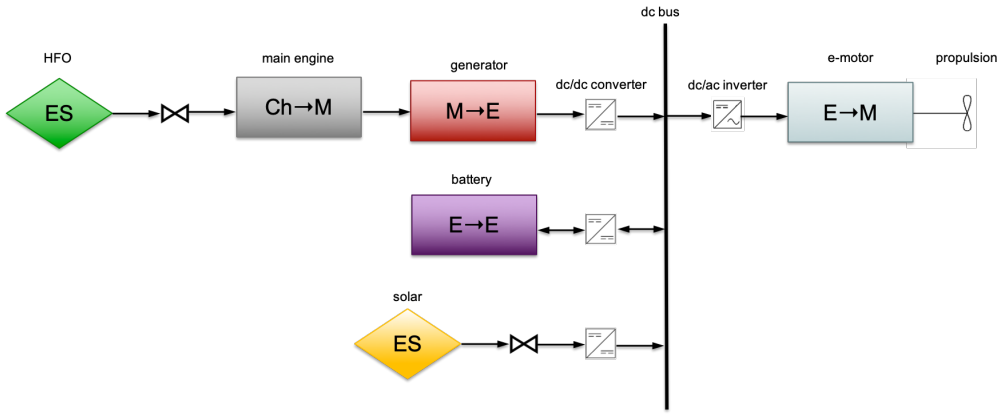

Figure 5.9: Schematic propulsion system using solar assist

The drive train of the propulsion system when also a solar hybrid is placed, is shown in figure 5.9.
The solar system generates electrical energy and is connected to the bus with a dc/dc converter. The rest of the layout of the drive train of this propulsion system is similar to the layout with a WASP type 2 system. Keep in mind that a lot of different layouts are possible. To compare all propulsion systems with the base case and with each other, the battery is placed the same in every drive train.

5.7 Overview systems for each propulsion drive train

	Base case	Biofuel	Hydrogen	Ammonia	WASP type 1	WASP type 2	Solar
Current main engine (Ch→M)	✓	✓	✗	✗	✓	✓	✓
Adjusments for new/ extra energy source (ES)	✗	✗	✓	✓	✓	✓	✓
Fuel cell (Ch→E)	✗	✗	✓	✓	✗	✗	✗
E-motor (E→M)	✗	✗	✓	✓	✗	✓	✓
Battery (E→E)	✗	✗	✓	✓	✗	✓	✓
Generator (M→E)	✗	✗	✗	✗	✗	✓	✓
Extra system(s)	✗	SCR	Heat insulation system + WHR	Ventillation system + WHR	✗	✗	✗

✓ System in drive train
✗ System not in drive train

Figure 5.10: Overview of the systems necessary for each propulsion drive train

Figure 5.10 shows an overview of each system necessary for each propulsion system drive train, as discussed in this chapter. The white boxes with the tick mark show which system is included in which propulsion drive train and the dark blue boxes with the cross are not included in the drive train.
In chapter 6 for each of these systems, the fuel cell, electric motor, battery and potential extra system, will be discussed and its properties such as efficiency, size, weight, lifetime and prices, are presented.

6 | Performances and sizes of the drive train components

In chapter 5 the drive train for each (hybrid) propulsion system is analysed separately. In this chapter each component of the different drive trains are elaborated and examined on their performances and their sizes. The efficiencies of the drive train components are needed to calculate the fuel consumption. When the fuel consumption and the sizes of each component is known, the costs of the components necessary for each propulsion system, can be determined. KPI 2, the costs per tonne collected nodules (defined in chapter 3) can then be established.
The structure of this chapter is as follows, first the components of the drive trains are discussed. Then, the total size results of each propulsion system with its drive train performance is established.

6.1 Fuel cell

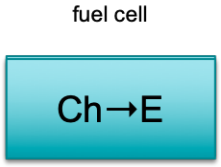

Figure 6.1: Fuel cell block

The fuel cell is only used in the drive trains of the hydrogen and ammonia propulsion. The two fuel cells that seem most promising at the moment are PEMFC and SOFC (Tronstad, Åstrand, Haugom, & Langfeldt, 2017).

PEMFC stands for proton exchange membrane fuel cell. The PEM fuel cell is the most mature fuel cell and is already successfully used in the marine sector. However, injection to the PEMFC requires pure hydrogen. Therefore fuels other than hydrogen need to be converted to hydrogen for operation. The operating temperature is low, which provides high tolerance for cycling operation (Battelle Memorial Institute, 2016).

Solid oxide fuel cell (SOFC) on the other hand, has a high operating temperature. Therefore, the start-up time for the SOFC is much longer than the start up time of PEMFC (Tronstad et al., 2017). Because the transport of the nodules is only one straight way back and forth, and no special or difficult operations happen during the transport of CCZ to Mexico and back, this disadvantage can be taken for granted.

Because of the high operating temperature, a waste heat recovery system (WHR) is feasible and can increase the efficiency of the fuel cell up to 80% (U.S. Department of Energy, 2016). Comparing this fuel cell with the PEMFC, with the use of SOFC is less experience in vessels. An advantage of the SOFC is that it can be used for different fuels as the reforming from hydrocarbons to hydrogen takes place within the fuel cell (Battelle Memorial Institute, 2016).
A summary of the properties of the PEMFC and the SOFC are shown in table 6.1.

Table 6.1: Comparison and properties PEMFC and SOFC (Battelle Memorial Institute, 2016) (U.S. Department of Energy, 2016) (Tronstad et al., 2017)

Fuel cell type	PEMFC	SOFC
Typical stack size [kW]	<1 kW–100 kW	1 kW–2 MW
Efficiency [%]	60%	60% (80% with WHR)
Capital costs [$/kW]	1,700-2,860	1,180-1,790
Life time [years]	3-5	3-5
Operating temperature [°C]	<120°C	500–1,000°C

For the propulsion of both hydrogen and ammonia is chosen for a SOFC, because of its higher efficiency (assuming a WHR system is also installed), its price and stack size.
A SOFC fuel cell stack of 500 kW from Sunfire, is given in figure 6.2. So for this transport 20 of these SOFC stacks are needed. The volume of this stack is around 3.5 m^3. The lifetime of this fuel cell is up to 40,000 hours (Sunfire, 2020).

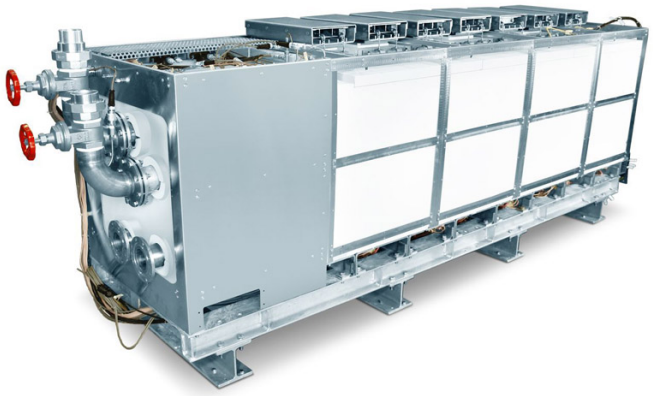

Figure 6.2: SOFC fuel cell of Sunfire (Sunfire, 2020)

6.2 Electro motor

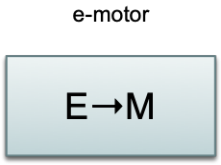

Figure 6.3: E-motor block

In this report it is assumed that the electric motor is an AC motor but in fact, this could also be a DC motor. In this section the advantages of direct current (DC) and alternating current (AC) motors are discussed and an AC electric motor is selected as starting point to continue with.

Table 6.2: Data electric motor and infrastructure (Ramme, 2021) (Reed, 2021)

Electric engine type	Permanent magnet RAMME
Size [rpm]	100-800
Size [m^3]	~10
Efficiency [%]	98%
Life time [years]	30
Efficiency inverters (AC/DC) and converters (DC/DC) [%]	95%

In this report there is chosen for a DC infrastructure, because it will help improve grid integration of RE sources and improve their overall economic and environmental value proposition. Besides this, renewable energy sources are compatible with DC power. Also all propulsion systems in this report are combined with batteries. Almost all battery technologies are based on direct current as well, this will increase integration efficiency and decrease the operating losses. DC becomes a more naturally compatible interface when using both RE sources and batteries (Reed, 2021).

Figure 6.4: Permanent magnet motor of RAMME (Ramme, 2021)

When looking at the electric motor, there is chosen for a AC motor. As there is more known about the AC motor, this electric motor is less expensive, smaller and needs less maintenance. There are three types of AC motors, AC induction motors, AC synchronous electrically excited motors and AC synchronous motor with permanent magnet. Two AC types were considered, an AC induction motor and a AC permanent magnet motor. The permanent magnet motor is more efficient, smaller and there is no need for a gearbox, which is required for the induction motor. A disadvantage of the permanent magnet motors, is that they are expensive. The costs of the electric motor are discussed in chapter 7. The chosen e-motor is shown in figure 6.4 and only one motor is necessary. The data of this chosen electric motor is given in table 6.2. The size of the electric motor does not depend on the installed power of the vessel but depends on torque.

6.3 Generator

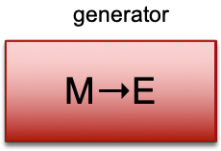

Figure 6.5: Generator block

AC motors, including permanent magnet AC motors, can also be used as generators. As mentioned in chapter 5, the function of a generator is to convert mechanical energy into electrical energy. An AC motor usually can be used as a generator, without any internal modifications (Wildi, 2004).
Combining the generator with the motor is called a genset. This needed for the hybrid propulsion system with WASP and solar systems and as well for the drive train systems with hydrogen and ammonia. For these propulsion systems it is assumed the AC permanent magnet motor also functions as a generator. Therefore, its efficiency is decreased to 95% (Sajip, 2021).
The generator must match with the diesel engine, otherwise the genset will be overloaded. The engine can be overloaded when the load connected to the generator exceeds the rated kW. The generator can be overloaded if the load exceeds the rated kVA of the generator (Sajip, 2021).
For the propulsion system with a WASP type 2 system, another generator is needed to convert the mechanical energy generated with this WASP system into electrical energy. Also, a generator to start the active sails of WASP type 1, a generator is needed. It is assumed, for both types this generator is integrated in the WASP system.

6.4 Battery

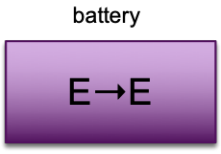

Figure 6.6: Battery block

In almost all propulsion systems discussed in chapter 5, a battery is used. This battery is not used as main energy source, but functions as buffer for peak shaving, as emergency energy source or for boosting scenarios.
Peak shaving is another word for load shedding and reduces power consumption quickly and for a short period of time to avoid a spike in energy consumption. The storage system is then continually charged from the electricity grid (Next, n.d.).
The battery can also function as an emergency energy source. For each vessel built, the classification of each vessel states how much this emergency energy is.
Lastly, the battery can function as a booster. This happens, for example, when the vessel needs to be on DP (dynamic positioning). DP is presumably needed for the transfer of the nodules from the Hidden Gem to the transport vessel. This transfer of nodules and DP is elaborated in appendix A.

The most promising battery at the moment for marine application is the lithium-ion battery (DNV.GL, 2020). Five main advantages of this type of battery are firstly, that li-ion batteries reduce engine maintenance and need less maintenance than other batteries as they do not need to be watered. Besides this, the lifespan of a lithium-ion battery is eight or more years, depending on its use. Also, this type of battery is more safe because it eliminates exposure to flammable fuels and battery acids with the lithium-ion technology. Several Li-ion batteries exist. According to a study into electrical storage on ships by DNV.GL in 2020 (DNV.GL, 2020), lithium-ion batteries (lithium-ion nickel manganese cobalt oxide (NMC)), are reviewed best for maritime applications, idem according to a review about current li-ion battery technologies in electric vehicles (Miao, Hynan, von Jouanne, & Yokochi, 2019). From this last research, the summary of all reviewed li-ion batteries is shown in figure 6.7 and analysed on their capacity, specific power, safety, performance, life span and cost. With performance in this graph is meant the material and thermal characteristics of the battery.

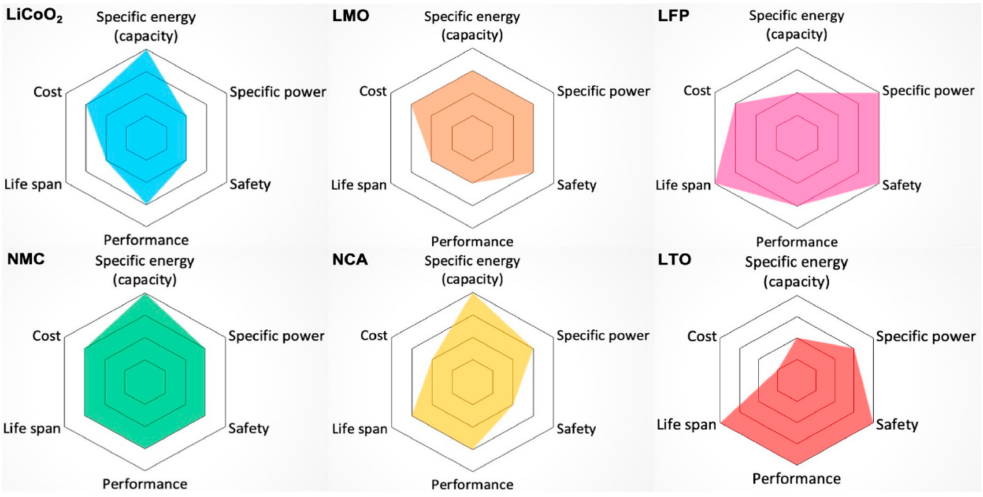

Figure 6.7: Comparison of different types of li-ion batteries from six perspectives, capacity, specific power, safety, performance, life span and cost (Miao et al., 2019)

The greater the area of the graph, the better the overall performance of the battery. As can be seen in the graph, the NMC battery scores well on every perspective. For this function, the

outer hexagon is most desirable for the battery.
The NMC battery is the most used chemistry in marine applications at present. Advantages of the NMC battery are that the battery can be combined for high specific energy, its power density is adjustable, the energy density is high, the costs are relatively low and the battery is safe. Also, NMC has a flexible design with respect to energy and power capabilities.

An example of a NMC litium ion battery, is the Catl 50 battery, shown in figure 6.8. This battery has a capacity of 50Ah (amp-hour) and a nominal voltage of 3.65V, which gives a energy of 182.5Wh. Its weight is 0.9kg and is has a volume of 148mm*98mm*27mm, $3.9 * 10^{-4}$ m^3 (Zaozhuang Evlithium Electronic Technology Co., 2018). To store for example 2.5% of the total power needed for the transport, around 250,000 batteries are needed, which has a volume of more than 100m^3 and weights 225 tonnes. Also air is between the batteries and battery management systems need to be installed, therefore a factor of 10% is added to the size and weight, so these end up to be 110m^3 and 250 tonne. Further calculations were made with these numbers.

Figure 6.8: Nmc 811 Lithium Ion Li Polymer Ternay Battery (Zaozhuang Evlithium Electronic Technology Co., 2018)

6.5 Additional systems needed for the drive trains

Implementing alternative fuels brings as well extra systems to function safely, sustainable or more efficient. In this section the extra systems necessary for some of the different propulsion systems are mentioned. For biofuel, this is the SCR katalysator, for hydrogen a high-performance heat insulation system, for ammonia a ventilation system and to increase the efficiency of the SOFC used for hydrogen and ammonia, a WHR system.

Selective catalytic reduction (SCR) system

A selective catalytic reactor (SCR) technology is used for the propulsion system using biofuel as main energy source, to reduce NO_x emissions. The working of the SCR with ammonia as reductor, is shown in figure 6.9. SCR converts nitrogen oxides with the aid of a catalyst into N_2 and water. A reducing agent, such as ammonia or aqueous ammonia (NH_4OH), or an urea ($CO(NH_2)_2$) solution, is added to a stream of exhaust gas and is reacted onto a catalyst (Wartsila, 2017).

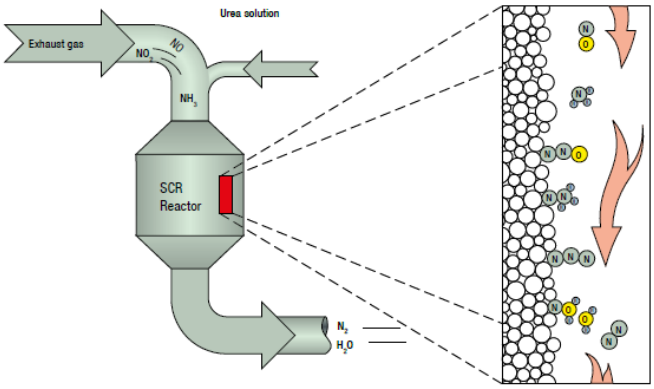

Figure 6.9: SCR reactor (JSTRA & MLIT, 2020)

High-performance heat insulation system

As said is section 4, because hydrogen is stored below -253 °C, a high-performance heat insulation system is needed. Therefore, vacuum heat insulation was adopted.Each tank will have a double wall, and the space between these walls will be filled with vacuum for heat insulation (DNV.GL, 2019).

Ventilation system

When using ammonia as the main fuel, a ventilation system is necessary because ammonia is highly toxic. The ventilation requirements set for the ammonia engine room are to ensure safety. The ventilation systems monitors and prevents the build-up of refrigerant in the engine room, which can occur by a leak to a concentration. This leak would be flammable or harmful or would lead to oxygen deficiency. Therefore the ventilation system requires detection to activate at a specific concentration of ammonia in the air (DualTemp, 2020).
Besides the ventilation system, additional safety measures in accordance with the IGF Code, such as the adoption of a double-pipe structure in the engine room, are also necessary.

Waste heat recovery system

Waste heat recovery systems are used with the SOFC, implemented in the propulsion drive train of hydrogen and ammonia to improve its efficiency and increase it from 60% to 85%. A waste heat recovery system recovers the lost thermal energy and converts it into electrical energy. The WHR system can consist of an flue gas boiler (or combined with oil-fired boiler), a power turbine and/or a steam turbine with alternator. By redesigning the ship layout, the boilers on the ship can be efficiently accommodated to better fit this system (Glomeep & DNV.GL, 2021b).

6.6 Total size results of each propulsion system drive train

Table 6.4 gives the total efficiencies and the relative measurements of the complete drive train of each propulsion system. The necessary tank size depends on the tank to propeller efficiency, given for each propulsion system in table 6.3. So, the efficiencies of the battery and the WASP and solar systems are not taken into account in this calculation.

Table 6.3: Efficiencies of the drive train components and total efficiency for each propulsion system

	Base case	Biofuel	Hydrogen	Ammonia	WASP type 1	WASP type 2	Solar
Efficiency current main engine	50%	50%	×	×	50%	50%	50%
Efficiency fuel cell	×	×	80%	80%	×	×	×
Efficiency e-motor	×	×	98%	98%	×	98%	98%
Efficiency converter	×	×	95%	95%	×	95%	95%
Efficiency inverter	×	×	95%	95%	×	95%	95%
Efficiency Generator	×	×	×	×	×	95%	95%
Total efficiency (tank to propeller)	50%	50%	71%	71%	50%	42%	42%

The tank to propeller efficiency is the total efficiency of the propulsion system from the tank to the propeller. For the base case the tank to propeller efficiency depends only on the efficiency of the 2 stroke main engine, which is 50%, this also applies for the propulsion system using biofuel and for WASP type 1. For the hybrid propulsion system using WASP type 2 and Solar systems, the main energy source remains the current engine with HFO, with has an assumed total volume of 1000 m^3, see table 6.4. Because a generator and electric motor are placed in the drive train, the total efficiency decreases to 42%. The total efficiency is calculated by multiplying the efficiencies of the different components of the drive train. Here, these are the efficiency of the current engine, the efficiency of the converter, the inverter and the electric motor. This tank to propeller efficiency is for WASP type 2 and solar systems the same. The layout of the drive trains of these propulsion systems are, however, not the same. As for the WASP system type 2 an extra generator is added. This generator does not influence the efficiency of the tank to the propeller, but has only influence on the efficiency from the WASP system to the propeller. Also, as said before, this generator is integrated in this WASP system. Because of this, the total efficiency of the propulsion system using WASP and solar are similar.
The installed HFO tank capacity for the Panamax Leda C is 2500m^3 (Target Marina S.A., 2011). Looking at the fuel consumption of the propulsion systems with WASP type 1, this is less than the fuel consumption of the base case. The tank size for each of these systems remains the same, however how full the tanks are compared with each other may differ. The total efficiencies of the drive train for WASP type 2 and the solar systems are decreased due to the added components. Because of this, the amount of fuel required will be greater, however the WASP or solar system will also generate energy making the required amount of fuel in the tanks smaller. The fuel consumption is taken into account in calculating the total costs of each propulsion system in chapter 7.

Table 6.4: Total efficiencies and sizes systems required for each propulsion system

	Base case	Biofuel	Hydrogen	Ammonia	WASP type 1	WASP type 2	Solar
Total efficiency (tank to propeller)	50%	50%	71%	71%	50%	42%	42%
Total tank capacity [m3]	2500	2500	6000	3750	< 2500	2500	2500
Current engine size [m3]	1000	1000	x	x	1000	1000	1000
Fuel cell size [m3]	x	x	70	70	x	x	x
E-motor size [m3]	x	x	10	10	x	10	10
Battery size [m3]	x	x	110	110	x	110	110
Total tank capacity [m3]	2500	2500	6000	3750	< 2500	2500	2500
Total size tank compared with base case [%]	0%	0%	140%	50%	0%	0%	0%
Total size propulsion drive train [m3]	1000	1000	190	190	1000	3620	3620
Total size propulsion drive train compared with base case [%]	0%	0%	-81%	-81%	0%	262%	262%
Total size propulsion drive train with tank [m3]	3500	3500	6190	3940	<5000	6120	6120
Total size propulsion drive train with tank compared with base case [%]	0%	0%	31%	-17%	0%	29%	29%

The total efficiency using hydrogen or ammonia is determined to be 71% (depending on the efficiency of the fuel cell, inverter, converter and electric motor), keeping in mind a WHR system is also installed. Comparing the size of the storage capacity necessary for hydrogen and the storage capacity of the base case, the storage limit of the existing tanks is way exceeded. As the efficiency of the drive train of hydrogen and ammonia is increased, the storage capacity is not exceeded by a factor of 4.2 as stated in section 4.2, but is exceeded with 140% (which gives a factor of 2.4) as shown in table 6.4. An advantage of hydrogen, as said before, is that it has a light weight. Because of this advantage, hydrogen tanks can be placed on the deck of the Panamax Leda C. On the deck is enough space. For example, one tank of 3500 m^3 can be placed on deck. The feasibility, safety and the influence on the draught of the vessel have to be further investigated.
Ammonia as main energy source on board will exceed the storage limit of the current tanks as well. Also, because of the higher total efficiency, the ratio with the HFO tank is not 2.7 as said section 4 but 1.5. One tank of 1500 m^3 needs to be placed on deck for this, which should be feasible. When hydrogen is placed hybrid and for example is combined with a WASP system and stored on deck, there is a possibility that there is not enough space for the number of propulsors of the WASP system. This should be kept in mind when thinking about hybrid propulsion.

7 | Costs analysis

In addition to the performance of each propulsion system discussed in this report, a cost analysis is also done to determine the KPIs set in chapter 3 and to know which system is individually most cost efficient compared with the base case.
In this chapter KPI 2 is examined. First the different components of the cost analysis such as initial investments and additional costs of each propulsion system are explained, then cost analysis examples are given of three different propulsion systems, one of the base case, one with an alternative fuel and one with a WASP system installed. Lastly, the total costs of each system over 30 years is given on the premise that all fuel prices and the costs for the technology systems remain the same as they are determined at the moment.

7.1 Cost analysis components

This section describes what must be taken into account when calculating the total expenses after 30 years for each propulsion system. This total expense depends on the initial investment made for purchasing a system and on the additional costs that needs to be payed each year.
To validate the cost of a certain product or technology, mostly CAPEX (major purchases to be used over the long term) and (day-to-day expenses) are used. Also in this section, both these expenditures are explained and included in this costs analysis.
Keep in mind that the revenue from the transported nodules are not taken into account for each propulsion system as it is assumed that this stays unchanged for all options.

7.1.1 Initial investment

The initial investment of each propulsion system consists of the research costs, which depend on the technology readiness level (TRL) of each propulsion system, the CAPEX and the installation costs.

Research costs

'Research costs' revers to how much should be invested to realize the propulsion system, as some of the propulsion systems are not yet ready to be realized at the moment. The total research investments of some of the propulsion systems can reach millions of dollars. In this cost analysis is looked at only one system, assuming more will be produced. To estimate the research costs of this one propulsion system, a percentage of the total CAPEX is taken, depending on the TRLs, which are determined in chapter 2.
When the TRL is high, the research costs are low. The research costs are determined as follows:

$$C_{research} = (100\% - 10 \cdot TRL) \cdot CAPEX \tag{7.1}$$

So when the TRL for example is 4, the research costs are 60% of the CAPEX costs. The resulting percentages for the research costs are given in table 7.1.

		Research costs [% of total CAPEX]
Base case	HFO	0%
Alternative fuels	Biofuel (HVO)	40%
	Hydrogen	60%
	Ammonia	40%
WASP system	Kites	50%
	Dyna rig	40%
	Wing sail	20%
	Turbo sails	40%
	Flettner rotor	10%
	Wind turbine	20%
Solar system	Solar panels	40%
	Solar in sails	60%

Figure 7.1: Research costs in percentages of total CAPEX hardware

CAPEX

CAPEX is the capital expense. This is the companies' spending on this certain product or technology. The value of CAPEX is each year reduced by depreciation (Fernando, 2021). Depreciation is the expenditure of a fixed asset over its useful life. The depreciation method used in this costs analysis is the straight-line depreciation method, which is also the most common used. To calculate the amount of annual depreciation expense using the straight-line method, the CAPEX of the total hardware of the propulsion system divided by its lifetime. So, for example, the CAPEX of the fuel cell is 14 m$ and the lifetime is 4 years, then the depreciation each year is $\frac{14m\$}{4years}$, which is 3,5m$. After these 4 years, the fuel cell has to be replaced.

Installation costs

The installation costs are the costs to install the equipment necessary for each propulsion system. The rule of thumb that is used to estimate the installation costs in the maritime sector, is that the installation costs range from 1-3 times the CAPEX costs, depending on the size and the complexity of the system. Most of the time the installation and CAPEX costs of the equipment are the same [1]. This rule of thumb is used when the installation costs are not specified.

7.1.2 Additional costs (OPEX)

OPEX are the operating expenses, which are required for the day-to-day functioning of the new product or technology. These additional costs need to be payed yearly for each propulsion system and includes the fuel costs, the operating and maintenance costs of the propulsion system and the CO_2 tax. (Fernando, n.d.)

[1] This guideline to estimate the installation costs is discussed with a sustainability expert Taco Straathof, who is a Sustainability Engineer at Allseas.

Fuel costs

The fuel costs are the costs for the total annual fuel consumption of each propulsion system and depend on the type of fuel. The costs of each type of fuel discussed in this report, are given in table 7.1. These fuel prices of alternative fuels vary a lot at the moment, so assumptions about the price had to be made.
The price for HVO is around 2000$/tonne according to (Squadrin, 2021). A reason for this high price, is the expensive production of HVO as expensive equipment for the hydrogenation process are needed. A reason for the fluctuations is that HVO can be produced in multiple ways. Therefore, the assumed price for HVO is set on 1300$/tonne.

The production costs for green hydrogen are currently between $2500 and $4500 per tonne, according to an analysis by Bloomberg (Dezem, 2021). In this same analysis is stated that this price would need to be below 1000$/tonne to become competitive with grey hydrogen, which is made from fossil fuel. Bloomberg predicts this price will be reached by 2030 and sink to 800$/tonne by 2050. The cost of production of hydrogen varies greatly depending on the price of electricity (in the case of electrolysis), the scale of the production plant, the need for transport and liquefaction (DNV.GL, 2019). For this cost analysis, the price of liquid hydrogen is assumed to be 3500$/tonne.

According to Argus Media (Brown, 2020) , the production cost of green ammonia today would be between a rate of 650$/tonne and 1500$/tonne, which is more than twice the market price of ammonia made from fossil fuels. Recently, Argus Media published a model with an overview of the market potential of green ammonia and estimates that green ammonia could cost just $250 per ton by 2040. (Media, 2021) A price of 1000$/ tonne is assumed for green ammonia in this cost analysis.

Table 7.1: Fuel costs (Stopford, 2009) (DNV.GL, 2019)

Fuel type	**Costs [$/t]**
HFO	450 [$/t]
Biofuel (HVO)	2000 [$/t]
Liquid hydrogen	3500 [$/t]
Ammonia	1000 [$/t]

The reference vessel uses 20ton/day when sailing at a fixed ship speed of 12 knts (Healy & Graichen, 2019), sailing 250 days per year, this is 5000 tonne HFO per year for the transport of the polymetallic nodules. Using the energy density of alternative fuels, given in chapter 4, the efficiencies of the drive trains given in chapter 6 and the percentages of reduction of fuel for the WASP and solar systems, determined in chapter 4, the annual fuel consumption can be calculated and with that the annual fuel costs. The annual fuel consumption and costs for each propulsion system are given in table 7.2 (DNV.GL, 2019).

Table 7.2: Annual fuel consumption and fuel costs

2 Panamac Leda C bulks carriers at 12 knts							
			Alternative fuel or technologies	Costs fuel [$/t]	Fuel reduction [%]	Total annual fuel consumption [t]	Costs fuel consumption per year for entire fleet [m$/year]
Alternative fuels			Biofuels	2000	0%	4592	9.2
			Hydrogen	3500	0%	1188	4.2
			Ammonia	1000	0%	7667	7.7
Alternative energy generation	Wind	Soft sails	Kites	450	7%	4650	2.1
			Dyna rig	450	7%	4640	2.1
		Wing sails	Wing sail	450	11%	4450	2.0
		Active sail	Turbosail	450	6%	4689	2.1
			Flettner rotor	450	12%	4399	2.0
		Other	Wind turbine	450	3%	5802	2.6
	Solar		Solar panels	450	3%	5802	2.6
			Solar in sails	450	1%	5902	2.7
Base case			HFO	450	0%	5000	2.3

As can be seen in table 7.2, the total annual fuel consumption of ships equipped with solar or WASP type 2 are even higher than that of the base case. This is because the efficiency of its main drive train is decreased by adding the generator and an electric motor. The energy generated by these system cannot compete, as it were, with this new efficiency.

O&M costs

The operating and maintenance (O&M) costs depend also on the capital expenditures. According to Stopford[2] (Stopford, 2009), and generally accepted, the O&M costs of a vessel are 4.75% of the CAPEX costs. For a ship this size, the O&M costs for the HFO fuel tanks are is 0.5$ per year. This value is also used for the O&M costs of the electric motor and the extra systems.
From research of the Pusan National University (PNU, South Korea) it is assumed that the O&M costs of the fuel cell is only 1% of the CAPEX (Kim et al., 2020). For the O&M costs of the WASP systems, an economic analysis of previous WASP research (Schinas & Metzger, 2019) is assumed, which is estimated to be the CAPEX costs divided by 3.
For the propulsion systems of the base case, using biofuel, with WASP system and with the solar system, the maintenance costs of the current engine need to be taken into account as well.

CO_2 tax

To reach the Dutch emission reduction targets (that comply with those of the European Union), a CO_2 tax is intended to set a minimum price for CO_2 emissions relative to the EU Emissions Trading System (EU ETS) price. The tax rates at the moment are typically around $5-$30 per tonne of CO_2 (a.o., 2020). For 2021, a CO_2 tax of $35 is proposed. This is expected to rise to $150 per tonne carbon emissions in 2050 (Parry, Heine, Kizzier, & Smith, 2018).

[2]Martin Stopford is an economist who has enjoyed a distinguished career in the shipping industry as Director of Business Development with British Shipbuilders, Global Shipping Economist with the Chase Manhattan Bank N.A., Chief Executive of Lloyds Maritime Information Services; Managing Director of Clarkson Research Services and an executive Director of Clarksons PLC. His book 'Maritime Economics' uses historical and theoretical analysis as the framework for a practical explanation of how the shipping industry works today.

For this costs-analysis this carbon tax needs to be taken into account as it will be able to contribute to the total expenses for each propulsion system. In chapter 3.2, it is stated that there is 3.2 tonne emission of CO_2 per tonne fuel HFO. Annually this means a fuel consumption of 5000 tonne, resulting in a carbon emission of more than 15,000 tonne.
The effective tax price will therefore be based on the difference between the EU ETS price per tonne of CO_2 emitted and the legal CO_2 emissions rate of that year. However, it cannot lead to a negative effective carbon tax rate, as this would imply that the government would have to refund if the EU ETS price is higher than the national legal price.

7.2 Initial investment and additional costs per propulsion system

In this section the initial investments for each of the propulsion system is discussed. For every propulsion system a table is given with an overview of the costs included. The CO_2 tax is not yet determined (explained as 't.b.d.' in the tables). This will be discussed in chapter 8, when this tax will change will depend on the goals set concerning the energy transition.

Costs propulsion system of base case

No initial investments for the HFO tank with the current engine are necessary as they are already installed. This means no research costs and no CAPEX costs. The lifetime of the engine and tank is the same as the lifetime of the ship. The costs for the propulsion of the base case only consist of the additional costs, this includes the fuel costs and the O$M costs. The fuel costs were calculated in the previous section and the O$M were estimated on 0.5m$ per year (Stopford, 2009). The costs of the base case are given in table 7.3.

Table 7.3: Costs base case

Base case			
Initial investment	CAPEX total hardware [m$]	HFO tank and current engine [m$]	0
	Installation costs [m$]	HFO tank and curren engine [m$]	0
	Research costs (0% of total CAPEX) [m$]		0
		Total [m$]	0
Annual additional costs (OPEX)	Fuel costs [m$]	HFO fuel [m$]	2.3
	O&M costs [m$]	HFO tank and current engine [m$]	0.5
	CO2 tax [m$]		t.b.d.
		Total [m$]	2.8

Costs propulsion system with: Biofuel

Looking at the costs for the propulsion system with biofuel as energy source, they are similar with the costs for the base case. But a SRC is added to be able to emit zero emissions on board. This SCR is explained in chapter 6. The costs for the SCR used for the drive train with biofuel as main energy source to reduce NO_x, is already determined by Taco Straathof, Sustainability Engineer at Allseas. This resulted in a CAPEX of 21500$ per MW.

Keep in mind that the research costs for biofuel in the other calculations are actually higher as the total CAPEX costs for the biofuel drive train are relatively low. This is because almost no modifications to the drive train of the base case have to be executed.

The CO_2 tax, which is added later in this research, is assumed to be zero at all times for biofuel, as it is assumed to generate no emissions when using biofuel as main energy source. The costs for the propulsion system with biofuel as main energy source, is given in table 7.4.

Table 7.4: Costs biofuel

Biofuel			
Initial investment	CAPEX total hardware [m$]	HVO tank and current engine [m$]	0
		SCR [m$]	0.2
		Total	0.2
	Installation costs [m$]	HVO tank and current engine [m$]	0
		SCR [m$]	0.2
		Total	0.2
	Research costs (40% of total CAPEX) [m$]		0.08
		Total [m$]	0.88
Annual additional costs (OPEX)	Fuel costs [m$]	HVO fuel [m$]	9.2
	O&M costs [m$]	HVO tank and current engine [m$]	0.5
		SCR [m$]	0.01
		Total	0.51
	CO2 tax [m$]		t.b.d.
		Total [m$]	10.2

Costs propulsion system with: Hydrogen

The initial investment for installing liquid hydrogen on board of the Panamax Leda C consist of the CAPEX costs for the hydrogen tank, the fuel cell, electric motor, WHR and a ventilation system.

A research analysis including the investments costs for the storage of hydrogen and ammonia is done by the National Renewable Energy Laboratory of Colorado (Amos, 2014). This analysis is used to determine the CAPEX of the storage tanks and additional systems such as the heat insulation system (for hydrogen) and the ventilation system (for ammonia). Their target price of 400\$/^{3} for the total tank capacity (6000m^3 as stated in chapter 6) is used. The systems that already are established in chapter 6 such as the fuel cell, electric motor and heat insulation system, the CAPEX costs of their suppliers are used.

The costs for the WHR, again research done by Glomeep and DNV.GL, were used as guidance (Glomeep & DNV.GL, 2021b). This research states that for the CAPEX and installation of the WHR system, a lot of costs are involved and are more or less independent of size. The guideline for this cost estimation indicates that the costs grow linearly with the ship size.

As said before, the thumb rule for the installation costs depend on the size and complexity of the system and range from 1-3 times the CAPEX costs. Therefore the installation costs of the hydrogen tank is set on three times its CAPEX costs.

For the research, 60% is taken from its total CAPEX costs for all components of the hydrogen drive train. So, the research costs for Hydrogen, consists of 60% of the CAPEX of the new tanks and pipes, plus 60% of the CAPEX of the fuel cell plus 60% of the CAPEX of e-motor, plus 60% of the CAPEX of the battery, plus 60% of the CAPEX of the heat insulation system.

The lifetime of the hydrogen tank is as long as the lifetime of the reference vessel. The lifetime of

the other components of the drive train were already given in chapter 6, which is for the electric motor, 30 years, the fuel cell 4 years and the heat insulation system 10 years. Keep in mind that these system need to be replaced after these years.
The additional costs include the fuel costs (were established in the previous section) and the O&M costs. The O&M costs are 4.75% of the CAPEX costs of the hydrogen tank ((Stopford, 2009)) on top of the O&M costs of the base case.
The CO_2 tax is, like biofuel and ammonia, assumed to be zero at all times for hydrogen.
An overview of the total costs for the propulsion system with hydrogen as main energy source, is shown in table 7.5.

Table 7.5: Costs hydrogen

Hydrogen			
Initial investment	CAPEX total hardware [m$]	Hydrogen tank [m$]	2.4
		Fuel cell [m$]	14
		Electric motor [m$]	5
		Heat insulation system [m$]	0.2
		WHR system [m$]	7.5
		Total	16.4
	Installation costs [m$]	Hydrogen tank [m$]	7.2
		Fuel cell [m$]	14
		Electric motor [m$]	5
		Heat insulation system [m$]	0.2
		WHR system [m$]	0.02
		Total	26.42
	Research costs (60% of total CAPEX) [m$]		9.84
		Total [m$]	52.66
Annual additional costs (OPEX)	Fuel costs [m$]	Hydrogen fuel [m$]	4.2
	O&M costs [m$]	Hydrogen tank [m$]	0.6
		Fuel cell [m$]	0.1
		Electric motor [m$]	0.2
		Heat insulation system [m$]	0.01
		WHR system [m$]	7.5
		Total	8.5
	CO2 tax [m$]		t.b.d.
		Total [m$]	12.7

Costs propulsion system with: Ammonia

As said before, the research of the National Renewable Energy Laboratory of Colorado (Amos, 2014) analyses the investment costs for the storage of ammonia. This research gives a target price of 500\$/m^3 for the capacity of the installed ammonia tanks (from chapter 6, which is 3750m^3).
Like the hydrogen propulsion system, costs for the fuel cell, electric motor and WHR are included as well. Instead of a waste heat recovery system, the propulsion system with ammonia as main energy source, needs a ventilation system, explained in chapter 6. The research costs are 40% of the total CAPEX hardware (see explanation of the research costs in the previous section). The rule of thumb is used here by multiplying the CAPEX costs by 3 for the installation costs of the ammonia tank and piping system.
The fuel costs and the O&M costs are the additional costs. Like the estimation of the O&M costs for the hydrogen tank, 4.75% ((Stopford, 2009)) of the CAPEX costs of the ammonia tank on top of the O&M costs of the base case is used.
As said before, the CO_2 tax is assumed to be zero at all times for ammonia.
The initial investments and the additional costs of ammonia are displayed in table 7.6.

Table 7.6: Costs ammonia

Ammonia			
Initial investment	CAPEX total hardware [m$]	Ammonia tank [m$]	1.9
		Fuel cell [m$]	14
		Electric motor [m$]	5
		Ventilation system [m$]	0.2
		WHR system [m$]	7.5
		Total	15.9
	Installation costs [m$]	Ammonia tank [m$]	5.6
		Fuel cell [m$]	14
		Electric motor [m$]	5
		Ventilation system [m$]	0.2
		WHR system [m$]	0.02
		Total	24.82
	Research costs (40% of total CAPEX) [m$]		6.36
		Total [m$]	47.08
Annual additional costs (OPEX)	Fuel costs [m$]	Ammonia fuel [m$]	7.7
	O&M costs [m$]	Ammonia tank [m$]	0.6
		Fuel cell [m$]	0.1
		Electric motor [m$]	0.2
		Ventilation system [m$]	0.01
		WHR system [m$]	7.5
		Total	8.5
	CO2 tax [m$]		t.b.d.
		Total [m$]	16.2

Costs propulsion system with: WASP

To estimate the CAPEX and OPEX of new technologies, such as the WASP systems, is another challenge. Especially as not a lot of research is done regarding the costs for these propulsion systems, not as much as for the prediction of the CAPEX of the alternative fuels.
To estimate the installation and O$M costs of the WASP systems, the same percentages of the CAPEX costs is assumed. The costs for the propulsion system with WASP type 1 consists of the costs for the current engine and the costs for WASP type 1 system. For the propulsion system with WASP type 2, the extra costs of an electric motor have to be added.

For the CAPEX costs for most of the WASP systems (not kites and wind turbines) research of (Schinas & Metzger, 2019), (Clodic, Babarit, & Gilloteaux, 2018) and information of expert Giovanni Bordogna of BlueWASP are used. (Schinas & Metzger, 2019) states that Turbosails sails will cost 0.5$ per unit. In this price the installation costs is included as well which is 25% of these investment costs. For the Flettner rotor, (Schinas & Metzger, 2019) estimates a price of 1$m per unit. Again, the installation costs is included in these costs (25%). Bordogna confirms that the costs for the Flettner rotor that is used in this research, will be about 1 million dollar. Bordogna states that the maintenance costs of the WASP systems is about 2% annually of the purchasing and installation costs, so for the Flettner rotor this is 2% annually of 1 m$.

Therefore, in this costs analysis, for the installation 1/3 of the CAPEX costs of the total hardware of the WASP system and 2% of the CAPEX costs for the O$M costs are taken.
Research of (Clodic et al., 2018), gives the ratios of the CAPEX costs to each other. This analysis points out the different WASP systems and examines them on their performance, robustness, costs and feasibility. Looking at the cost grades, figures are given from 0 to 10. In these costs, the replacement time of the specific system is also included. This should be kept in mind by estimating the costs, because in this costs analysis, the lifetime of the WASP systems is not included in the CAPEX. This research grades the turbo sail and Flettner rotor an 8.5, the wing sail a 7.5 and the dyna rig and kite an 6.5 (Clodic et al., 2018). The lower grades for the rigid sails are thus

because of their relatively short lifespan, therefore they must be replaced more often.
For most of the WASP systems, a lifetime of 20 years is assumed (Nelissen et al., 2016). It is likely that the lifetime of these system will increase when these systems will be more developed. Because the kite and the dyna rig consist mostly of a softsail, the lifetime for these systems is much shorter. Roland Schmehl of the TU Delft states that the lifetime of a kite is 1 year and mentions that this is already quite positive. For the dyna rig, the lifetime of softsails are assumed and are set to be 3 years (Quantum Sails, 2016).

The research costs are different for each WASP system and their percentages are given in the previous section.

Kite

For the CAPEX of the kites, research performed by Roland Schmehl and Pietro Faggiani of the TU Delft is used (Faggiani & Schmehl, 2018b). They have already made a cost analysis of a pumping kite wind park. The CAPEX costs of one 100m^3 kite of this kite park is 98800$. As a result, for a 640m^3 kite, CAPEX costs 450000$ is assumed. Systems needed for the kite system, have the same value as the value of the kite in the reference research and do not increase when the kite increases.
This research also includes installation and maintenance costs of the entire kite park. Because this is much larger than one kite, the ratios mentioned earlier, are used to estimate the installation and O&M costs. Table 7.7 shows an overview of the costs when using a propulsion assisting kite.

Table 7.7: Costs kite

Kites			
Initial investment	CAPEX total hardware [m$]	HFO tank and current engine [m$]	0
		Kite [m$]	0.5
		Total	0.5
	Installation costs [m$]	HFO tank and current engine [m$]	0
		Kite [m$]	0.2
		Total	0.2
	Research costs (50% of total CAPEX) [m$]		0.25
		Total [m$]	1.65
Annual additional costs (OPEX)	Fuel costs [m$]	HFO fuel [m$]	2.1
	O&M costs [m$]	HFO tank and current engine [m$]	0.5
		Kite [m$]	0.01
		Total	0.51
	CO2 tax [m$]		t.b.d.
		Total [m$]	2.61

Dyna rig

The Dyna rig is a soft sail, like the kite, but does not need the complex control system that is necessary for kites. Because of this, the CAPEX costs are estimated on 400 000 $ per unit. 5 wingsails are installed and the research costs is 40% of the CAPEX costs of total hardware of the Dyna rig. The costs are shown in table 7.8.

Table 7.8: Costs dyna rig

Dyna rig			
Initial investment	CAPEX total hardware [m$]	HFO tank and current engine [m$]	0
		Dyna rig [m$]	2
		Total	2
	Installation costs [m$]	HFO tank and current engine [m$]	0
		Dyna rig [m$]	0.7
		Total	0.7
	Research costs (40% of total CAPEX) [m$]		0.8
		Total [m$]	6.2
Annual additional costs (OPEX)	Fuel costs [m$]	HFO fuel [m$]	2.1
	O&M costs [m$]	HFO tank and current engine [m$]	0.04
		Dyna rig [m$]	0.01
		Total	0.05
	CO2 tax [m$]		t.b.d.
		Total [m$]	2.15

Wing sail

The wing sail is more robust than the dyna rig as it includes a frame as well. Using the ratio given by (Clodic et al., 2018), the CAPEX costs are estimated on 450 000 $ per unit, so 3.6m$ in total, as 8 wing sails are installed. The costs for the wing sails are displayed in table 7.9.

Table 7.9: Costs wing sail

Wing sail			
Initial investment	CAPEX total hardware [m$]	HFO tank and current engine [m$]	0
		Wing sail [m$]	3.6
		Total	3.6
	Installation costs [m$]	HFO tank and current engine [m$]	0
		Wing sail [m$]	1.2
		Total	1.2
	Research costs (20% of total CAPEX) [m$]		0.72
		Total [m$]	10.32
Annual additional costs (OPEX)	Fuel costs [m$]	HFO fuel [m$]	2.0
	O&M costs [m$]	HFO tank and current engine [m$]	0.5
		Wing sail [m$]	0.07
		Total	0.6
	CO2 tax [m$]		t.b.d.
		Total [m$]	2.57

Turbo sail

The investment costs of the Turbo sail were estimated on 500.000$ per unit, of which 25% are the installation costs (Schinas & Metzger, 2019). So the CAPEX costs of one Turbo sail is 375.000$. 12 units need to be installed and the research costs are 40% of its total CAPEX costs. An overview of the costs are shown in table 7.10.

Table 7.10: Costs turbo sail

Turbo sail			
Initial investment	CAPEX total hardware [m$]	HFO tank and current engine [m$]	0
		Turbo sail [m$]	4.5
		Total	4.5
	Installation costs [m$]	HFO tank and current engine [m$]	0
		Turbo sail [m$]	1.5
		Total	0.2
	Research costs (40% of total CAPEX) [m$]		1.8
		Total [m$]	6.5
Annual additional costs (OPEX)	Fuel costs [m$]	HFO fuel [m$]	2.1
	O&M costs [m$]	HFO tank and current engine [m$]	0.5
		Turbo sail [m$]	0.09
		Total	0.6
	CO2 tax [m$]		t.b.d.
		Total [m$]	2.69

Flettner rotor

(Schinas & Metzger, 2019) states that the CAPEX costs of the total hardware of the Flettner rotor is 750.000$ per unit. On the Panamax Leda C, 6 Flettner rotors are installed. Because of the technology readiness level of this WASP system, the research costs are only 10% of the total CAPEX costs. An overview of the costs estimation for the Flettner rotor is given in table 7.11.

Table 7.11: Costs flettner rotor

Flettner rotor			
Initial investment	CAPEX total hardware [m$]	HFO tank and current engine [m$]	0
		Flettner rotor [m$]	4.5
		Total	4.5
	Installation costs [m$]	HFO tank and current engine [m$]	0
		Flettner rotor [m$]	1.5
		Total	1.5
	Research costs (10% of total CAPEX) [m$]		0.45
		Total [m$]	6.45
Annual additional costs (OPEX)	Fuel costs [m$]	HFO fuel [m$]	2.0
	O&M costs [m$]	HFO tank and current engine [m$]	0.5
		Flettner rotor [m$]	0.01
		Total	0.5
	CO2 tax [m$]		t.b.d.
		Total [m$]	2.51

Wind turbine

Wind turbines stand alone in the CAPEX costs of the WASP systems, therefore research is used from Cranfield University (UK) and University of Strathclyde (Scotland) (Kolios & Brennan, 2018). This research states that the CAPEX costs of one wind turbine of 5MW is around 5million$. Therefore, 300.000$ is estimated for the CAPEX costs. This is the WASP system with the lowest CAPEX costs.

The research costs of a wind turbine is 20% of the total CAPEX hardware. Table 7.12 shows an overview of the cost estimation of retrofitting the wind turbine on the reference ship.
Keep in mind that for this WASP type, an electric motor must be installed as well.

Table 7.12: Costs wind turbine

Wind turbine			
Initial investment	CAPEX total hardware [m$]	HFO tank and current engine [m$]	0
		Wind turbine [m$]	0.3
		Electric motor [m$]	5
		Total	0.3
	Installation costs [m$]	HFO tank and current engine [m$]	0
		Wind turbine [m$]	0.1
		Electric motor [m$]	5
		Total	5.1
	Research costs (20% of total CAPEX) [m$]		0.06
		Total [m$]	5.46
Annual additional costs (OPEX)	Fuel costs [m$]	HFO fuel [m$]	2.6
	O&M costs [m$]	HFO tank and current engine [m$]	0.5
		Wind turbine [m$]	0.01
		Electric motor [m$]	0.2
		Total	0.8
	CO2 tax [m$]		t.b.d.
		Total [m$]	3.4

Costs of propulsion system with: Solar

For the solar systems, guidelines stated by Glomeep and DNV.GL were used (Glomeep & DNV.GL, 2021a), specifically regarding the CAPEX and installations for solar systems on board of a vessel. This research states that the costs of solar modules for ships is currently about 0.6$/Watt of installed capacity. For installing these solar modules, cables and the mounting structure are needed as well. These costs are included in the installation costs and this price is set to 2.8 to 3.4 $/Watt of installed capacity (Glomeep & DNV.GL, 2021a). Because of this, for solar the installation costs are estimated to be 1.00.000$ and the total CAPEX costs are 180.000$ costs. This research expects this value to decrease over time.

Besides the costs of the solar system, the costs of the electric motor must be included as well. The fuel costs are discussed in the previous section. And for the O$M costs, 4.75% of the total CAPEX is used. This percentage is from Stopford (Stopford, 2009) and used in estimating O$M costs of maritime systems. Table 7.13 shows the costs for the solar panels when installing them on board of the Panamax Leda C.

Table 7.13: Costs solar

Solar			
Initial investment	CAPEX total hardware [m$]	HFO tank and current engine [m$]	0
		Solar system [m$]	0.2
		Electric motor [m$]	5
		Total	0.2
	Installation costs [m$]	HFO tank and current engine [m$]	0
		Solar system [m$]	1
		Electric motor [m$]	5
		Total	6
	Research costs (20% of total CAPEX) [m$]		0.04
		Total [m$]	6.24
Annual additional costs (OPEX)	Fuel costs [m$]	HFO fuel [m$]	2.6
	O&M costs [m$]	HFO tank and current engine [m$]	0.5
		Solar system [m$]	0.05
		Electric motor [m$]	0.2
		Total	0.8
	CO2 tax [m$]		t.b.d.
		Total [m$]	3.4

7.3 Total costs after 30 years

The total costs for the propulsion systems using renewable energy on board come close to each other. The costs for the propulsion systems will be analysed first. The most competitive technology will then be compared with the total costs of the propulsion systems using biofuel, hydrogen and ammonia.

Total costs after 30 years - renewable energy generation on board

The total costs of the propulsion systems using renewable energy on board, which include the WASP systems and solar systems, are analysed in this subsection.
Figure 7.2 shows the expenditures of these systems using an annual cumulative sum chart (per year over 30 years added to the year before). In this way, it is easier to see when one propulsion system becomes more expensive than the other.
In year zero the initial investment for each propulsion system is given, these are the total purchase costs of the new systems and is the starting point. There are 'step ups' for the years that systems need to be replaced, e.g. for the Dyna rig system, this is every three years. There are a lot of step ups at year 20 because most of the WASP systems have a lifetime of 20 years. The rest of the time the graphs shows a straight diagonal line with a constant slope, as it is assumed that the annual additional costs remain the same each year.
30 years is used as this is the standard lifetime of a bulk carrier (IMO, 2015). For the total expenditures, the carbon tax is not included and set here to be zero, in chapter 8, the CO_2 tax is included and its influence on the total costs will be analysed. Also, for this calculation it is assumed that the OPEX costs of the systems remain unchanged. These costs could also shift, which is explained in chapter 8.
Batteries are only used during emergencies or for peak shaving and therefore left out in this cost analysis.
The annual costs of the base case stay the lowest, this can be explained by the fact that no new equipment has to be purchased.
Of the propulsion systems using renewable energy on board, in lowest costs after 30 years, are the wing sail and the Flettner rotor. These systems have both a lifetime of 20 years and are somewhat cheaper than the other WASP systems. Besides this, their fuel costs are the lowest of the WASP systems as these systems have the best performances in terms of fuel reduction.
The highest lines belong to solar and the wind turbine. An explanation for this is the high fuel costs as these systems are connected to the main drive train, wherefore its efficiency will be decreased and the fuel costs will increase. Besides this, the costs for these systems also include the costs for an electric motor.
The highest total costs per tonne nodules for the WASP is for the dyna rig. The high costs of the Dyna rig can be explained by the fact that this system must be replaced every 3 years.
The most increasing lines belong to the WASP system of the kite. This is because the kite must be replaced every year.

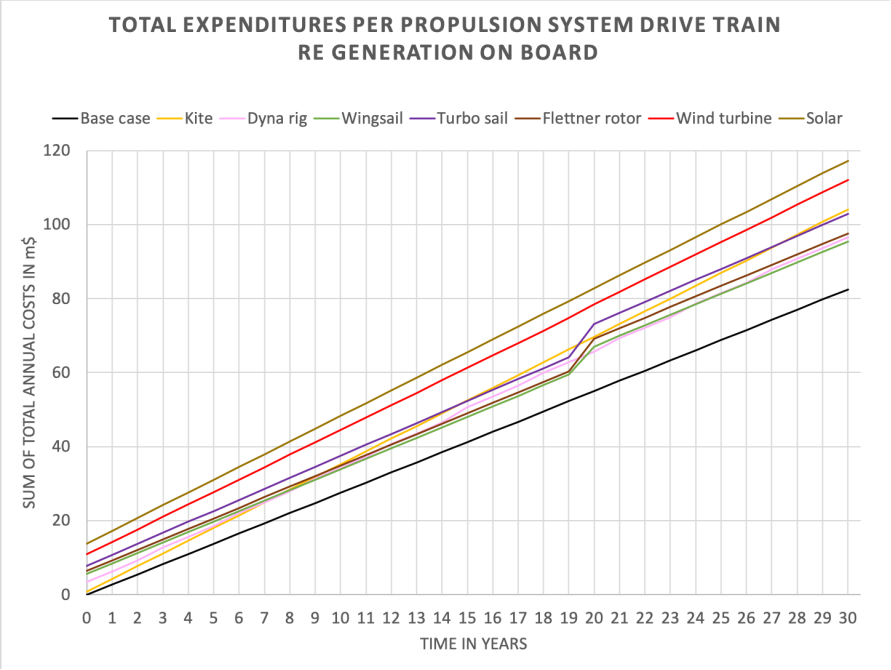

Figure 7.2: Expenditures for each total propulsion system with RE generation on board after 30 years

The highest total costs per tonne nodules for the RE on board systems are for solar systems, the wind turbine and dyna rig. The reason behind the high costs for the wind turbine and solar system is explained earlier, this is due to their increase in fuel costs and the extra costs for having an electric motor in their drive train. The high costs of the Dyna rig can be explained by the fact that this system must be replaced every 3 years.
What is notable, is that there seem to be major differences in the total costs per tonne nodules between the WASP systems. However, this is relative. In the next section the Flettner rotor will be plotted against the alternative fuels as comparison as a representative of the WASP systems.

Total costs after 30 years - alternative fuels, Flettner rotor

Figure 7.3 shows the expenditures of the propulsion system with the base case, Flettner rotor and alternative fuels in an annual cumulative sum chart.
As said before, the carbon tax is not included, the OPEX costs of the systems remain unchanged and batteries are left out in this cost analysis.
The initial investment for each propulsion starts in year zero. There are 'step ups' for the years that systems need to be replaced, for the WHR systems this is every ten years and for the fuel cells of hydrogen and ammonia this is every four years. This is the reason of the number of steps in the line of hydrogen and ammonia.
As shown in figure 7.2, the annual costs of the base case stay the lowest. Second place in lowest costs after 30 years, is the Flettner rotor. No other changes in the drive train have to be done. The most increasing lines belong to ammonia. The reason regarding this increase for ammonia, is that the energy content of ammonia is very low compared to the other fuel types and there-

fore the annual fuel costs are high. Besides this, every four years the fuel cell must be replaced, which is quite expensive. Comparing the alternative fuels, the lowest costs are for biofuel. This is because no other equipment is needed to install biofuel, only the fuel costs play a large role in estimating the expenditures on biofuel.

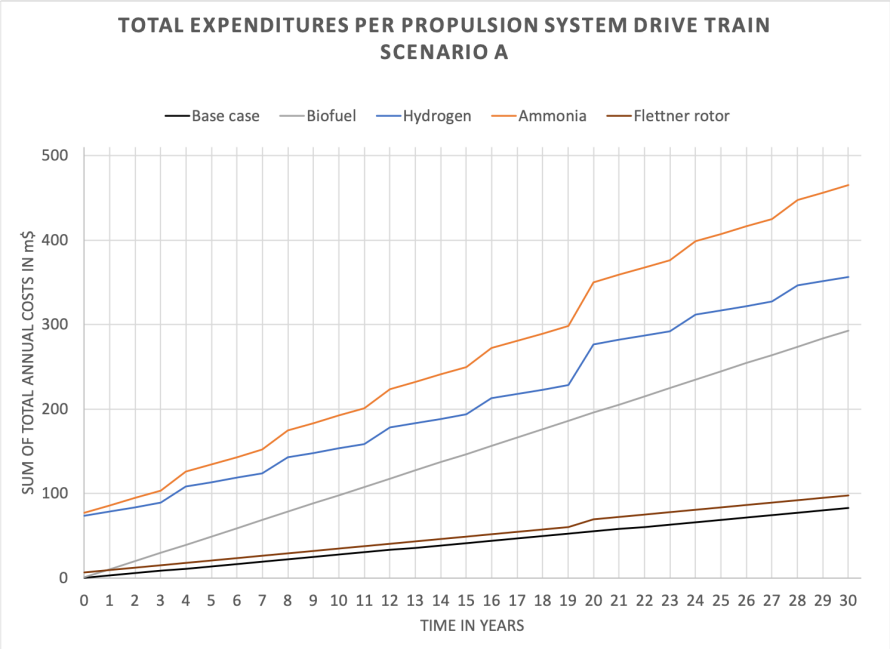

Figure 7.3: Expenditures for each total propulsion system after 30 years

8 | Three different scenarios concerning the energy transition

To understand which of the discussed systems and alternative fuels are likely to become the most cost-efficient in reducing emissions, is complicated. With cost-efficiency in this thesis is meant, the relation between the costs and the amount of emission reduction. The most cost efficient system is the optimum of low costs and a high emission reduction. The costs of each potential varies depending mostly on the fuel prices and the international policies and guidelines. The costs of the different systems differ as they depend on the scale of the market, the development period and the startup development time. A positive startup development period is when economies of scale are achievable. Only as the market will grow, the costs may decrease over time.

Achieving zero emissions in shipping by 2050, and even more by 2030, is a challenge, so determined action is needed. This is because, with a ship's lifespan of about 25-30 years and many markets for low-emission technologies still under development, concerted action is required involving multiple parties such as the shipping industry, governments, technology and fuel industries, representatives of the international shipping industry and others. Therefore, three different scenarios are outlined in this chapter over a time period of 30 years, assuming this is the lifespan of the Panamax Leda C.

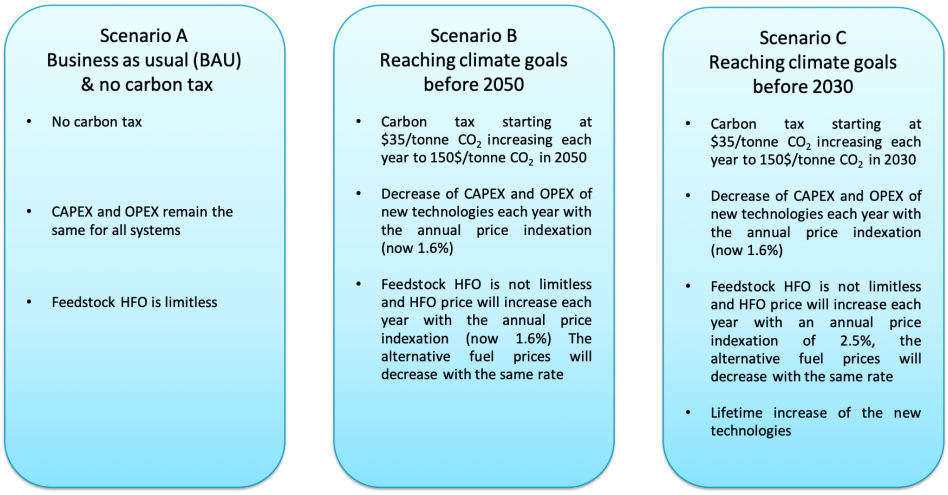

Figure 8.1: Overview scenarios

Scenario A is the business as usual (BAU) case, under the current policies and regulations, without a carbon tax. Scenario C is the situation when the strictest regulations regarding the amount of allowed emissions are met. Scenario B is of the improving propulsion systems the most feasible scenario as the CO_2 tax is expected to come (DNV.GL, 2019) and therefore the most likely scenario that will happen. Figure 8.1 gives an overview of the three different scenarios discussed in this chapter.

In this chapter per scenario the total costs per year over 30 years are considered (tables given in appendix 3.6). The resulting KPIs of each propulsion system can be found in chapter 3:

- Emission reduction per tonne collected nodules [%/tonne]
- Costs per tonne collected nodules [$/tonne]

For clarification, the most cost-effective propulsion system of the newly developed systems using renewable energy on board, will be chosen from scenario A. This 'pinned' propulsion system will be used for the comparison with the alternative fuels, for all scenarios.

8.1 Scenario A - Business as usual (BAU) without carbon tax

Scenario A is the business as usual (BAU) case without a carbon tax. This means that the costs paid for the different systems and fuels at the moment will remain the same over the next years. Although in chapter 7 is said at the moment the CO_2 tax is set on 35$/tonne, no carbon tax is included for this scenario.
In this section first the propulsion systems using renewable energy on board will be analysed. The most cost-effective propulsion system using renewable energy on board will be chosen. As all the costs of the WASP and solar systems are increased and decreased with the same rates, the proportions to each other will remain the same. This propulsion system is used for the comparison with the alternative fuels, for this scenario and for scenario B and C. For scenario A, this analysis is in the second part of this section.

Scenario A - for RE generation propulsion systems on board

The expenditures for scenario A for RE generation propulsion systems on board were already analysed in chapter 7 and shown in figure 7.2. The two resulting KPIs are given in this section for these RE systems.
Figure 8.2 shows the two resulting KPIs plotted against each other. On the y-axis the costs per tonne collected nodules is given and on the x-axis the emission reduction compared with the base case is given in percentage. At the left of the scatter plot, the base case, the different WASP systems and the solar system are given.
The most optimal propulsion system in terms of cost-effectiveness, stands at the bottom right of the scatter plot, here the largest percentage of emission reduction is given and the lowest costs. Here this is the Flettner rotor. This is explained by the assumption that not many adjustments have to be made to the current propulsion system, the Flettner rotor has a relatively long life time compared with other WASP system and the performances of the Flettner rotor are the highest. The solar panels are relatively expensive regarding their efficiency in reducing emissions.
The Flettner rotor is used in the next part of this section, against which the alternative fuels will be compared. This also applies to scenario B and C as the Flettner rotor is the most optimal system in terms of cost effectiveness.

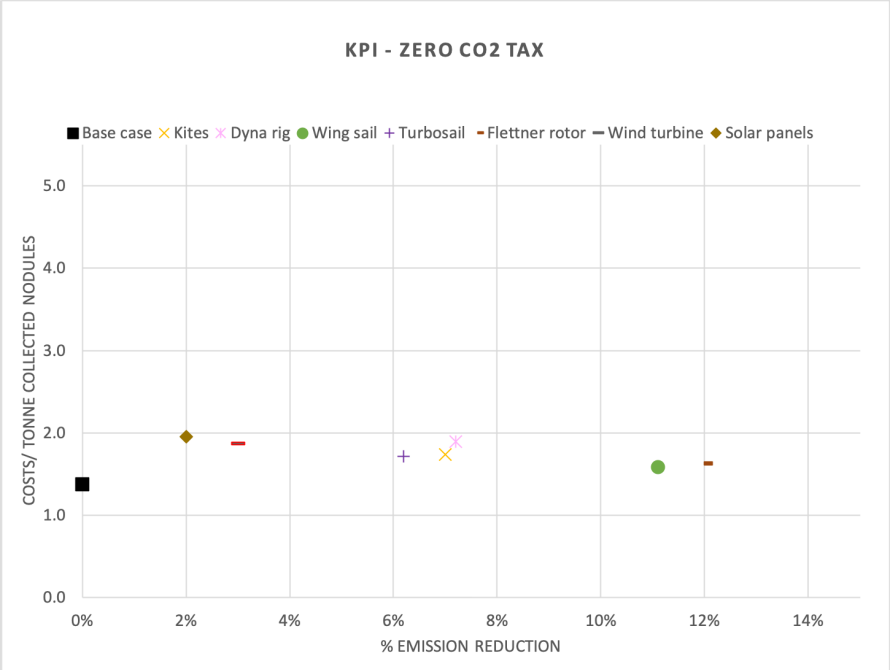

Figure 8.2: Resulting KPIs of scenario A for renewable energy generation on board

Scenario A - All propulsion systems

The annual expenditures for this scenario are given in figure 7.3 in chapter 7 and are analysed. In this subsection, the resulting KPIs for scenario A for the Flettner rotor, base case and alternative fuels is analysed.

Figure 8.3 shows the plot of the two resulting KPIs. At the left of the scatter plot, the base case and the Flettner rotor are given. At the right the three alternative fuels discussed in this report, are given. As said before, in chapter 2 and 4, it is assumed that the alternative fuels mentioned in this report, reduce the emissions with 100% and these fuels originate from sustainable energy sources.

As explained before, the most optimal propulsion system in terms of cost-effectiveness, stands at the bottom right of the scatter plot. The alternative fuel that is the most cost-effective, is biofuel. This is explained by the assumptions that not many adjustments have to be made to the current propulsion system, the costs of the fuel will be comparable and there are zero emissions using biofuel.

On the bottom left the base case is plotted. The base case has the lowest costs per collected nodules, but an emission reduction of 0%.

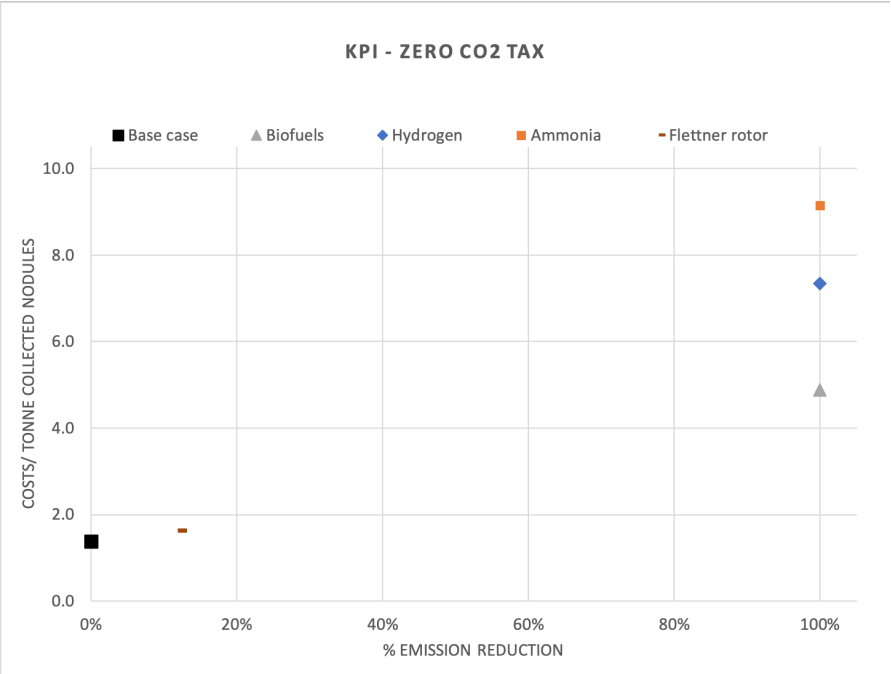

Figure 8.3: Resulting KPIs of scenario A

8.2 Scenario B - achieving the climate goals before 2050

Scenario B is the most feasible scenario when meeting regulations and therefore the most likely case that will happen. It is predicted that stricter policies and regulations will be established concerning emissions to achieve the sustainability goals set by the IMO, some driven by existing regulation and some by market forces. A higher carbon tax will probably be one of the regulations. As said before, at the moment it is set at 35$/tonne carbon emissions and is predicted to become 150$/tonne in 2050. Besides the carbon tax another regulation concerning the sustainability will influence the general costs. It is very likely the price for HFO will rise as HFO is not endless. For this scenario an fuel price increase of 1.6% each year for HFO is assumed. This 1.6% is the indexation rate (Stopford, 2009). Indexation compensates for the inflation. By using indexation, the purchase price of an investment can be adjusted to reflect the impact of inflation. The inflation rate at the moment is 1.24%, as said before in chapter 3.
Besides the fuel price increase of 1.6% for HFO, for this scenario it is expected that the prices of the alternative fuels will decrease with 1.6% each year as more research will be done and a better network will be build. Also, a minimum energy efficiency level is set by the IMO, which will increase the fuel efficiency, this is taken into account in the decreasing fuel price.
Another point expected in this scenario is the drop in OPEX costs for the new systems. New systems will in time be more commonly used, as more will be made and they will be more and more developed, so the overall prices will fall. A decrease of 1.6% has been assumed (indexation rate -1.6%).

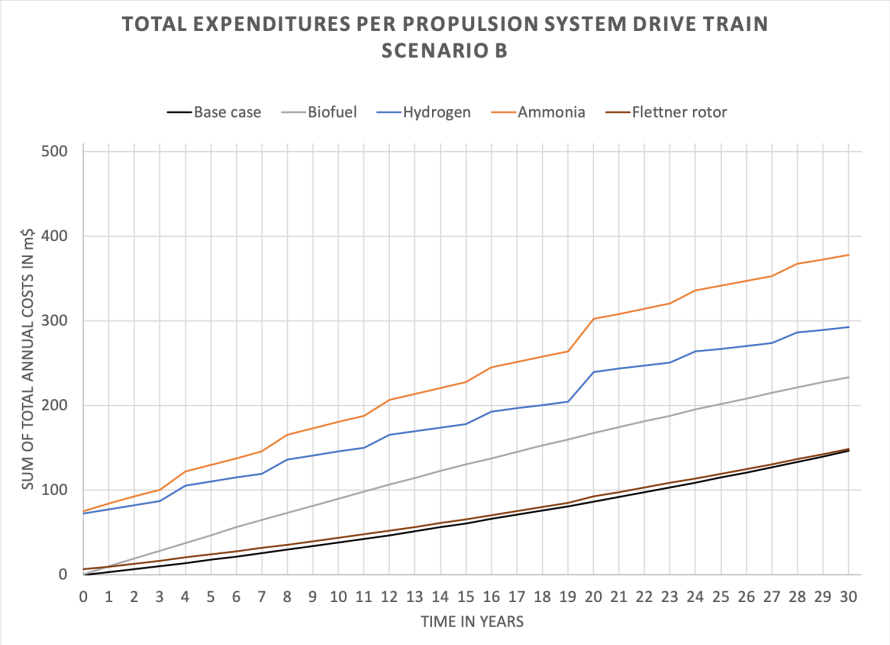

Figure 8.4: Expenditures for each total propulsion system after 30 years per tonne collected nodules for scenario B

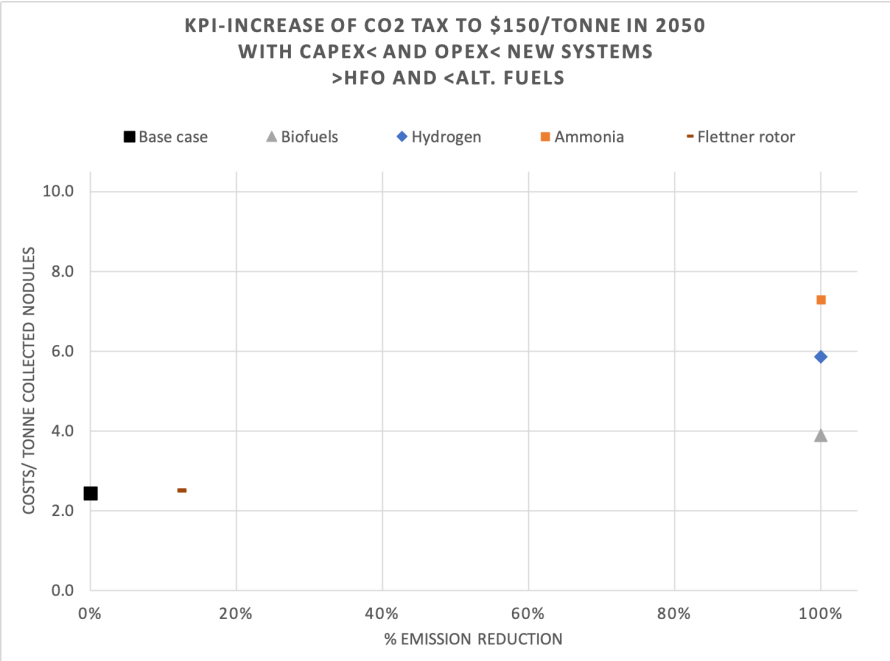

Figure 8.5: Resulting KPIs of scenario B

Looking at the annual expenditures in figure 8.4, the lines are gradually steeper for the WASP system (Flettner rotor is chosen) and the base case. Although the OPEX costs of the Flettner rotor decrease, the expenditures will keep increasing. This is because these systems can not be used solely, but depend on other propulsion systems, in this case the 2 stroke diesel engine which runs on HFO. Other factors are the increasing carbon tax and the HFO fuel price, that both will not be outweighed by the reduction of their OPEX costs.
The graph lines for the costs for the alternative fuels slowly flatten. The reason for this, is that the carbon tax and the fuel price will drop for the alternative fuels. However, because the hydrogen and ammonia fuel cell needs to be replaced every 4 years, which is the unchanged lifetime of this fuel cell, the expenditures of hydrogen and ammonia will be more expensive. As can be seen from figure 8.4, for this scenario, no renewable energy propulsion system expenditures will be lower than the base case. After more than 30 years the Flettner rotor has lower expenditures than the base case for this scenario, which is a positive outcome in terms of sustainability.

The resulting KPIs for this scenario are shown in figure 8.5. Comparing this figure with figure 8.3, the propulsion systems on the left go all up and the alternative fuels will go down, which is because of the carbon tax and the change in fuel prices. The Flettner rotor is the most cost-efficient outcome for this scenario and comes to almost the same costs per tonne nodules as the base case. For the alternative fuels, the most cost-effective is biofuel.

8.3 Scenario C - achieving the climate goals before 2030

This last scenario is the situation in which the conditions to reach the climate goals before 2030 are described. Therefore, strict regulations are necessary in terms of reduction of emissions. For this scenario the carbon tax will start in 2021 at 35$/tonne CO_2 and will increase to 150$/tonne in 2030. This is a raise of almost 13$/tonne per year. The carbon tax will keep rising with this rate, also after 2030. Another strict rule for this scenario compared to the previous one, is the increase of the HFO fuel price of 2.5% per year. The increase of the lifetime for the new systems is also a reasonable but expected difference. The lifetime of the WASP systems and the fuel cell will shift from 4 years to 6 years.
The lifetime of the kite is short and will stay the same, therefore one year remains set for a kite. According to R. Schmell (TU Delft) a life time of one year is already 'long' for a kite.
Expectations for the Dyna rig are a little bit more positive, it will need to be replaced every 4 years instead of 3 years.

The resulting annual expenditures for the propulsion systems over 30 years are given in figure 8.6. Looking at these expenditures, they will increase more and more for the Flettner rotor as well as for the base case. The costs for the propulsion systems using alternative fuels will flatten; in the end all alternative fuels will become lower in costs than the base case. The expenditures for biofuel will be lower after 28 years than that of the base case and for hydrogen this will happen several years later. The reason for the relatively low expenditures of biofuel is the fact that no equipment needs to be replaced within this time frame and that the fuel costs will keep decreasing.
In figure 8.7 the resulting KPIs for this scenario are plotted. In this figure can be seen as well that the costs per tonne nodules for the propulsion system using Flettner rotors are lower than using the base case.
The resulting costs per collected nodules are even closer together for the alternative fuels compared with the previous scenario. The resulting costs of biofuel will also become lower than the base case. The propulsion systems using hydrogen and ammonia as main energy source stay more expensive than the base case.

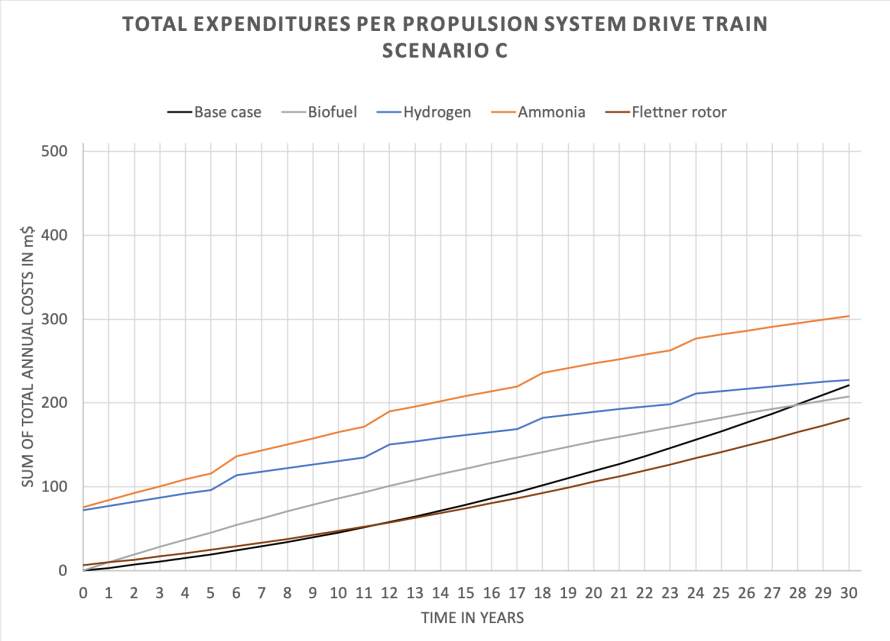

Figure 8.6: Expenditures for each total propulsion system after 30 years per tonne collected nodules for scenario C

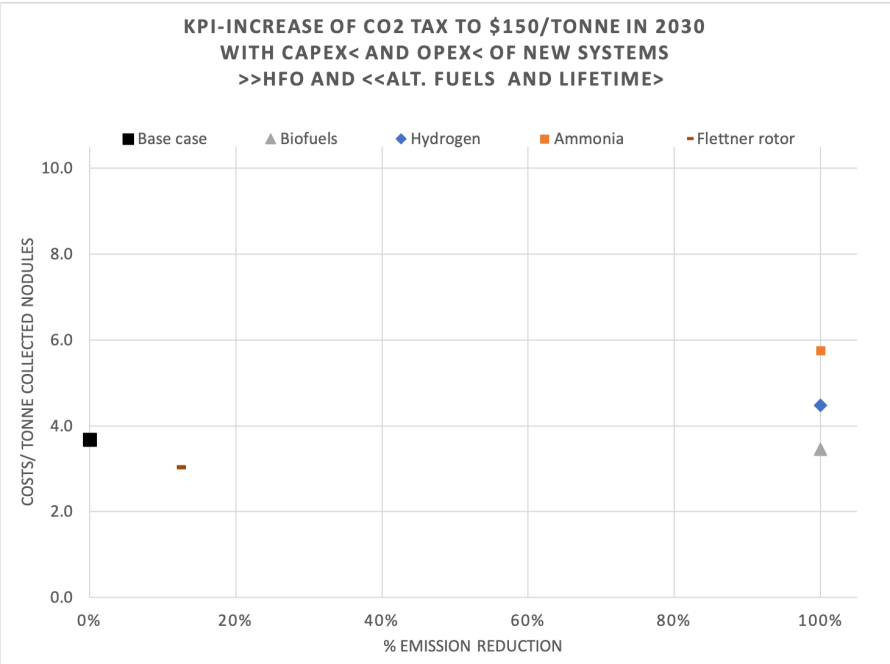

Figure 8.7: Resulting KPIs of scenario C

Comparison between the three scenarios

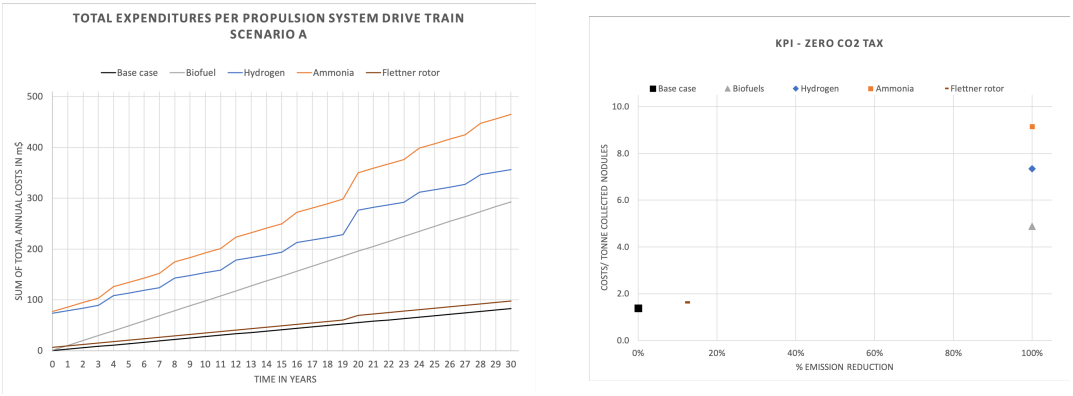

Figure 8.8: Scenario A - Expenditures and resulting KPIs

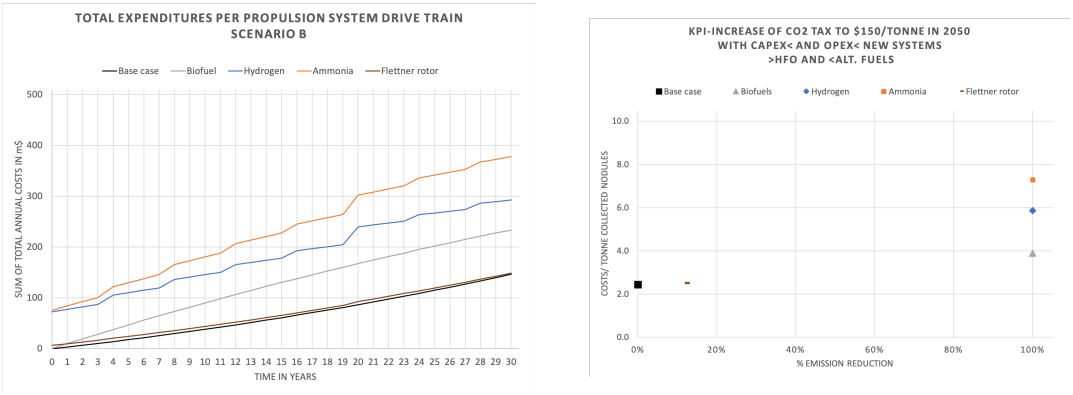

Figure 8.9: Scenario B - Expenditures and resulting KPIs

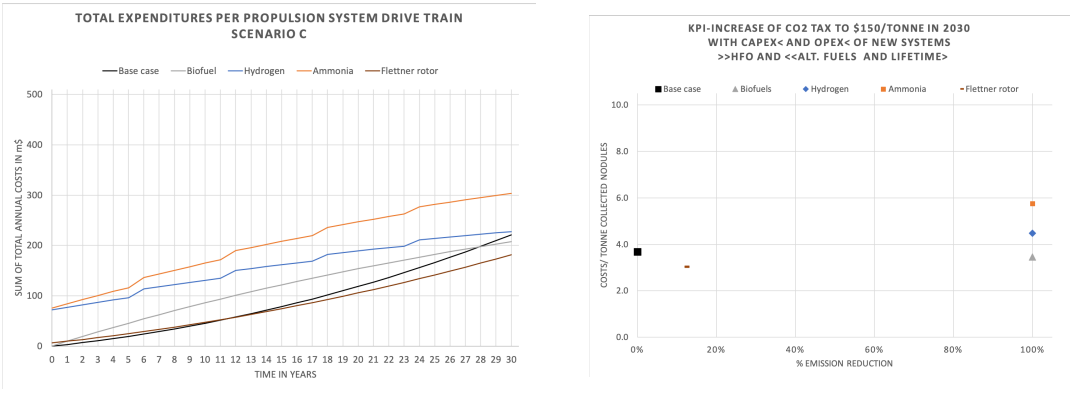

Figure 8.10: Scenario C - Expenditures and resulting KPIs

From these scenarios it can be concluded that the resulting costs depend to a large extent on the fuel prices and the CO_2 tax set.
The most likely scenario that will occur, is scenario B, due to feasibility as explained earlier. It follows from scenario B that the most cost-effective system is a hybrid propulsion system. The conclusion from the WASP systems in terms of sustainability, the Flettner rotor is the most cost-efficient. Therefore, it can be advised to use this system together with HFO as main energy source.
However, in terms of costs, the base case will still be the least expensive. Because of this, a CO_2 tax must be introduced and implemented to make the hybrid propulsion more attractive. Looking at the graph, figure 8.5, the lines will cross after 30 years, so after this period this will likely be a more attractive solution.
Looking at shifting to alternative fuels, this is still very expensive. Although biofuels are most cost-efficient of the alternative fuels, hydrogen is advised over biofuels as for biofuels there are several side notes concerning their emissions.

As can be seen from the resulting KPI scatter plots, there is a large gap for the percentage of emission reduction between the Flettner rotor (which also is the case for the other WASP and solar systems) and the alternative fuels. A hybrid propulsion system, using different energy sources can fill this gap. For example the combination of WASP with solar. But as stated in chapter 7, the efficiency of the drive train of the solar system is lower than that of the base case. So, combining a WASP type 1 system with solar, will negatively impact the output of the total drive train. Adding the systems together will not contribute to a large effect and will increase the total costs of this hybrid propulsion system.
What should be noted also, is that the batteries are left out from the cost determination. As said before, batteries are now only used during emergencies or for peak shaving. Batteries could also be used as one of the energy sources when fully charged in addition to use as energy storage. When batteries are used in that way, the costs of these hybrid systems will increase, but the emissions will decrease as well, although the batteries have to be loaded ashore using other (renewable) energy sources. The feasibility of this mentioned hybrid solution together with the likely increasing complexity of the system must be looked into as well.

9 | Conclusions

In this research available technologies that will help the shipping sector to achieve the climate goals set by the IMO are examined. The goal of this research was to investigate the possibilities to apply renewable energy sources to a vessel that transports polymetallic nodules from the Clarion-Clipperton Zone to Mexico in order to reduce the carbon footprint.
The propulsion systems using renewable energy discussed are solar systems and WASP systems. The WASP systems discussed in this thesis are the kite, Dyna rig, Wing sail, Turbosail, Flettner rotor and wind turbine. Besides energy generation on board, alternative fuels as biofuel, hydrogen and ammonia are discussed as well.
Two different key performance indicators (KPIs) were set to analyse the different propulsion systems. These KPIs are the emission reduction per tonne collected nodules in %/tonne and the costs per tonne collected nodules in $/tonne.

Looking at the overall performances in terms of emission reduction (KPI 1) of the WASP systems and comparing these with the maxima of their performances stated in chapter 2, it can be concluded that their performances are not that high. The reason for this are the weak wind conditions on the route. Another conclusion that can be drawn is that the WASP systems need to be placed hybrid, in combination with another energy source. In this research this energy source is HFO. The best performances for the WASP systems are that of the Flettner rotor and the lowest performances have been reached with the wind turbine at a ship speed of 12 knts. With a lower ship speed, even larger reductions turned out. However, these were economical less attractive as an extra ship would be needed for the fleet consisting of the determined Panamax bulk carrier, the Leda C. Of all the RE on board systems, it can be concluded that the lowest fuel consumption reduction is reached when using only solar systems as second propulsion. This is due to the fact the ship requires a lot of energy wherefore a solar system with a large area is needed and the area is limited on the vessel.
It can be concluded that the drive train of hydrogen (with fuel cell and electric motor) is much more efficient (50% of the base case and 71% of the fuel cell and electric motor combination). The same applies to the drive train with ammonia. The drive trains for WASP type 2 (wind turbine) and solar systems are the least efficient, 42%. This is due to the added electric motor. Looking at the storage of these alternative fuels, biofuels can be stored in the current fuel tanks and do not exceed the current tank volume. Hydrogen storage will exceed the tank capacity of the base case with 140%, this is due its low energy density (MJ/m^3) and ammonia storage will exceed the tank capacity of base case with 50%. Keep in mind that for all alternative fuels it is required that the production of the sustainability-certified alternative fuels has to be in such quantities that they can fully replace the HFO as used in the current engine.

KPI 2 examined the costs of the different propulsion systems. The highest costs for the propulsion systems generating energy on board, is for solar and the wind turbine (WASP type

2), this is due to their low drive train efficiency. The lowest costs are for the WAPS systems using a wing sail and the Flettner rotor.
The costs for all alternative fuels result to be very high. This is because the current fuel price for these alternative fuels is very high. The costs by using hydrogen and ammonia are even higher due to the fact that the costs for renewing the fuel cell are added every 4 years and the costs for the waste heat recovery (WHR), necessary for the fuel cells to increase their efficiency from 60% to 80%, is quite expensive as well.
It can be concluded that KPI 2 is largely determined by fuel prices.

The most cost-effective technology for the RE on board systems is the Flettner rotor and for the alternative fuels this is biofuel. All propulsion systems discussed will only be attractive when the CO_2 tax will increase. Although the annual costs of biofuels are lower than that of hydrogen, hydrogen is advised over biofuels as for biofuels there are several side notes concerning their emissions. It is concluded that the higher the carbon tax, the more attractive the alternative fuels become in terms of cost effectiveness. Comparing the energy content of the alternative fuels, the energy content (MJ/kg) of ammonia is very low. This ensures high annual fuel costs, especially compared with hydrogen which has much lower annual fuel expenditures.

Advice for Allseas

Of the technologies considered, it is reasonable to anticipate that the costs for conventional components will not change significantly. However, the costs for fuel cells, batteries, electric motor, WASP and solar system could all reduce significantly. These costs will decrease, especially if they become important components of the decarbonisation in another sector or if these technologies are more developed and elaborated during the energy transition of the shipping sector.
If nothing changes, the advice for Allseas will be to not install a sustainable energy propulsion system. Because all investigated systems will be more expensive than the base case.
If case regulations make it necessary to reduce emissions, it is advised to install the Flettner rotor in hybrid with the current engine as concluded in chapter 8 using the resulting KPIs.
All in all, HFO is becoming scarce, and future international legislation concerning the maritime environment will push and accelerate the process of the transition to renewable energy and green power systems for the shipping sector. Technology and processes are currently low in terms of maturity but have definite potential for improvements and economies of scale.

This research includes two different aspects to assess the different options, from the sustainable point of view and the business point of view.
Previous investigations only explained the performances of new technologies, but none of these studies have listed all the options and no study has compared them with each other on both performances and total costs.
Although this thesis describes only one case study, it is the first report that compares WASP systems, solar systems and biofuels regarding the emission reduction, the costs and their feasibility.

10 | Recommendations

The results of this study mostly depend on assumptions and simplifications made. The main reason behind this, is the lack of information currently available. Because of this, the reliability of the results presented in the previous chapters is influenced. In this chapter recommendations are given for further research to make the outcomes of this thesis more certain and to elaborate the results.

First of all, the goal of this research was to look at different energy sources that will reduce emissions and pollutants. This can also be done by making the ship more efficient with the use of different systems. For example, installing an exhaust scrubber, advance the rudder and propeller or install a speed nozzle.A speed nozzle is a non-rotating nozzle placed at the propeller to improve its efficiency.
Besides these devices, lowering speed can reduce the fuel consumption of the vessel, but than more ships are needed or larger ships to compensate, or more days at sea are required to do the same amount of transport work (Abbasov, 2020). In this thesis an optimum for the ship speed was found at 11.5 knts. All this confirms the fact that more research has to be done to understand the consequences of speed reduction and the effect this has on the total fuel consumption of the fleet but also on the WASP systems.

A route optimization device is another device that can make this transport more efficient. Route optimization uses global weather forecasts to build optimal routes and to avoid storms and undercurrents. For the WASP systems it can also be used to adjust the route in order to increase the performances of the WASP systems. This will improve the safety and will save fuel. Research regarding route optimization is required to find the optimal route to decrease the fuel consumption even more.

What is not included in the calculations in this thesis, but will play a role on the background, is when newer generation ships will enter the fleet. Since 2012, the Marine Environment Protection Committee (MEPC) of the IMO approved several guidelines assisting in implementation of the mandatory regulations on energy efficiency for new ships and the Ship Energy Efficiency Management Plan (SEEMP) for all ships. Meaning that from 1 January 2013 new ship design needs to comply with the reference level for their ship type, which is tightened incrementally every five years to keep pace with development of new efficiency and reduction measures. The Energy Efficiency Design Index (EEDI) is developed for the largest and most energy intensive segments of the world fleet (IMO, 2013).
This thesis examines only retrofit (improvement of existing vessels) of new energy sources on the Panamax Leda C. It is expected that when building a new vessel and adapt it to the new energy source, such as hydrogen or a WASP system, the new propulsion system will function more efficient and the fuel consumption will decrease as well. Besides examining the performance of this option when using a new vessel, it is also recommended to investigate the final costs to have

a complete picture of this option.

Multiple energy sources were examined, different fuels, wind and solar systems. Hydrogen is discussed only in liquid form; as is concluded from chapter 2, hydrogen in gas form gives an even larger storage problem. However, at the moment, research is also performed with solid hydrogen combined with other particles. In this way the hydrogen can be stored in powder form with a lower energy density (MJ/m^3) so a much smaller storage capacity is needed.
Another energy source but not discussed in this report, is nuclear energy. At the moment thorium nuclear energy is considered as an energy source to provide power to a vessel. Thorium is more efficient than fossil fuel and generates no carbon emissions as a byproduct. Also, their energy density (MJ/m^3) is very high, so high that only a cube of the size of a hand is needed to provide energy for an entire ship.
To find out if these new technologies are viable, safe, feasible and could indeed be options as main energy sources for the Panamax Leda C, research is necessary.

Three different alternative fuels are discussed in this project, biofuels (HVO), hydrogen and ammonia. Other fuels can be used as well, such as LPG, LNG and methanol (mentioned in chapter2). As concluded in this report, at the moment these other alternative fuels cannot reduce emissions completely. However, more research has to be done about alternative fuels to investigate the possibility and way to improve their emission reduction.
Concerning the alternative fuels discussed in this thesis (biofuels, hydrogen and ammonia), it is assumed that these raw materials are limitless, that they all are generated using renewable energy sources, they reduce harmful emissions completely and their network is already laid down. To verify the conclusion of this report, research into the production of these alternative fuels needs to be done as well.

As how the systems will develop and the impact of sustainability regulations is uncertain, different scenarios are sketched in this report. A more comprehensive analysis using more detailed modeling consistent with another approach could lead to different results. In the time that was used for this study, three different pragmatic and proportional scenarios were investigated. It should be noted that these scenarios have limitations and therefore the results should be considered as indicative.
Also, whether the systems discussed in this study will result in a taking a share of overall shipping energy sources, or if practical limits on production causing prices to rise remains unknown and needs further work.
Another scenario which is interesting to look into, is the influence of a crisis, such as the Covid-19 pandemic that slowed down the growth of the global economy. This can decrease the annual ship's sailing days, the sailing efficiency and therefore has influence on the costs and performances of the different propulsion systems using renewable energy on board. To draw conclusions from this scenario, further research is necessary.

Lastly, this project started with a research about the current state of sustainable technologies that can be installed on vessels. Sustainable technologies and systems that are currently under development. What not had been considered in this research, are new possibilities that do not yet exist. Or sustainable energy generation options, not on board, but, for example, on the Hidden Gem or at the CCZ. Options such as floating wind turbines or floating solar systems in the middle of the pacific where renewable energy can be collected. To answer the question to what other options are there, which are feasible and fit for this case, more research is needed.

References

Abbasov, F. (2020). *Shipping and the environment.* Retrieved from https://www.transportenvironment.org/what-we-do/shipping-and-environment

Abramowski, T., & Cepowski, T. (2013, 09). Preliminary design considerations for a ship to mine polymetallic nodules in the clarion-clipperton zone.. doi: 10.13140/RG.2.1.1977.9284

Airseas. (2018, Sept). *Seawing the automated kite that tows ships...* Retrieved from https://www.airseas.com/assets/media/documents/Press-Book-Sept2018.pdf

Amos, W. A. (2014). *Costs of storing and transporting hydrogen and ammonia.* Retrieved from https://www.energy.gov/sites/default/files/2014/03/f12/25106.pdf

a.o., L. J. (2020). Retrieved from https://www.dentons.com/en/insights/alerts/2020/november/26/the-dutch-carbon-emission-tax

Autonaut. (2020). *Autonaut.* Retrieved from https://www.autonautusv.com

Battelle Memorial Institute. (2016). *Manufacturing cost analysis of 100 and 250 kw fuel cell systems for primary power and combined heat and power applications.* Retrieved from https://www.energy.gov/sites/prod/files/2016/07/f33/fcto_battelle_mfg_cost_analysis_pp_chp_fc_systems.pdf

Boonstra, S. (2020). *An investigation of the internal airflow system behavior of a turbosail.* Retrieved from http://resolver.tudelft.nl/uuid:24bd44e8-36c9-485c-bd8d-e47a5bb07931

Bordogna, G. (2020). *Aerodynamics of wind-assisted ships: Interaction effects on the aerodynamic performance of multiple wind-propulsion systems.* doi: https://doi.org/10.4233/uuid:96eda9cd-3163-4c6b-9b9fe9fa329df071

Bordogna, G., Markey, D., Huijsmans, R., Keuning, L., & Fossati, F. (2014). Wind-assisted ship propulsion: a review and development of a performance prediction program for commercial ships. In S. Tan, X. Wang, W. Gho, & J. Chua (Eds.), *Proceedings of the 11th international conference on hydrodynamics (ichd 2014)*. ICHD. (ICHD 2014: 11th International Conference on Hydrodynamics ; Conference date: 19-10-2014 Through 24-10-2014)

Brown, T. (2020). Retrieved from https://www.ammoniaenergy.org/articles/industry-report-sees-multi-billion-ton-market-for-green-ammonia/

Carlson, O., & Nilsson, P. A. (2014). *Development and demonstration of new technology for the use of wind turbines on ships, final report.* Retrieved from hhttps://www.chalmers.se/SiteCollectionDocuments/Energy20och20miljÃű/Elteknik/Final20report.pdf

Cepowski, T., & Kacprzak, P. (2019). An analysis of vertical shear forces and bending moments during nodule loading for a standard bulk carrier in the clarion-clipperton zone. *60 Scientific Journals of the Maritime University of Szczecin, no. 60 / 2019*, 184-191. Retrieved from http://repository.scientific-journals.eu/handle/123456789/2566 doi: 10.17402/388

C-job. (2015). *R&d project - flettner freighter.* Retrieved from https://c-job.com/project/rd-project-flettner-freighter/

Clodic, G., Babarit, A., & Gilloteaux, J.-C. (2018). Wind propulsion options for energy ships. In *International conference on offshore mechanics and arctic engineering* (Vol. 51975, p. V001T01A002).

Cousteau. (2011). *Cousteau's turbosail.* Retrieved from https://www.cousteau.org/legacy/technology/turbosail/

CRAIN. (2010). *Suction wing propeller.* Retrieved from http://site.craintechnologies.com/index.php/en/wind-propulsion-en/suction-wing-en

Cummins, K. (2012, 05 09). *Harnessing the sun, the wind and the sea with e/s orcelle.* Retrieved from https://www.offshore-energy.biz/nyk-steps-into-the-future-with-super-eco-ship-2050/

Daluar Hussain Sumon, M. (2017, 12). A conceptual analysis of green ship technology using wind propulsion system to reduce fuel consumption and emission..

DeCicco, J. (2016, October 5). Biofuels turn out to be a climate mistake – here's why. *The Conversation*. Retrieved from https://theconversation.com/biofuels-turn-out-to-be-a-climate-mistake-heres-why-64463

Dezem, V. (2021). *Why hydrogen is the hottest thing in green energy.* Retrieved from https://www.bloomberg.com/news/articles/2021-06-19/why-hydrogen-is-the-hottest-thing-in-green-energy-quicktake

Dimitriadis, A., Natsios, I., Dimaratos, A., Katsaounis, D., Samaras, Z., Bezergianni, S., & Lehto, K. (2018). *Evaluation of a hydrotreated vegetable oil (hvo) and effects on emissions of a passenger car diesel engine.* doi: 10.3389/fmech.2018.00007

DNV.GL. (2016). *Liquefied gas carriers with independent cylindrical tanks of type c.* Retrieved from https://rules.dnv.com/docs/pdf/DNV/CG/2016-02/DNVGL-CG-0135.pdf

DNV.GL. (2019, July). *Assessment of selected alternative fuels and technologies.*

DNV.GL. (2019). *Comparison of alternative marine fuels.* Retrieved from https://safety4sea.com/wp-content/uploads/2019/09/SEA-LNG-DNV-GL-Comparison-of-Alternative-Marine-Fuels-2019_09.pdf

DNV.GL. (2020). *Study on electrical energy storage for ships.*

Donker, I., van Herwaarden, P., Stuurman, L., & van Zutphen, O. (2010, 01 25). *Energy from the sea for seagoing vessels.*

DSEC. (2016). *Technical development overview.* Retrieved from https://dsec.com/english/04_rd/rd_01.php

DualTemp. (2020). *Ammonia machinery room requirements.* Retrieved from https://dualtempclauger.com/wp-content/uploads/2020/04/DTC-Engineering-Bulletin-4.pdf

Dykstra-NA. (2013). *Wasp (ecoliner) / sailing cargo ship.* Retrieved from https://www.dykstra-na.nl/designs/wasp-ecoliner/

Eco Marine Power. (2016). *Eco marine power research institute | research and development.* Retrieved from https://www.ecomarinepower.com/en/research

Econowind. (2019). *Flatrack ventifoil.* Retrieved from https://www.econowind.nl

Eirik Bøckmann, S. S. (2011). Wind turbine propulsion of ships. *Norwegian University of Science and Technology Department of Marine Technology*. Retrieved from https://www.sciencedirect.com/science/article/pii/S0029801816301718

Entec. (2002). *2. quantification of ship emissions.* Retrieved from https://ec.europa.eu/environment/air/pdf/chapter2_ship_emissions.pdf

Faggiani, P., & Schmehl, R. (2018a). *Design and economics of a pumping kitewind park.* Springer. doi: https://doi.org/10.1007/978-981-10-1947-0_16

Faggiani, P., & Schmehl, R. (2018b). Design and economics of a pumping kite wind park. *Airborne Wind Energy e Advances in Technology Development and Research*, 391e411.

Fernando, J. (n.d.).
Fernando, J. (2021, 4). *Capital expenditure (capex)*. Retrieved from https://businesstown.com/articles/depreciation-and-amortization-basics/
Fulwood, M. (2021). The role of hydrogen in the energy transition.
Glomeep & DNV.GL. (2021a). *Solar panels.* Retrieved from https://glomeep.imo.org/technology/solar-panels/
Glomeep & DNV.GL. (2021b). *Waste heat recovery systems.* Retrieved from https://glomeep.imo.org/technology/waste-heat-recovery-systems/
"Grow". (n.d.). *Technology readiness levels.* Retrieved from https://www.grow-offshorewind.nl/technology-readiness-levels
Hanania, J., Stenhouse, K., & Donev, J. (2016). *Energy education - anthropogenic carbon emissions.* Retrieved from https://energyeducation.ca/encyclopedia/Anthropogenic_carbon_emissions#cite_note-IPCC_SREX-2
Healy, S., & Graichen, J. (2019). *Impact of slow steaming for different types of ships carrying bulk cargo.* Retrieved from https://seas-at-risk.org/images/pdf/190507_Impact_of_Slow_Steaming_Final_Report.pdf
Hellenic Shipping News. (2018, 06 18). *Aquarius eco ship project: Japanese companies push for renewable energy in vessels.* Retrieved from https://www.hellenicshippingnews.com/aquarius-eco-ship-project-japanese-companies-push-for-renewable-energy-in-vessels/
Hsieh, e. a., C. (2017). *Biofuels for the marine shipping sector, an overview and analysis of sector infrastructure, fuel technologies and regulations.*
IMO. (2013). *2013 guidance on treatment of innovative energy efficiency technologies for calculation and verification of the attained eedi.* Retrieved from https://www.classnk.or.jp/hp/pdf/activities/statutory/eedi/mepc_1-circ_815.pdf
IMO. (2015). *Improving the safety of bulk carriers.*
Inerjy. (2015). *Ecovert™ 300: Next generation of vertical axis wind power turbines.* Retrieved from https://www.inerjy.com/ecovert/
Inhabitat. (2008, 02 26). *The suntory mermaid ii wave-powered boat.* Retrieved from https://inhabitat.com/transportation-tuesday-the-wave-powered-boat/
IRCLASS. (2014).
IWSA. (2016). Seagate sail. *IWSA*. Retrieved from http://wind-ship.org/seagate-sail/
JSTRA & MLIT. (2020, march). *Roadmap to zero emission from international shipping.* Retrieved from https://wwwcdn.imo.org/localresources/en/OurWork/Environment/Documents/Air%20pollution/Roadmap%20to%20Zero%20Emission%20from%20International%20Shipping%20-%20Japan%20March%202020.pdf
Julià, E., Tillig, F., & Ringsberg, J. W. (2020). Concept design and performance evaluation of a fossil-free operated cargo ship with unlimited range. *Sustainability*, *12*(16). Retrieved from https://www.mdpi.com/2071-1050/12/16/6609 doi: 10.3390/su12166609
Kim, K., Roh, G., Kim, W., & Chun, K. (2020). A preliminary study on an alternative ship propulsion system fueled by ammonia: Environmental and economic assessments. *Journal of Marine Science and Engineering*, *8*(3). Retrieved from https://www.mdpi.com/2077-1312/8/3/183 doi: 10.3390/jmse8030183
Kolios, A., & Brennan, F. (2018). *Romeo d8. 1-review of existing cost and o&m models, and development of a high-fidelity cost/revenue model for impact assessment.*
Lindstrand, N. (2021). *Unlocking ammoniaś potential for shipping.* Retrieved from https://www.man-es.com/discover/two-stroke-ammonia-engine
Liquid Robotics, Inc. (2020). *The wave glider.* Retrieved from https://www.liquid-robotics.com/wave-glider/how-it-works/

Lloyd's Register. (2015). *Wind-powered shipping, a review of the commercial, regulatory and technical factors affecting uptake of wind-assisted propulsion.* Retrieved from http://www.nsrsail.eu/wp-content/uploads/2015/12/Wind_powered_shipping-Lloyds-Register.pdf

Lucie Kirstein, R. H., & Merk, O. (2018). *Decarbonising maritime transport - pathways to zero-carbon shipping by 2035* (Vol. 84) (No. 1). Retrieved from https://www.itf-oecd.org/sites/default/files/docs/decarbonising-maritime-transport-2035.pdf

Magnuss. (2020). *How global shipping could be powered by the wind.* Retrieved from http://www.magnuss.com

Mallouppas, G., & Yfantis, E. A. (2021). Decarbonization in shipping industry: A review of research, technology development, and innovation proposals. *Journal of Marine Science and Engineering*, *9*(4). Retrieved from https://www.mdpi.com/2077-1312/9/4/415 doi: 10.3390/jmse9040415

MAN Diesel A/S. (2010, April). *Man b&w s60mc-c8-tii project guide camshaft controlled two stroke engines.* Retrieved from https://man-es.com/applications/projectguides/2stroke/content/printed/s60mcc8.pdf

MAN Diesel A/S. (2020, november). *Man b&w two-stroke engine operating on ammonia.* Retrieved from https://www.man-es.com/docs/default-source/marine/tools/man-b-w-two-stroke-engine-operating-on-ammonia.pdf

marinetraffic.com. (2011). *Leda c.* Retrieved from hhttps://www.marinetraffic.com/nl/ais/details/ships/shipid:713545/mmsi:538004349/imo:9583768/vessel:LEDA_C

Maritime Industry Decarbonisation Council (MIDC). (2018). *Alternative marine fuels?* Retrieved from https://midc.be/alternative-marine-fuels/

Media, A. (2021). Retrieved from https://www.argusmedia.com/en/press-releases/2021/green-ammonia-prices-double-that-of-regular-supplies

Melkert, J. A., Gibson, A., & Hulshoff, S. J. (2003). Design-synthesis exercise in aerospace engineering, global journal of engineering education. *GJEE*, *7*(1), 121 - 130. Retrieved from http://www.wiete.com.au/journals/GJEE/Publish/vol7no1/Melkert.pdf

Miao, Y., Hynan, P., von Jouanne, A., & Yokochi, A. (2019, 03). Current li-ion battery technologies in electric vehicles and opportunities for advancements. *Energies*, *12*, 1074-1094. doi: 10.3390/en12061074

Moosmann, L., Urrutia, C., Siemons, A., Cames, M., & Schneider, L. (2019). *International climate negotiations* (Tech. Rep.). Retrieved from http://www.europarl.europa.eu/RegData/etudes/STUD/2019/642344/IPOL_STU(2019)642344_EN.pdf

Naaijen, P., & Koster, V. (2014, 01). *Performance of auxiliary wind propulsion for merchant ships using a kite.*

Nelissen, D., Traut, M., Kohler, J., Mao, W., Faber, J., & Ahdour, S. (2016). *Study on the analysis of market potentials and market barriers for wind propulsion technologies for ships.* Retrieved from https://www.hellenicshippingnews.com/wp-content/uploads/2017/04/CE-Delft-Study-on-the-analysis-of-market-potentials-and-market-barriers-for-wind-propulsion-technologies-for-shipsb.pdf doi: 10.2834/68747

Neoline. (2020). *The neoline project.* Retrieved from https://www.neoline.eu/en/the-project/

Neste Oil. (2018). *Hydrotreated vegetable oil (hvo) - premium renewable biofuel for diesel engines.* Retrieved from http://artfuelsforum.eu/wp-content/uploads/2018/05/Acrobat-Document-1.pdf

Next. (n.d.). *What does peak shaving mean?* Retrieved from https://www.next-kraftwerke.com/knowledge/what-is-peak-shaving

Norsepower. (2014). *Rotor sails installed in 2014 & 2015.* Retrieved from https://www.norsepower.com/ro-ro/

Offshore Energy. (2018, 11 15). *Nyk steps into the future with super eco ship 2050.* Retrieved from https://www.offshore-energy.biz/nyk-steps-into-the-future-with-super-eco-ship-2050/

Parry, I., Heine, M. D., Kizzier, K., & Smith, T. (2018). *Carbon taxation for international maritime fuels: Assessing the options.* International Monetary Fund.

Pietro Faggiani, R. S. (2017). *Wind assisted ship propulsion, savings predictions.*

Pilato, F. (2012). *Planetsolar 100 catamaran has 38,000 photovoltaic solar cells, set to sail in march.* Retrieved from http://www.mobilemag.com/2010/02/26/planetsolar-100-catamarn-has-38000-photovaltaic-solar-cells-set-to-sail-in-march/

Platform Duurzame Biobrandstoffen. (2018). *Overview of biofuel options for shipping.* Retrieved from https://platformduurzamebiobrandstoffen.nl/overview-of-biofuel-options-for-shipping/

Poulsen Hybrid. (2012). *The poulsen hybrid monorotor.* Retrieved from http://cfd.mace.manchester.ac.uk/twiki/pub/Main/FlettnerRotors/Poulsen_Monorotor_011612.pdf

Quantum Sails. (2016). *How long do sails last?* Retrieved from https://www.quantumsails.com/en/resources-and-expertise/articles/how-long-do-sails-last

Ramme. (2021). *Permanent magnet motors.* Retrieved from https://www.ramme.de/en/bannerleiste/innovative-technologies/torque-motors

Reed, G. (2021). *9 reasons why dc may replace ac.* Retrieved from https://www.electricalindustry.ca/latest-news/1018-9-reasons-why-dc-may-replace-ac

Rehmatulla, N., Parker, S., Smith, T., & Stulgis, V. (2017). Wind technologies: Opportunities and barriers to a low carbon shipping industry. *Marine Policy*, *75*, 217 - 226. Retrieved from http://www.sciencedirect.com/science/article/pii/S0308597X15003917 doi: https://doi.org/10.1016/j.marpol.2015.12.021

Ridden, P. (2018, 03 26). *Autonomous boat gets around under wave power.* Retrieved from https://newatlas.com/autonaut-autonomous-unmanned-surface-vessel/53949/

Sajip, J. (2021). *Understanding diesel genset specifications: kw, kva and power factor.* Retrieved from https://www.ny-engineers.com/blog/diesel-genset-specifications-kw-kva-and-power-factor

Schinas, O., & Metzger, D. (2019, 09). *Financing ships with wind-assisted propulsion technologies.*

Sea World. (2020). *2020 hurricane season in mexico.*

Shadbolt, P. (2015, 11). *'vindskip' cargo ship uses its hull as a giant sail.* Retrieved from www.edition.cnn.com

Ship & Bunker. (2021). *World bunker prices.* Retrieved from https://shipandbunker.com/prices

SKYSAILS GROUP. (n.d.). *Skysails group.* Retrieved from https://skysails-group.com/index.html

Smart Green Shipping. (2020). *Fast technologies.* Retrieved from https://smartgreenshipping.com/fast-technologies

Smulders, P. S. (2017). *Using a breakwater in offshore operations: An enquiry into the effectiveness and economic viability of using a breakwater in offshore operations.* doi: http://resolver.tudelft.nl/uuid:617b70c3-99b8-4dcb-ae27-a1a1077ff467

Squadrin, G. (2021). *Nwe hvo, saf at records on feedstocks prices, demand.* Retrieved from https://www.argusmedia.com/en/news/2220328-nwe-hvo-saf-at-records-on-feedstocks-prices-demand

Stam, B. (2020, 03 17). *Rogier eggers (marin) over hulp bij windvoortstuwing 'voor substantiële besparing is nieuw ontwerp nodig'.* Retrieved from https://www.maritiemnederland.com/

artikelen/techniek-innovatie/voor-substantiele-besparing-is-een-nieuw-ontwerp-nodig

Stopford, M. (2009). *Maritime economics (3rd edition)*.

Sunfire. (2020). *Liquefied gas carriers with independent cylindrical tanks of type c.* Retrieved from https://www.sunfire.de/en/news/detail/sunfire-supplies-thyssenkrupp-marine-systems

Talluri, L., Nalianda, D., Kyprianidis, K., Nikolaidis, T., & Pilidis, P. (2016). Techno economic and environmental assessment of wind assisted marine propulsion systems. *Ocean Engineering*, *121*, 301-311. Retrieved from https://www.sciencedirect.com/science/article/pii/S0029801816301718 doi: https://doi.org/10.1016/j.oceaneng.2016.05.047

Tamalm. (2004). *t 09.08- zonnestraling op het aardoppervlak.* Retrieved from https://tamtalm.nl/zon-aard/

Target Marina S.A. (2011). *Leda c.* Retrieved from https://targetmaritime.gr/fleet-list/target-marine-leda-c/

Tatar, V., & ÖZER, M. B. (2018). The impacts of co2 emissions from maritime transport on the environment and climate change. *Uluslararası Çevresel Eğilimler Dergisi*, *2*(1), 5–24.

The Maritime Executive. (2017a). *Report: Oceanfoil wingsails achieve 14 percent average fuel savings.* Retrieved from https://www.maritime-executive.com/corporate/report-oceanfoil-wingsails-achieve-average-14-percent-fuel-savings

The Maritime Executive. (2017b, 02 08). *Wave energy concept ready for ship propulsion.* Retrieved from https://www.maritime-executive.com/article/wave-energy-concept-ready-for-ship-propulsion

The Metals Company. (2021). *A battery in a rock. polymetallic nodules are the cleanest path toward electric vehicles.* Retrieved from https://metals.co/nodules/

Thiiink. (2015). *Flettner rotor.* Retrieved from http://www.thiiink.com/flettner-rotor/

TNO. (2013). *Ghg emission reduction potential of eu-related maritime transport and on its impacts.* Retrieved from https://ec.europa.eu/clima/sites/clima/files/transport/shipping/docs/report_ghg_reduction_potential_en.pdf

Traut, M., Gilbert, P., Walsh, C., Bows, A., Filippone, A., Stansby, P., & Wood, R. (2014). Propulsive power contribution of a kite and a flettner rotor on selected shipping routes. *Applied Energy*, *113*, 362-372. Retrieved from https://www.sciencedirect.com/science/article/pii/S0306261913005928 doi: https://doi.org/10.1016/j.apenergy.2013.07.026

Tronstad, T., Åstrand, H. H., Haugom, G. P., & Langfeldt, L. (2017). *Study on the use of fuel cells in shipping.*

TWI Ltd. (2021). *What are the technology readiness levels (trl)?* Retrieved from https://www.twi-global.com/technical-knowledge/faqs/technology-readiness-levels

U.S. Department of Energy. (2016). *Comparison of fuel cell technologies.* Retrieved from https://www.energy.gov/eere/fuelcells/comparison-fuel-cell-technologies

van der Kolk, Nico. (2020). *Sailing efficiency and course keeping ability of wind assisted ships* (Doctoral dissertation, Delft University of Technology). doi: 10.4233/uuid:8707309f-b9a3-4e09-916d-8fb64328a138

van der Kolk, N. (2020). *Sailing Efficiency and Course Keeping Ability of Wind Assisted Ships.* doi: https://doi.org/10.4233/uuid:8707309f-b9a3-4e09-916d-8fb64328a138

van der Kolk, N., Bordogna, G., Mason, J. C., Desprairies, P., & Vrijdag, A. (2019). Case study: Windassisted ship propulsion performance prediction, routing, and economic modelling. *the International Conference Power & Propulsion Alternatives for Ships The Royal Institution of Naval Architects (RINA)*. doi: https://doi.org/10.1016/j.apenergy.2013.07.026

Van Hoecke, L., Laffineur, L., Campe, R., Perreault, P., Verbruggen, S. W., & Lenaerts, S. (2021). Challenges in the use of hydrogen for maritime applications. *Energy & Environmental Sci-*

ence, *14*(2), 815–843.

Vos, B. (2019). *The Sailing Tug: A feasibility study on the application of Wind-Assisted towing of the Thialf.* doi: http://resolver.tudelft.nl/uuid:2b970216-3650-46f4-8fae-747a15eeacdf

Wartsila. (2017). *Environmental product guide.* Retrieved from `https://cdn.wartsila.com/docs/default-source/product-files/egc/product-guide-o-env-environmental-solutions.pdf`

Wildi, T. (2004). *Celectrical machines, drives, and power systems, 4th edition.* Prentice Hall.

Zaozhuang Evlithium Electronic Technology Co., L. (2018). *Catl nmc ncm 811 lithium ion li polymer ternay battery 50ah 3.7v.* Retrieved from `https://winston-battery.en.made-in-china.com/product/rXRmNobEnCUw/China-Catl-Nmc-Ncm-811-Lithium-Ion-Li-Polymer-Ternay-Battery-50ah-3-7V.html`

Appendices

A | Multi-Criteria Analysis

Table A.1: Multi-criteria analysis

	Alternative fuel or technologies	Price	Infrastructure	Regulation	Scalability	Environmental impact	Propulsive performance	Technology	Robusness	Controlability	CAPEX	OPEX	Total
	Weight	2	2	1	3	5	10	3	3	2	2	2	
Alternative fuels													
	Biofuels	3	3	5	7	8		6			9	6	**126**
	Methanol	5	5	6	7	3		4			7	6	**100**
	LNG	8	6	10	8	5		9			5	6	**136**
	Hydrogen	8	4	6	10	9		7			5	6	**148**
	LPG	6	5	1	6	4		4			7	6	**99**
Alternative technologies													
	Batteries/electrical	8	9	6	6	9		5			6	7	**144**
	Fuel cells	5	4	5	4	9		4			3	5	**108**
Alternative energy generation													
Wind													
Soft sails													
	Kites			4	2			5	3	2	1	2	**44**
	Square rig			4	9		1.60	10	3	2	9	5	**118**
	Bermuda rig			4	9		1.65	9	4	4	9	8	**128**
	Dyna rig			7	8		2.12	8	3	9	7	7	**131**
	Aero rig			4	8		2.53	4	4	9	6	7	**121**
Wing sails													
	Wing sail			8	8		3.00	8	9	7	3	10	**153**
Active sail													
	Turbo sails			4	7		3.41	6	8	6	2	4	**125**
	Flettner rotor			8	6		4.86	6	7	10	3	4	**148**
Other													
	Wind turbine			4	8			7	4		6	5	**83**
Solar													
	Solar panels			6	7			6	8		3	5	**85**
	Solar in sails			6	8			4	8		2	6	**82**
Waves													
	Wave energy			3	2			1	2		2	1	**24**
	Dolphin system			7	4			2	2		3	4	**45**

B | Requirement discovery tree

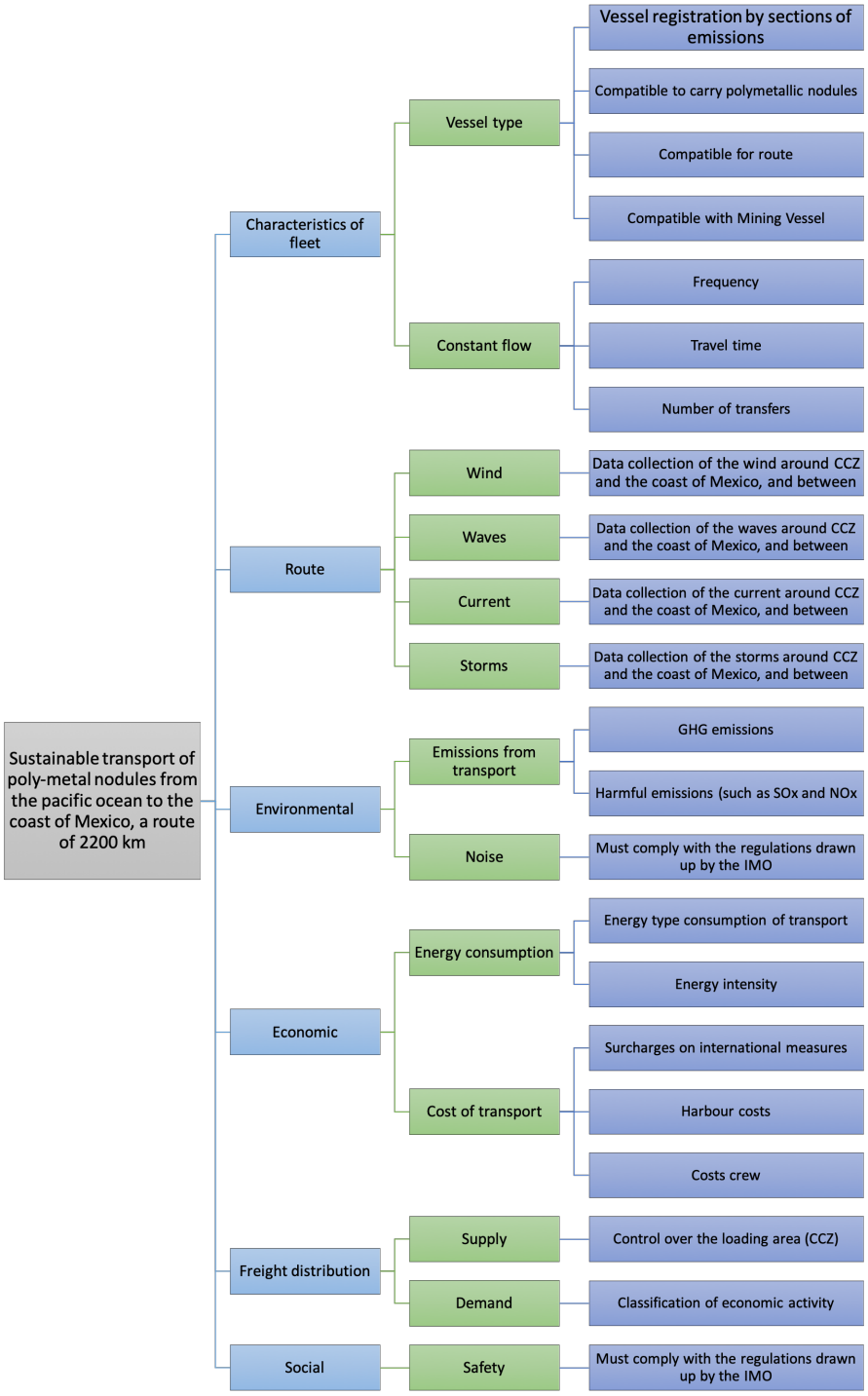

Figure B.1: Requirement discovery tree

C | Transfer of the nodules

Before the polymetallic nodules are transported from the CCZ to Mexico, first they are transferred from the Hidden Gem to the transport vessel.This transfer can be done in different ways, depending on the status of the nodules. Two different modes of transfer have been considered: in "dry" or "wet" condition.

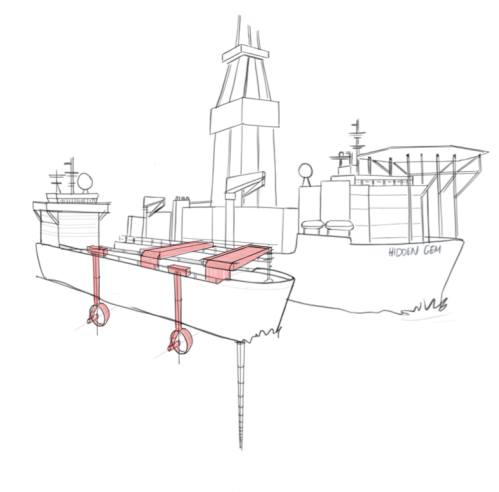

Figure C.1: Side by side transfer 'dry' cargo

When the nodules are in 'dry' conditions, the nodules are passive dehydrated on board of the Hidden Gem and not centrifuged. When the nodules are in this state, they can be transferred with conveyor belts. The transport vessel is placed side by side with the Hidden Gem, see figure C.1. The transfer speed for the nodules in this state is 5000 t per hour. Although the transfer speed is 15 times faster then the harvesting speed, the work-ability for this transfer is low. The connecting time of the conveyor belts would be only 4 to 6 hours. However, due to the fact that the freeboard of the transport vessel and the Hidden Gem should be aligned and because side by side transfer can only take place within certain weather restrictions, it is not always possible to connect the vessels. When the wave height is too high, the freeboard of the vessels can not be aligned to make the transfer possible. This wave height depends on the allowed distance between the two vessels and the size of the transport vessel. Both of these requirements are not yet established. This low work ability is the reason why a day is set for the connecting time for side by side connection, as shown in table 3.1.

Not only the freeboard of the vessels must be aligned, but also the location of the two vessels must be within a certain footprint. To keep the transport vessel in place dynamic positioning (DP) is necessary, this is explained further in the section. Because the work-ability of this transfer is low, due to the alignment of the freeboard, and because the transport vessel consumes more energy to be on DP, the transport vessel disconnects when the buffer of the Hidden Gem is empty and lays still next to the Hidden Gem. For a ship to lay still in the middle of the Pacific, it is assumed that the transport vessel uses 5% of its energy consumption when sailing. When the buffer of the Hidden Gem is almost full, the transport vessel reconnects to continue with the transfer of the nodules. This re-connecting is only necessary when the capacity of the transport vessel is smaller then the buffer of the Hidden Gem (25,000 dwt).

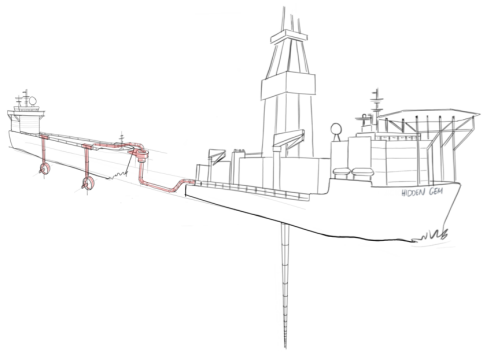

Figure C.2: Tandem transfer 'wet' cargo

The nodules can also be transferred in 'wet' conditions. For this transfer the transport vessel is placed behind the Hidden Gem, shown in figure C.2. With a large tube, the slurry, consisting of water and nodules, is transferred to the transport vessel with 666 tonne nodules per hour, so two times faster then the harvesting speed. To connect the vessels tandem takes 8 hours, but it requires many men to make this connection possible. This is one of the reasons why the transport vessel stays connected to the Hidden Gem, even tough the buffer of the Hidden Gem is empty. The transport vessel still needs to stay within a certain footprint, it needs DP as well but less accurate, this is explained further in this section.
A disadvantage of this transfer is the slurry exist for 90 % of water and 10% of nodules. This water needs to be pumped back into the ocean, below a specific depth. Pumps or filters are therefore needed which is more time consuming and increases the energy consumption.

As said before, for both transfers the ships need to stay in a specific footprint and needs DP. Figure C.3 shows these footprints. In this figure, HG is the Hidden Gem in normal weather conditions, T1 is the transport vessel when the transfer is done side by side with the Hidden Gem using conveyor belts and T2 is the transport vessel if the transfer is done tandem through a large tube.
The smaller the footprint, the more accurate the DP needs to be, the more power the transport vessel needs to deliver and the higher its fuel consumption. This extra energy consumption is calculated with the DP tool off Allseas. For the accuracy, the peak to mean factor of the incoming wave is used. The peak to mean factor is, as it were, the stiffness of the incoming wave. Increas-

ing this factor, the accuracy of the DP increases, which decreases the footprint while all the other terms are set to remain the same. The incoming wave is usually between 30° on one side and 30°C on the other side, so worst case will be 30°. The peak to mean factor is 1.2 for T2 and 1.6 for T3, then it was examined how much the power linked to the peak to mean factors differ from each other [1]. Thus, it is determined for T1 30% extra energy is consumed during the transfer and for T2 this is 10%.

Thus, it is determined for T1 30% extra energy is consumed during the transfer and for T2 this is 10%.
Both transfers require thrusters to stay in place, this is not taken into account for determining the energy consumption and costs of base case because it falls outside the scope of this project.

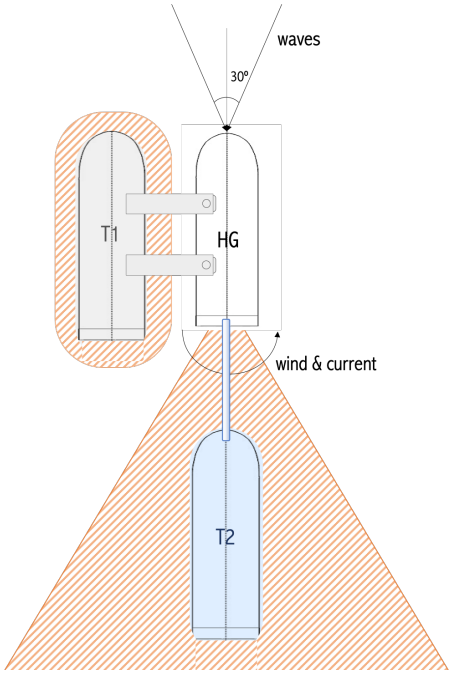

Figure C.3: Footprints of side by side transfer for dry cargo (T1) and tandem transfer for wet cargo (T2)

Both these transfer configurations have disadvantages and advantages. If the disadvantages of both of these configurations are combined, a third configuration arises. This third configuration is shown in figure C.4. The transport vessel is placed behind the Hidden Gem, tandem transfer. The nodules are transferred in dry conditions, so using one conveyor belt which ensures a transfer speed of 5000 tonne nodules per hour. For this configuration the work ability is still high and the connection time is only 6 hours. To save energy, the transport vessel disconnects when the buffer of the Hidden Gem is empty and waits next to the Hidden Gem until it is reloaded. To calculate the footprint of this configuration a peak to mean factor for the incoming wave is set 1.4. This number is lower then configuration 1 because it is tandem transfer, but higher then figuration 2 because the transfer is done by a conveyor belt which is more static then

[1] this is determined in consultation with Niels Mallon Senior R&D Engineer at Allseas

a tube. This gives an extra energy consumption of 20%.

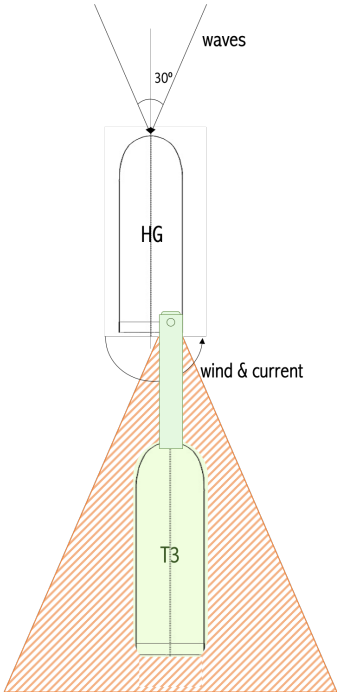

Figure C.4: Footprint of tandem transfer for dry cargo (T3)

D | Wind probability matrix

RELATIVE TO NORTH - Global Shipping Routes Wind Probability Matrix

TWS [m/s] \ TWA [deg] ->	0	5	10	15	20	25	30	35	40	45	50	55
0.5	3.4506556	6.90E-05	1.73E-05	0.00E+00	3.45E-05	5.18E-05	5.18E-05	3.45E-05	3.45E-05	5.18E-05	6.90E-05	3.45E-05
1.5	5.18E-05	1.21E-04	8.63E-05	8.63E-05	1.55E-04	1.21E-04	1.04E-04	8.63E-05	1.21E-04	1.55E-04	2.24E-04	1.04E-04
2.5	1.73E-04	3.28E-04	2.76E-04	2.42E-04	1.55E-04	1.90E-04	2.24E-04	2.76E-04	2.93E-04	4.14E-04	2.24E-04	2.42E-04
3.5	8.63E-05	2.93E-04	4.66E-04	3.97E-04	2.93E-04	3.45E-04	2.42E-04	4.66E-04	4.14E-04	3.11E-04	4.14E-04	4.31E-04
4.5	1.73E-04	3.97E-04	4.49E-04	5.00E-04	5.18E-04	8.28E-04	5.35E-04	4.83E-04	7.94E-04	3.80E-04	6.56E-04	7.59E-04
5.5	2.24E-04	6.56E-04	5.69E-04	6.04E-04	7.59E-04	7.42E-04	5.87E-04	6.38E-04	8.11E-04	9.83E-04	8.45E-04	8.28E-04
6.5	3.97E-04	5.35E-04	9.14E-04	7.59E-04	7.25E-04	7.76E-04	9.32E-04	9.83E-04	8.97E-04	1.10E-03	1.05E-03	1.05E-03
7.5	3.11E-04	8.45E-04	1.00E-03	9.14E-04	9.66E-04	8.63E-04	9.14E-04	1.00E-03	8.80E-04	1.17E-03	1.26E-03	1.28E-03
8.5	4.31E-04	6.90E-04	9.14E-04	1.10E-03	1.12E-03	1.16E-03	1.00E-03	1.10E-03	1.54E-03	1.04E-03	1.05E-03	1.26E-03
9.5	3.80E-04	1.29E-03	1.21E-03	1.57E-03	1.21E-03	1.76E-03	1.48E-03	1.47E-03	1.81E-03	1.41E-03	1.52E-03	1.40E-03
10.5	3.45E-04	9.66E-04	1.50E-03	1.17E-03	1.54E-03	1.55E-03	1.59E-03	1.41E-03	2.04E-03	1.74E-03	1.90E-03	1.48E-03
11.5	6.04E-04	1.09E-03	1.24E-03	1.90E-03	2.04E-03	2.24E-03	2.61E-03	2.38E-03	2.52E-03	2.12E-03	1.85E-03	1.64E-03
12.5	4.14E-04	9.32E-04	1.55E-03	2.07E-03	2.17E-03	2.97E-03	2.42E-03	2.45E-03	2.21E-03	1.90E-03	2.12E-03	1.67E-03
13.5	4.14E-04	1.31E-03	1.21E-03	2.33E-03	2.74E-03	2.62E-03	2.31E-03	2.24E-03	2.07E-03	2.04E-03	2.14E-03	1.48E-03
14.5	4.49E-04	1.04E-03	1.41E-03	2.02E-03	2.26E-03	2.14E-03	2.40E-03	2.17E-03	2.07E-03	1.60E-03	1.88E-03	1.19E-03
15.5	2.93E-04	9.14E-04	1.19E-03	1.66E-03	1.88E-03	2.35E-03	1.97E-03	2.57E-03	2.00E-03	1.55E-03	1.26E-03	1.14E-03
16.5	1.38E-04	9.83E-04	1.29E-03	1.28E-03	1.45E-03	1.43E-03	2.00E-03	1.76E-03	1.47E-03	1.41E-03	1.09E-03	7.42E-04
17.5	6.56E-04	1.62E-03	2.50E-03	3.55E-03	4.02E-03	4.40E-03	4.18E-03	3.74E-03	3.50E-03	2.38E-03	1.73E-03	1.17E-03

TWS [m/s] \ TWA [deg] ->	60	65	70	75	80	85	90	95	100	105	110	115
0.5	3.45E-05	1.04E-04	1.73E-05	8.63E-05	0.00E+00	5.18E-05	5.18E-05	3.45E-05	5.18E-05	0.00E+00	0.00E+00	3.45E-05
1.5	2.07E-04	6.90E-05	1.90E-04	1.21E-04	1.04E-04	1.38E-04	1.90E-04	1.38E-04	3.45E-05	5.18E-05	5.18E-05	1.38E-04
2.5	2.07E-04	3.80E-04	3.28E-04	2.93E-04	2.24E-04	3.45E-04	2.76E-04	1.90E-04	2.59E-04	2.24E-04	1.73E-04	1.38E-04
3.5	2.42E-04	4.49E-04	3.45E-04	3.62E-04	2.24E-04	2.24E-04	2.59E-04	3.11E-04	2.59E-04	2.07E-04	3.45E-04	1.73E-04
4.5	6.56E-04	6.56E-04	5.69E-04	7.42E-04	5.52E-04	3.80E-04	5.69E-04	3.97E-04	5.00E-04	3.28E-04	3.97E-04	2.42E-04
5.5	8.11E-04	7.59E-04	7.59E-04	6.04E-04	6.73E-04	6.90E-04	5.18E-04	5.35E-04	5.35E-04	4.83E-04	5.35E-04	5.18E-04
6.5	8.80E-04	7.07E-04	8.45E-04	8.80E-04	8.11E-04	6.21E-04	7.07E-04	5.52E-04	4.31E-04	4.14E-04	4.31E-04	3.80E-04
7.5	1.09E-03	7.59E-04	8.45E-04	7.76E-04	8.28E-04	7.42E-04	6.04E-04	5.52E-04	6.56E-04	5.00E-04	4.14E-04	5.52E-04
8.5	1.28E-03	1.29E-03	1.02E-03	8.80E-04	9.32E-04	8.63E-04	6.73E-04	4.83E-04	4.66E-04	5.87E-04	4.31E-04	4.66E-04
9.5	1.00E-03	1.40E-03	1.14E-03	1.22E-03	9.14E-04	4.49E-04	7.42E-04	4.83E-04	5.69E-04	3.97E-04	3.97E-04	4.14E-04
10.5	1.41E-03	1.73E-03	1.09E-03	8.28E-04	9.49E-04	5.87E-04	5.18E-04	5.87E-04	4.66E-04	3.80E-04	2.24E-04	2.07E-04
11.5	1.19E-03	9.32E-04	1.16E-03	6.56E-04	8.63E-04	4.83E-04	5.18E-04	3.80E-04	3.45E-04	3.62E-04	3.11E-04	8.63E-05
12.5	1.22E-03	1.17E-03	8.63E-04	7.07E-04	6.04E-04	6.04E-04	3.80E-04	1.21E-04	1.38E-04	1.90E-04	1.73E-04	1.04E-04
13.5	1.24E-03	1.00E-03	8.80E-04	6.38E-04	5.52E-04	4.49E-04	3.97E-04	2.42E-04	1.73E-04	2.24E-04	5.18E-05	8.63E-05
14.5	9.66E-04	8.97E-04	7.25E-04	3.28E-04	3.28E-04	3.45E-04	1.21E-04	1.73E-04	2.07E-04	8.63E-05	1.38E-04	8.63E-05
15.5	6.38E-04	4.83E-04	4.83E-04	4.66E-04	1.73E-04	2.42E-04	2.07E-04	5.18E-05	8.63E-05	5.18E-05	0.00E+00	1.73E-05
16.5	5.52E-04	5.00E-04	2.76E-04	2.24E-04	8.63E-05	1.55E-04	5.18E-05	1.73E-05	3.45E-05	5.18E-05	0.00E+00	1.73E-05
17.5	8.28E-04	6.38E-04	5.87E-04	3.80E-04	3.28E-04	1.04E-04	3.45E-05	0.00E+00	5.18E-05	0.00E+00	3.45E-05	3.45E-05

TWS [m/s] \ TWA [deg] ->	120	125	130	135	140	145	150	155	160	165	170
0.5	1.21E-04	0.00E+00	3.45E-05	1.73E-05	8.63E-05	6.90E-05	1.73E-05	1.73E-05	3.45E-05	1.04E-04	0.00E+00
1.5	6.90E-05	1.21E-04	6.90E-05	1.21E-04	1.55E-04	1.04E-04	1.21E-04	1.21E-04	8.63E-05	1.38E-04	1.21E-04
2.5	3.11E-04	1.90E-04	2.59E-04	2.24E-04	1.38E-04	1.73E-04	1.38E-04	1.55E-04	1.21E-04	2.24E-04	1.55E-04
3.5	2.76E-04	3.80E-04	2.59E-04	2.93E-04	2.42E-04	2.76E-04	2.24E-04	2.59E-04	2.76E-04	2.24E-04	2.24E-04
4.5	3.97E-04	4.14E-04	3.28E-04	2.76E-04	2.42E-04	3.62E-04	3.97E-04	2.24E-04	2.42E-04	2.07E-04	3.28E-04
5.5	3.45E-04	5.00E-04	3.45E-04	3.80E-04	2.59E-04	2.93E-04	2.76E-04	2.93E-04	2.07E-04	1.21E-04	2.07E-04
6.5	2.93E-04	2.59E-04	3.28E-04	3.28E-04	2.42E-04	3.11E-04	3.28E-04	3.62E-04	2.42E-04	2.24E-04	3.11E-04
7.5	3.45E-04	3.28E-04	2.93E-04	2.24E-04	1.38E-04	2.24E-04	1.90E-04	1.38E-04	1.73E-04	1.55E-04	3.62E-04
8.5	2.93E-04	2.24E-04	1.21E-04	2.07E-04	1.90E-04	1.21E-04	1.90E-04	1.55E-04	1.90E-04	1.04E-04	2.24E-04
9.5	3.97E-04	4.14E-04	1.55E-04	1.38E-04	2.07E-04	1.73E-04	1.21E-04	1.73E-04	2.07E-04	2.07E-04	2.24E-04
10.5	2.76E-04	2.59E-04	1.73E-04	1.55E-04	1.55E-04	6.90E-05	1.04E-04	1.55E-04	1.55E-04	1.38E-04	1.21E-04
11.5	1.90E-04	6.90E-05	3.45E-05	1.73E-04	1.73E-05	3.45E-05	1.04E-04	8.63E-05	5.18E-05	8.63E-05	6.90E-05
12.5	1.21E-04	1.38E-04	8.63E-05	1.04E-04	5.18E-05	1.73E-05	3.45E-05	1.73E-05	0.00E+00	5.18E-05	8.63E-05
13.5	6.90E-05	6.90E-05	5.18E-05	1.73E-05	3.45E-05	1.73E-05	3.45E-05	5.18E-05	3.45E-05	1.73E-05	0.00E+00
14.5	3.45E-05	1.73E-05	5.18E-05	1.73E-05	5.18E-05	1.73E-05	0.00E+00	1.73E-05	0.00E+00	1.73E-05	3.45E-05
15.5	0.00E+00	1.73E-05	1.73E-05	0.00E+00	0.00E+00	0.00E+00	0.00E+00	3.45E-05	0.00E+00	0.00E+00	0.00E+00
16.5	0.00E+00	0.00E+00	0.00E+00	1.73E-05	0.00E+00	0.00E+00	1.73E-05	0.00E+00	0.00E+00	0.00E+00	0.00E+00
17.5	0.00E+00	1.73E-05	0.00E+00	5.18E-05	0.00E+00	1.73E-05	0.00E+00	0.00E+00	0.00E+00	0.00E+00	1.73E-05

TWS [m/s] \ TWA [deg] ->	175	180	185	190	195	200	205	210	215	220	225	230	235
0.5	5.18E-05	3.45E-05	1.04E-04	8.63E-05	0.00E+00	3.45E-05	5.18E-05	5.18E-05	5.18E-05	1.73E-05	6.90E-05	3.45E-05	3.45E-05
1.5	6.90E-05	5.18E-05	1.21E-04	1.55E-04	1.73E-04	1.55E-04	5.18E-05	3.45E-05	1.04E-04	1.38E-04	1.04E-04	8.63E-05	1.21E-04
2.5	1.90E-04	3.28E-04	1.55E-04	1.90E-04	2.42E-04	2.24E-04	2.42E-04	2.07E-04	2.42E-04	2.59E-04	1.73E-04	1.73E-04	2.24E-04
3.5	2.59E-04	1.90E-04	6.90E-05	3.97E-04	3.11E-04	3.28E-04	2.93E-04	2.93E-04	2.93E-04	3.62E-04	3.11E-04	3.11E-04	4.14E-04
4.5	2.93E-04	3.62E-04	3.80E-04	4.31E-04	2.59E-04	3.28E-04	3.45E-04	5.69E-04	3.97E-04	3.80E-04	3.62E-04	5.00E-04	5.52E-04
5.5	2.76E-04	4.31E-04	2.24E-04	2.93E-04	2.42E-04	6.04E-04	4.14E-04	3.62E-04	6.21E-04	6.73E-04	4.31E-04	7.25E-04	8.28E-04
6.5	2.93E-04	3.62E-04	4.49E-04	4.49E-04	3.80E-04	4.49E-04	5.69E-04	6.04E-04	6.21E-04	6.04E-04	6.90E-04	6.56E-04	9.66E-04
7.5	2.76E-04	1.73E-04	2.93E-04	3.45E-04	3.62E-04	5.52E-04	4.66E-04	5.35E-04	5.00E-04	7.59E-04	7.94E-04	7.25E-04	1.02E-03
8.5	2.24E-04	2.76E-04	3.11E-04	2.76E-04	4.49E-04	3.97E-04	5.52E-04	4.14E-04	8.28E-04	9.32E-04	1.16E-03	1.04E-03	1.45E-03
9.5	1.38E-04	2.24E-04	2.24E-04	2.24E-04	2.24E-04	5.18E-04	5.69E-04	7.42E-04	8.28E-04	1.09E-03	9.83E-04	1.92E-03	1.71E-03
10.5	1.38E-04	1.90E-04	1.73E-04	2.76E-04	2.93E-04	5.18E-04	7.59E-04	6.90E-04	9.66E-04	1.33E-03	1.48E-03	1.98E-03	2.00E-03
11.5	6.90E-05	1.55E-04	1.38E-04	1.38E-04	5.18E-04	4.31E-04	5.35E-04	6.56E-04	1.10E-03	1.73E-03	1.78E-03	2.50E-03	3.02E-03
12.5	1.21E-04	8.63E-05	1.73E-04	2.24E-04	3.97E-04	5.87E-04	8.11E-04	1.09E-03	1.38E-03	1.98E-03	2.67E-03	3.49E-03	4.37E-03
13.5	6.90E-05	6.90E-05	8.63E-05	3.11E-04	2.93E-04	4.49E-04	7.25E-04	9.49E-04	1.38E-03	2.09E-03	3.36E-03	4.28E-03	4.88E-03
14.5	1.73E-05	3.45E-05	3.45E-05	5.18E-05	2.93E-04	4.49E-04	7.25E-04	8.28E-04	1.85E-03	2.61E-03	4.11E-03	4.81E-03	5.18E-03
15.5	0.00E+00	0.00E+00	1.73E-05	0.00E+00	1.04E-04	2.42E-04	5.18E-04	1.09E-03	1.81E-03	2.28E-03	3.38E-03	4.66E-03	5.16E-03
16.5	1.73E-05	0.00E+00	1.73E-05	5.18E-05	1.04E-04	2.59E-04	3.80E-04	8.28E-04	1.28E-03	2.43E-03	3.40E-03	4.28E-03	5.00E-03
17.5	1.73E-05	0.00E+00	5.18E-05	1.21E-04	1.38E-04	1.04E-04	5.00E-04	1.28E-03	2.45E-03	4.59E-03	6.83E-03	7.37E-03	7.80E-03

TWS [m/s] \ TWA [deg] ->	240	245	250	255	260	265	270	275	280	285	290	295
0.5	6.90E-05	1.04E-04	6.90E-05	1.73E-05	3.45E-05	1.21E-04	3.45E-05	0.00E+00	8.63E-05	3.45E-05	6.90E-05	3.45E-05
1.5	1.04E-04	1.55E-04	1.21E-04	1.21E-04	1.04E-04	2.42E-04	1.73E-04	8.63E-05	2.07E-04	1.38E-04	1.38E-04	1.21E-04
2.5	3.28E-04	1.55E-04	1.90E-04	1.55E-04	2.93E-04	2.76E-04	2.42E-04	3.28E-04	1.90E-04	2.76E-04	1.73E-04	2.42E-04
3.5	4.49E-04	4.31E-04	2.93E-04	4.66E-04	4.66E-04	3.11E-04	5.35E-04	3.97E-04	3.45E-04	4.14E-04	5.52E-04	2.76E-04
4.5	7.07E-04	6.56E-04	5.18E-04	7.42E-04	5.52E-04	5.87E-04	4.31E-04	5.52E-04	6.38E-04	6.90E-04	4.83E-04	5.87E-04
5.5	7.25E-04	8.97E-04	8.45E-04	9.14E-04	1.04E-03	7.94E-04	6.38E-04	6.38E-04	6.38E-04	7.25E-04	1.12E-03	6.90E-04
6.5	8.97E-04	1.00E-03	9.83E-04	1.36E-03	1.09E-03	1.12E-03	1.16E-03	1.14E-03	9.14E-04	9.83E-04	1.31E-03	1.09E-03
7.5	1.36E-03	1.64E-03	1.64E-03	1.54E-03	1.66E-03	1.41E-03	1.55E-03	1.33E-03	1.29E-03	1.16E-03	1.10E-03	1.09E-03
8.5	1.48E-03	2.05E-03	2.28E-03	2.47E-03	2.24E-03	1.85E-03	1.60E-03	1.66E-03	1.55E-03	1.47E-03	1.33E-03	9.14E-04
9.5	2.31E-03	2.29E-03	3.23E-03	2.71E-03	2.67E-03	2.35E-03	2.35E-03	1.90E-03	1.85E-03	1.43E-03	1.26E-03	8.63E-04
10.5	2.85E-03	3.21E-03	3.33E-03	3.74E-03	3.23E-03	3.26E-03	2.12E-03	2.09E-03	1.52E-03	1.40E-03	1.19E-03	6.90E-04
11.5	4.11E-03	4.69E-03	4.83E-03	4.80E-03	4.31E-03	4.02E-03	2.28E-03	2.12E-03	1.48E-03	1.29E-03	1.02E-03	6.56E-04
12.5	5.31E-03	4.93E-03	5.68E-03	5.40E-03	4.68E-03	3.42E-03	2.07E-03	2.02E-03	1.24E-03	9.66E-04	5.69E-04	2.93E-04
13.5	5.47E-03	5.90E-03	6.02E-03	5.54E-03	4.81E-03	3.49E-03	1.78E-03	1.73E-03	8.80E-04	8.11E-04	5.00E-04	2.42E-04
14.5	6.14E-03	5.71E-03	5.54E-03	5.50E-03	3.61E-03	2.80E-03	1.62E-03	9.32E-04	6.73E-04	5.00E-04	3.45E-04	1.55E-04
15.5	5.18E-03	5.75E-03	4.50E-03	4.11E-03	2.88E-03	1.83E-03	1.24E-03	7.94E-04	3.80E-04	3.11E-04	2.07E-04	1.21E-04
16.5	4.78E-03	4.47E-03	3.54E-03	2.09E-03	2.17E-03	1.07E-03	6.73E-04	4.14E-04	1.90E-04	1.73E-04	6.90E-05	5.18E-05
17.5	7.33E-03	5.80E-03	4.04E-03	2.90E-03	1.83E-03	1.16E-03	7.94E-04	5.00E-04	3.28E-04	2.07E-04	1.38E-04	6.90E-05

TWS [m/s] \ TWA [deg] ->	300	305	310	315	320	325	330	335	340	345	350	355
0.5	1.73E-05	1.73E-05	5.18E-05	1.73E-05	0.00E+00	5.18E-05	5.18E-05	3.45E-05	5.18E-05	5.18E-05	1.73E-05	5.18E-05
1.5	8.63E-05	2.07E-04	1.73E-04	5.18E-05	1.38E-04	1.04E-04	1.55E-04	6.90E-05	1.38E-04	1.04E-04	2.59E-04	2.59E-04
2.5	3.45E-04	2.76E-04	3.97E-04	3.11E-04	2.07E-04	3.11E-04	2.59E-04	3.28E-04	2.59E-04	2.07E-04	3.28E-04	3.28E-04
3.5	5.00E-04	5.87E-04	3.80E-04	2.93E-04	3.97E-04	3.97E-04	4.83E-04	3.80E-04	4.31E-04	4.31E-04	2.93E-04	6.21E-04
4.5	6.90E-04	5.52E-04	5.69E-04	5.69E-04	4.83E-04	4.31E-04	4.83E-04	6.56E-04	4.31E-04	4.49E-04	4.14E-04	8.63E-04
5.5	5.69E-04	6.38E-04	5.18E-04	6.21E-04	6.04E-04	6.56E-04	7.07E-04	5.18E-04	5.69E-04	6.73E-04	5.69E-04	8.63E-04
6.5	7.94E-04	6.21E-04	7.94E-04	4.66E-04	5.52E-04	6.73E-04	4.83E-04	6.56E-04	6.90E-04	5.35E-04	8.63E-04	8.80E-04
7.5	8.45E-04	7.25E-04	7.76E-04	7.76E-04	5.69E-04	6.04E-04	3.11E-04	6.56E-04	4.49E-04	6.56E-04	8.11E-04	9.66E-04
8.5	9.14E-04	7.07E-04	6.21E-04	6.04E-04	6.04E-04	4.66E-04	4.31E-04	4.14E-04	5.35E-04	6.04E-04	6.38E-04	1.28E-03
9.5	5.52E-04	7.07E-04	4.14E-04	4.66E-04	4.66E-04	5.00E-04	3.80E-04	2.59E-04	3.28E-04	4.31E-04	7.42E-04	1.33E-03
10.5	6.04E-04	4.31E-04	4.31E-04	4.14E-04	3.80E-04	2.93E-04	5.00E-04	3.28E-04	3.80E-04	5.35E-04	7.76E-04	1.02E-03
11.5	3.97E-04	4.83E-04	2.42E-04	1.38E-04	2.07E-04	2.59E-04	2.24E-04	3.80E-04	5.18E-04	4.83E-04	6.38E-04	1.09E-03
12.5	3.62E-04	1.21E-04	1.90E-04	1.21E-04	1.73E-04	1.21E-04	1.38E-04	1.55E-04	3.97E-04	3.28E-04	5.35E-04	1.00E-03
13.5	1.73E-04	1.21E-04	1.04E-04	1.04E-04	3.45E-05	1.21E-04	2.07E-04	1.90E-04	2.07E-04	2.42E-04	3.62E-04	9.83E-04
14.5	1.55E-04	1.38E-04	6.90E-05	1.73E-05	3.45E-05	6.90E-05	5.18E-05	8.63E-05	1.04E-04	3.80E-04	2.93E-04	9.32E-04
15.5	1.21E-04	8.63E-05	1.73E-05	8.63E-05	3.45E-05	3.45E-05	3.45E-05	6.90E-05	6.90E-05	8.63E-05	2.93E-04	8.28E-04
16.5	1.73E-05	6.90E-05	0.00E+00	1.73E-05	3.45E-05	0.00E+00	5.18E-05	1.73E-05	3.45E-05	8.63E-05	3.28E-04	6.73E-04
17.5	5.18E-05	6.90E-05	5.18E-05	3.45E-05	3.45E-05	3.45E-05	3.45E-05	1.73E-05	1.04E-04	2.07E-04	2.24E-04	9.32E-04

Table D.1: Wind probability matrix relative to north, route between CCZ and Mexico

E | Hand calculations of WASP systems

Table E.1: Hand calculations for a ship speed at 9 knts

		Kite	Dyna rig	Wingsail	Turbosail	Flettner rotor
	Vs [knts]	**9**	**9**	**9**	**9**	**9**
	Cl	1.25	2	3	7.5	10
	Cd	0.28	1	1	2.2	3.3
	A [m2]	640	496	324	60	150
	#	1	5	8	12	6
	TWS [knts]	**9.5**	**9.5**	**9.5**	**9.5**	**9.5**
forth	**TWA [º]**	**130**	**130**	**130**	**130**	**130**
	F [kN]	13	76	127	87	143
	P_{forth} [kW]	85	499	840	573	944
back	**TWA [º]**	**50**	**50**	**50**	**50**	**50**
	F [kN]	26	137	232	168	272
	P_{back} [kW]	170	903	1534	1111	1802
Resulting	P_{WASP} [kW]	127	701	1187	842	1373
	% reduction	2%	11%	19%	13%	22%

Table E.2: Hand calculations for a ship speed at 12 knts

		Kite	Dyna rig	Wingsail	Turbosail	Flettner rotor
	Vs [knts]	**12**	**12**	**12**	**12**	**12**
	Cl	1.25	2	3	7.5	10
	Cd	0.28	1	1	2.2	3.3
	A [m2]	640	496	324	60	150
	#	1	5	8	12	6
	TWS [knts]	**9.5**	**9.5**	**9.5**	**9.5**	**9.5**
forth	**TWA [º]**	**130**	**130**	**130**	**130**	**130**
	F [kN]	28	82	139	100	162
	P_{forth} [kW]	243	724	1230	878	1430
back	**TWA [º]**	**50**	**50**	**50**	**50**	**50**
	F [kN]	28	143	247	180	289
	P_{back} [kW]	243	1257	2180	1587	2549
Resulting	P_{WASP} [kW]	243	991	1705	1233	1990
	% reduction	3%	10%	18%	13%	21%

Table E.3: Hand calculations for a ship speed at 14 knts

		Kite	Dyna rig	Wingsail	Turbosail	Flettner rotor
	Vs [knts]	**14**	**14**	**14**	**14**	**14**
	Cl	1.25	2	3	7.5	10
	Cd	0.28	1	1	2.2	3.3
	A [m2]	640	496	324	60	150
	#	1	5	8	12	6
	TWS [knts]	**9.5**	**9.5**	**9.5**	**9.5**	**9.5**
forth	**TWA [º]**	**130**	**130**	**130**	**130**	**130**
	F [kN]	18	86	154	112	178
	P_{forth} [kW]	184	886	1580	1152	1827
back	**TWA [º]**	**50**	**50**	**50**	**50**	**50**
	F [kN]	57	155	275	196	320
	P_{back} [kW]	583	1595	2831	2017	3294
Resulting	P_{WASP} [kW]	384	1240	2206	1585	2560
	% reduction	3%	10%	18%	13%	20%

Table E.4: Hand calculations for a ship speed at 14 knts

		Wind turbine		
	Vs [knts]	**9**	**12**	**14**
	Cp	0.59	0.59	0.59
	A [m2]	1134	1134	1134
	#	1	1	1
	TWS [knts]	**9.5**	**9.5**	**9.5**
forth	P_{forth} [kW]	66	106	147
back	P_{back} [kW]	358	559	729
Resulting	P_{WASP} [kW]	212	333	438
	% reduction	3%	4%	3%

F | Ship speed, fuel consumption and costs of reference ship

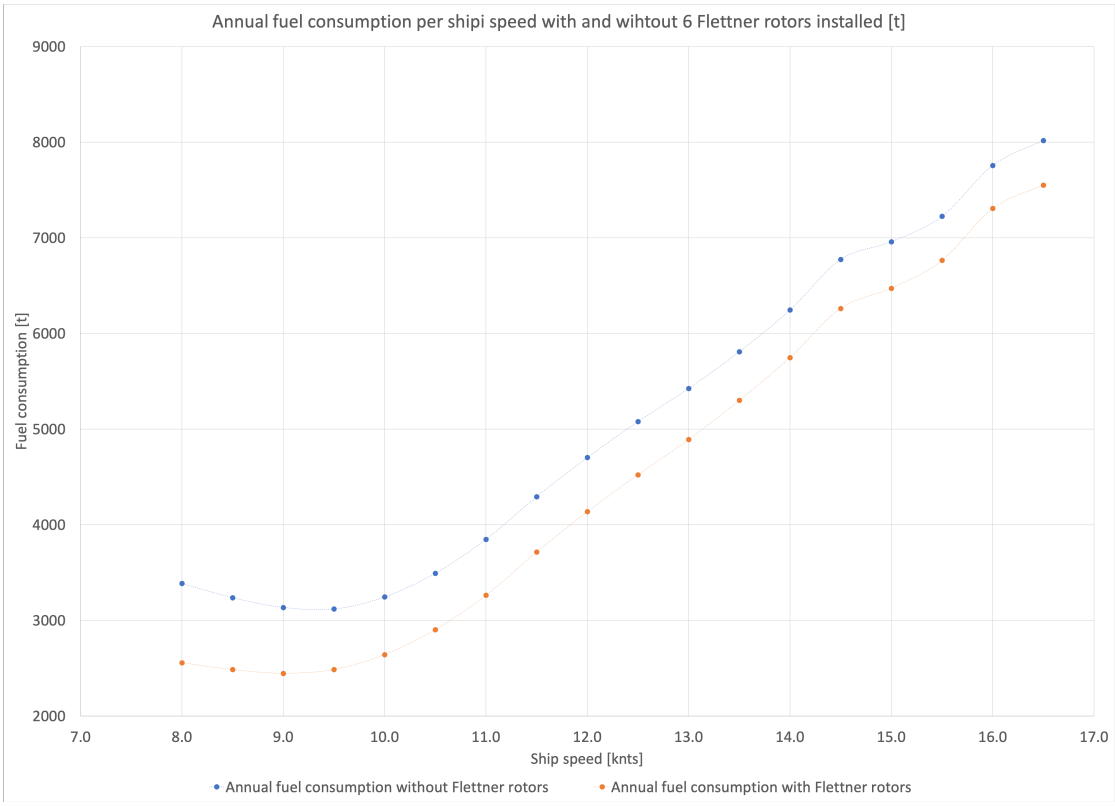

Figure F.1: Annual fuel consumption per ship speed for the reference vessel with and without installation of the Flettner rotors

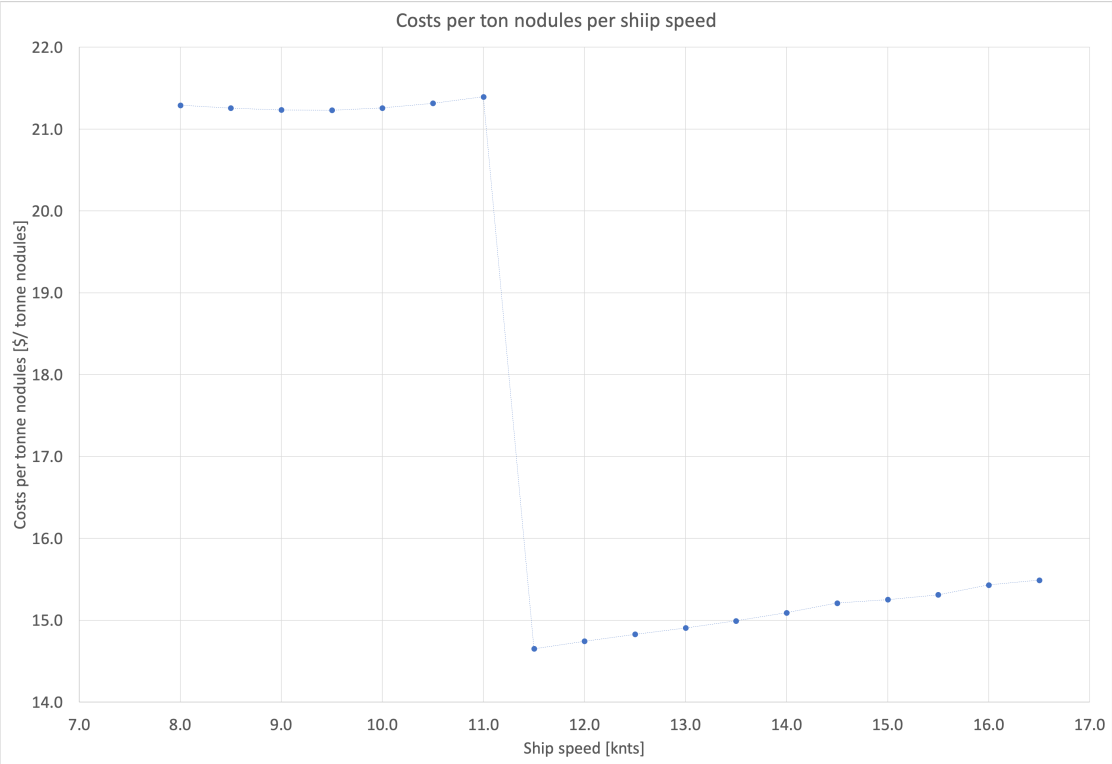

Figure F.2: Costs per tonne collected nodules per ship speed for the reference vessel

G | Performances and sizes WASP systems

Table G.1: Multi-criteria analysis

WASP systems		Number and size device	Fuel savings (% of total fuel consumption) (ship 9 knts)	Fuel savings (% of total fuel consumption) (ship 12 knts)	Fuel savings (% of total fuel consumption) (ship 14 knts)
Soft sails					
Kites	#	1	9.0%	7.0%	5.0%
	Area	640m^2			
	Cl	1.25			
	Cd	0.3			
Dyna rig	#	5	13.3%	7.2%	4.7%
	Height	34m			
	Width	14.6m			
	Cl	2			
	Cd	1			
Wing sails					
Wing sail	#	8	20.7%	11.1%	7.7%
	Height	36m			
	Width	9m			
	Cl	3			
	Cd	1			
Active sail					
Turbosail	#	12	11.9%	6.2%	4.0%
	Height	20m			
	Width	3m			
	Cl	7.5			
	Cd	2.2			
Flettner rotor	#	6	22.0%	12.0%	8.0%
	Height	30m			
	Diameter	5m			
	Cl	10			
	Cd	3+0.3			
	Rpm max	180 rpm			
	Power consumption max.	115 kW			
Other					
Wind turbine	#	1	1.9%	3.0%	3.9%
	Height	20m			
	Diameter	38m			
	Cp	16/27			